Czech University of Life Sciences Prague

Faculty of Forestry and Wood Sciences

Department of Forest Protection and Entomology

Disentangling pheromone biosynthesis in European spruce bark beetle, *Ips typographus*.

Dissertation Thesis

Author	**:**	**Rajarajan Ramakrishnan, M.Sc.**
Field of study	**:**	**Forest Biology**
Supervisor	**:**	**Ing. Anna Jirošová, Ph.D.**
Place & Year	**:**	**Prague, 2024.**

CZECH UNIVERSITY OF LIFE SCIENCES PRAGUE

Faculty of Forestry and Wood Sciences

Ph.D. THESIS ASSIGNMENT

Rajarajan Ramakrishnan, MSc

Forestry Engineering

Forest Biology

Thesis title

Disentangling pheromone biosynthesis in European spruce bark beetle (Ips typographus; Coleoptera; Scolytinae)

Objectives of thesis

European Spruce Bark Beetle (Ips typographus, Coleoptera, Scolytinae) is a devastating pest of spruce trees present in forests across Europe. This bark beetle uses pheromone-mediated aggregation to effectively overcome host defence. Considering pheromone communication, as an obvious key factor in mass attacks, intervention in pheromone biosynthesis of the beetle is a promising approach to curbing spruce killing behaviour.

Main goal of this dissertation thesis is to study Ips typographus aggregation pheromone biosynthetic pathways, related metabolism and underlying molecular mechanisms. The aim is to verify suggested reaction mechanisms of the aggregation pheromone components mainly 2-methyl-3-buten-2-ol and cis-verbenol as well as creation of monoterpenyl-esters as putative pheromone precursor. Furthermore, the candidates for involved genes and enzyme families will be targeted by differential genome expression approach and the functionality of these genes will be proved by functionally characterization techniques.

Methodology

This work will cover the broad range of “omic” approaches. The metabolomics will be used to determine the production profile of the pheromone compounds and related metabolites in the different beetle life stages and treatments (JHIII treatment). The beetle guts and corpuses will be dissected, extracted and measured by spectrometric methods to compare metabolom and quantify target compounds. The transcriptomic approach will cover the RNA sequencing of beetles tissues from various life stages and JHIII treatment and transcriptoms will be compared by Differential gene expression analysis with using sophisticated software tool such as CLC work bench. The highly upregulated genes with respect to pheromone biosynthesis will be selected and its production profile over the life stages will be supported with realtime quantitative polymerase chain reaction (RT-qPCR). The best candidate genes will be functionally characterized using specific expression among cell lines (bacterial, insect) and in vitro respected enzyme assays for achieving end products.

The proposed extent of the thesis

100-120

Keywords

Pheromone biosynthesis, Gene characterization, Transcriptomics, 2-methy-3-buten-2-ol, isoprenyl diphosphate synthase, verbenyl ester

---

Recommended information sources

Birgersson G.& Bergström, G; 1989. Volatiles released from individual spruce bark beetle entrance holes Quantitative variations during the first week of attack. J Chem Ecol., 15(10):2465-83.

Gilg, A.B., Bearfield, J.C., Tittiger, C., Welch, W.H., Blomquist, G.J., 2005. Isolation and functional expression of an animal geranyl diphosphate synthase and its role in bark beetle pheromone biosynthesis. Proc. Natl. Acad. Sci. U. S. A. 102, 9760–9765. https://doi.org/10.1073/pnas.0503277102

He, P., Mang, D.Z., Wang, H., Wang, M.M., Ma, Y.F., Wang, J., Chen, G.L., Zhang, F., He, M., 2020. Molecular characterization and functional analysis of a novel candidate of cuticle carboxylesterase in Spodoptera exigua degradating sex pheromones and plant volatile esters. Pestic. Biochem. Physiol. 163, 227–234. https://doi.org/10.1016/j.pestbp.2019.11.022

Chiu, C.C., Keeling, C.I., Bohlmann, J., 2018. Monoterpenyl esters in juvenile mountain pine beetle and sex-specific release of the aggregation pheromone trans -verbenol. PNAS 2–7. https://doi.org/10.1073/pnas.1722380115

Keeling, C.I., Blomquist, G.J., Tittiger, C., 2004. Coordinated gene expression for pheromone biosynthesis in the pine engraver beetle, Ips pini (Coleoptera: Scolytidae). Naturwissenschaften 91, 324–328. https://doi.org/10.1007/s00114-004-0523-y

Keeling, C.I., Li, M., Sandhu, H.K., Henderson, H., Man, M., Yuen, S., 2016. Quantitative metabolome , proteome and transcriptome analysis of midgut and fat body tissues in the mountain pine beetle , Dendroctonus ponderosae Hopkins , and insights into pheromone biosynthesis. Insect Biochem. Mol. Biol. 70, 170–183. https://doi.org/10.1016/j.ibmb.2016.01.002

Li, Z., Dai, L., Chu, H., Fu, D., Sun, Y., Chen, H., 2018. Identification, expression patterns, and functional characterization of chemosensory proteins in Dendroctonus armandi (Coleoptera: Curculionidae: Scolytinae). Front. Physiol. 9, 1–14. https://doi.org/10.3389/fphys.2018.00291

Roy, A., George, S., Palli, S.R., 2017. Multiple functions of CREB-binding protein during postembryonic development : identification of target genes. BMC Genomics 1–14. https://doi.org/10.1186/s12864-017-4373-3

Roy, A., Palli, S.R., 2018. Epigenetic modifications acetylation and deacetylation play important roles in juvenile hormone action. BMC Genomics 1–15. https://doi.org/10.1186/s12864-018-5323-4

Schlyter, F., Birgersson, G., Byers, J.A., Löfqvist, J., Bergström, G., 1987. Field response of spruce bark beetle, Ips typographus, to aggregation pheromone candidates. J. Chem. Ecol. 13, 701–716. https://doi.org/10.1007/BF01020153

Expected date
2024/25 WS – FFWS – State Doctoral Examinations

The Dissertation Thesis Supervisor
Ing. Anna Jirošová, Ph.D.

Supervising department
Department of Forest Protection and Entomology

Electronic approval: 17. 10. 2024

prof. Ing. Róbert Marušák, PhD.
Dean

Prague on 18. 10. 2024

ANNOTATION.

The European spruce bark beetle, *Ips typographus*, is a major pest in spruce forests across Eurasia, including the Czech Republic. The beetle's colonization in Norway spruce is mediated by an aggregation pheromone blend consisting of 2-methyl-3-buten-2-ol, ipsdienol, and ipsenol which are synthesized in the beetle's gut, along with *cis*-verbenol, produced by hydroxylation of host-derived pinene. *cis*-Verbenol has also been found as verbenyl fatty acid ester in the fat bodies of other bark beetles, potentially serving as a storage precursor. While pheromone communication is essential for mass beetle attacks on conifers, the detailed mechanisms of pheromone biosynthesis and its genetic basis in *I. typographus* remain largely underexplored.

This thesis focuses on elucidating the biosynthesis of key pheromone compounds at both metabolite and molecular levels, with emphasis on male beetles during pheromone-producing life stages. Additionally, juvenile hormone III (JH III) was applied to artificially induce pheromone production, providing insights into the hormonal regulation of this process and associated metabolic pathways. Using a multi-omics approach, we analyzed metabolites, gene transcripts, and protein expression in the gut and fat bodies of *I. typographus,* in both sexes and after JH III treatment.

The key findings showed that 2-methyl-3-buten-2-ol was produced at much higher levels in males feeding on trees and in those treated with JH III, suggesting *de novo* synthesis via the mevalonate pathway. *cis*-Verbenol levels were higher in both sexes of immature beetles compared to pheromone-producing adult males, while ipsdienol was detected in adult males post-mating. The storage precursor verbenyl oleate was most concentrated in both sexes of immature beetles and during the adult beetle stage, the compound was produced exclusively by males.

Differential gene expression (DGE) and differential protein expression (DPE) analyses identified candidate genes involved in pheromone biosynthesis. Genes in the mevalonate pathway were upregulated in the guts of feeding males and in response to JH III treatment, providing evidence for the *de novo* synthesis of 2-methyl-3-buten-2-ol and ipsdienol. Additionally, a novel gene encoding the first hemiterpenoid-synthesizing isoprenoid-diphosphate synthase (IPDS), which could be involved in the terminal step of 2-methyl-3-buten-2-ol synthesis, was identified. Cytochrome P450 (CYP450) enzymes were also pinpointed as potential catalysts for the hydroxylation of pinene into *cis*- and *trans*-verbenol, as well as for the detoxification of toxic monoterpenes. Genes from the esterase/lipase family were targeted for their roles in the formation and hydrolysis of *cis*-verbenol fatty acid esters stored in the fat body. Additionally, other genes involved in primary and secondary metabolic processes relevant to pheromone biosynthesis, detoxification, and juvenile hormone III regulation were identified and discussed.

Future research should focus on the functional characterization of these genes, with the potential to use genetic engineering to disrupt *I. typographus* aggregation behavior, thereby helping to prevent vegetation loss.

Keywords: *Ips typographus*, bark beetle, pheromone biosynthesis, multi-omics.

DECLARATION.

I declare that I have independently written the dissertation on the topic “Disentangling pheromone biosynthesis in European spruce bark beetle, *Ips typographus*”, with the use of literature and based on consultations and supervisor’s recommendations. I agree to publish the dissertation according to Act no. 111/1998 Coll., on schools, as amended, regardless of the outcome of its defence.

Prague, 2024. Rajarajan Ramakrishnan., M. Sc.,

ACKNOWLEDGEMENT.

For guidance and the opportunity to participate in the research project “Bark beetle, *Ips typographus* pheromone biosynthesis”, first, I thank my Ph.D. supervisor, Ing. Anna Jirošová, Ph.D. I also want to thank Dr. Amit Roy for providing molecular lab support. Furthermore, I appreciate the support of my friends and co-workers, and the rest of the staff and students from the Department of Excellent Mitigation Team and Faculty of Forestry and Wood Sciences at the Czech University of Life Sciences, Prague, Czech Republic.

I would like to thank Prof. Emeritus Fredrik Schlyter at the Department of Plant Protection Biology, Swedish University of Agricultural Sciences, Alnarp, Sweden for sharing his wide knowledge on the bark beetle research topic under the EU project EXTEMIT-K. I also want to thank Professor Dr. Jonathan Gershenzon, Department of Biochemistry, Max Planck Institute for Chemical Ecology, Jena, Germany for providing me the opportunity to complete abroad training in his group.

Finally, I would like to express my gratitude to my family in India and friends for their constant motivation, love, and support. I want to dedicate my Ph.D. thesis work in memory of my father, Mr. Ramakrishnan Kasi.

The dissertation was funded by an EU project: "EXTEMIT-K," No. CZ.02.1.01/0.0/0.0/15_003/0000433, Internal Grant Agency (IGA A_20_02 and IGA A_20_22, RAJARAJAN RAMAKRISHNAN) and the prestigious KORF scholarship from Faculty of Forestry and Wood Sciences at the Czech University of Life sciences, Prague, Czech Republic.

Motto

“DREAM is not what you see in sleep,
it is something that DOES NOT LET YOU SLEEP”.

- Dr. A.P.J. Abdul Kalam (scientist, 11th Indian President)

TABLE OF CONTENTS.

LIST OF FIGURES.

The permission to use Figures from relevant publications was obtained legally.

LIST OF TABLES:

LIST OF ABBREVIATIONS.

- AACT - Acetoacetyl-CoA thiolase.
- CYP450 - Cytochrome P450.
- CYP9T1/T2/T3 - Cytochrome P450 9.
- CYP6DE1like - Cytochrome P450 6.
- DGE - Differential Gene expression.
- DPE - Differential Protein expression.
- *ds*RNA - Double-stranded RNA.
- GC-MS - Gas Chromatograph coupled to Mass Spectrometer.
- GPPS - geranyl-di-phosphate synthase.
- HMG-S - 3-hydroxy-3methyl glutaryl Co-A synthase.
- HMG-R - 3-hydroxy-3methyl glutaryl Co-A reductase.
- IDOLDH - ipsdienol dehydrogenase.
- IDONER - ipsdienone reductase.
- IPPI - isopentenyl-di-phosphate isomerase.
- IPDS - isoprenoid-di-phosphate synthase.
- JH III - Juvenile Hormone III.
- MK - mevolnate-3-kinase.
- NHV - non-host volatiles.
- nLC-MS/MS - NanoLiquid Chromatography coupled to mass spectrometer.
- PMK - phosphomevalonate kinase.
- RbPL6 - Ribosomal protein L6.
- RbPS18 - Ribosomal protein S18.
- UHPLC-ESI-HRMS/MS - Ultra-high-performance liquid chromatography-electrospray ionization -high-resolution tandem mass spectrometry.

LIST OF PUBLISHED ARTICLES.

- **Ramakrishnan R**., Hradecký J., Roy A., Kalinová B., Mendezes C. R., Synek J., Bláha J., Svatoš A., Jirošová A*. 2022a. Metabolomics and transcriptomics of pheromone biosynthesis in an aggressive forest pest *Ips typographus*, Insect Biochemistry and Molecular Biology. https://doi.org/10.1016/j.ibmb.2021.103680

- **Ramakrishnan R**., Roy A., Kai M., Svatoš A., Jirošova A*. 2022b. Metabolome and transcriptome related dataset for pheromone biosynthesis in an aggressive forest pest *Ips typographus*. Data in Brief. https://doi.org/10.1016/j.dib.2022.107912

- **Ramakrishnan R**., Roy A., Hradecký J., Kai M., Harant K., Svatoš A., Jirošová A*. 2024. Juvenile Hormone III Induction Reveals Key Genes in General Metabolism, Pheromone Biosynthesis, and Detoxification in Eurasian Spruce Bark Beetle. Frontiers in Forests and Global change. http://doi.org/10.3389/ffgc.2023.1215813

Article yet to be published:

- **Ramakrishnan R.,** Shewale M. K., Strádal J., Hani U., Gershenzon J., Jirošová A*****. Aggregation Pheromones in the Bark Beetle genus *Ips*: Advances in Biosynthesis, Sensory Perception, and Forest Management Applications (unpublished Manuscript).

Article not included in this thesis:

- Jirošová A., Modlinger R., Hradecký J., **Ramakrishnan R**., Berankova K., Kandasamy D*. 2022. Ophiostomatoid fungi synergize attraction of the Eurasian spruce bark beetle, *Ips typographus* to its aggregation pheromone in field traps. Frontiers In Microbiology. https://doi.org/10.3389/fmicb.2022.980251

1. INTRODUCTION AND LITERARY ANALYSIS.

1.1. Bark beetle outbreaks in central Europe.

Bark beetle infestations in Eurasian conifer forests have become a critical issue for forest protection and ecological conservation. ***Ips typographus*** (L. 1758, Coleoptera; Curculionidae), commonly known as the European spruce bark beetle, is a major pest that causes widespread destruction of its host tree, Norway spruce (***Picea abies*** [L.] Karst.), across many European and Asian countries (Marini et al., 2017). The crisis caused by bark beetle activity in conifer forests has resulted in significant wood loss. Nevertheless, under balanced ecological conditions, bark beetle plays an essential role in spruce forests by decomposing dead and wind-fallen trees, thereby contributing to the ecological health of the forest (Peltonen, 1999).

One of the primary reasons for the recent outbreaks of *I. typographus* is the widespread planting of Norway spruce forest in Europe, driven by its high ecological adaptability and economic value (Schmidt Vogt, 1977). Spruce vegetation has been documented as far back as the 18th century (Andrle, 2017). Consequently, over the past few centuries, European forests have undergone significant changes in tree population variability, largely due to human activities (EEA 2014; Jansen et al., 2017). Despite government policies, such as the EU Commission's directive from December 2016, which aims to introduce more broadleaf species, the importance of spruce vegetation remains irreplaceable for these reasons (Szabó et al., 2017).

In the Czech Republic, *I. typographus* outbreaks, triggered by extreme climatic conditions in 2015 and 2018, were particularly severe (Figure 1). In 2018, the country experienced above-average temperatures (+2.1 °C deviation) and below-average precipitation (77% of normal levels) (Lubojácký et al., 2022), leading to exponential increases in *I. typographus* populations that exceeded epidemic levels in numerous regions (Lubojácký et al., 2022). As a result, thousands of hectares of spruce trees across the country were reported dead and rotting (Hlásny et al., 2021). Additionally,

salvage logging peaked at approximately 15 million m³ in 2019 and 2020, gradually decreasing to 5.5 million m³ in recent years (Figure 1, Lubojácký et al., 2022).

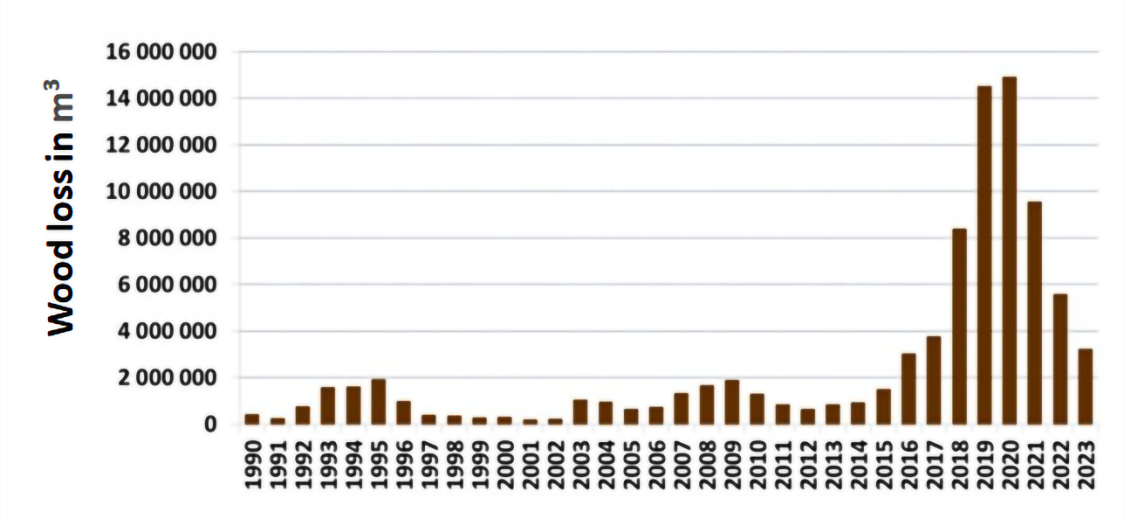

Figure 1: Recorded volume of wood loss due to bark beetle attacks in the Czech Republic. The wood loss showed per hectare of spruce stands from the year 1990 till 2023, representing 70% volume of the forest area in the Czech Republic) (source: https://www.vulhm.cz/en/what-are-the-current-threats-to-our-forests/, Lubojácký et al., 2022)

Bark beetle outbreaks have historically exhibited periodic fluctuations with recurrences every 20 to 30 years (as analyzed since 1945) and the outbreaks from 2018 to 2020 were the most severe on record (Hlásny et al., 2021). Due to changing climate conditions, another significant outbreak could occur in the near future. This highlights the critical need for extensive research on effective mitigation strategies for this highly aggressive forest pest, utilizing the latest scientific techniques and findings. In this context, studying the production of bark beetle pheromones, which serve as potent aggregation agents driving their aggressive behavior, is particularly important.

1.2. Host tree selection by bark beetles.

The success of bark beetle populations depends on selecting appropriate host trees with optimal resources and physiological conditions (Raffa et al., 2016). The selection of suitable trees involves an energy trade-off for the bark beetles over time and plays a crucial role in the success of the next generation (Raffa, 1983; Bohlmann and Gershenzon, 2009). This host selection process varies among different bark beetle

species depending on their population dynamics (Biedermann et al., 2019). For example, in the genus *Dendroctonus*, female beetles act as pioneer seekers, whereas in the genus *Ips*, male beetles serve as pioneers (Schmitz 1972; Amman 1989).

The behavioral mechanisms of host selection by bark beetles are explained by two main theories: active primary attraction to weakened trees based on their specific odors (Lehmanski et al., 2023) and random landing by emerging dispersing bark beetles, followed by a decision step based on the tree's smell and taste upon close encounter (Byers, 1989; Netherer et al., 2021).

In *I. typographus*, as in other *Ips* species, males are the pioneering sex in host selection (Bakke 1976; Seidl et al., 2016; Lehmanski et al., 2023). The exact mechanisms underlying the selection of suitable host trees remain unclear, as is the case with many other bark beetle species. However, it is known that *I. typographus* can detect monoterpenes emitted by host spruce trees, which primarily indicate habitat suitability. Additional volatiles from non-host species, such as broadleaf trees and their associated fungi, signal suitable and unfavorable conditions for colonization (Netherer et al., 2021, Figure 2). Furthermore, changes in tree metabolites, along with weakened defense mechanisms, help the bark beetles identify potential hosts (Schiebe, 2019; Netherer et al., 2024; Basile et al., 2024). After selecting a host, the pioneer bark beetle uses chemical cues to recruit conspecifics, facilitating colony establishment despite the host's defense mechanisms. This strategy helps bark beetles overcome the tree's chemical defenses, such as resins and toxic phenolic substances.

I. typographus pioneer male beetles produce the aggregation pheromone that consists of 2-methyl-3-buten-2-ol, *cis*-verbenol, and traces of ipsdienol, making it a highly effective attractant (Bakke et al., 1977; Schlyter et al., 1987). The aggregation pheromone is species-specific. The attractive function of this pheromone can also be

triggered by host spruce monoterpenes and volatiles produced by symbiotic fungi (Erbilgin, 2007; Jirošová et al., 2022).

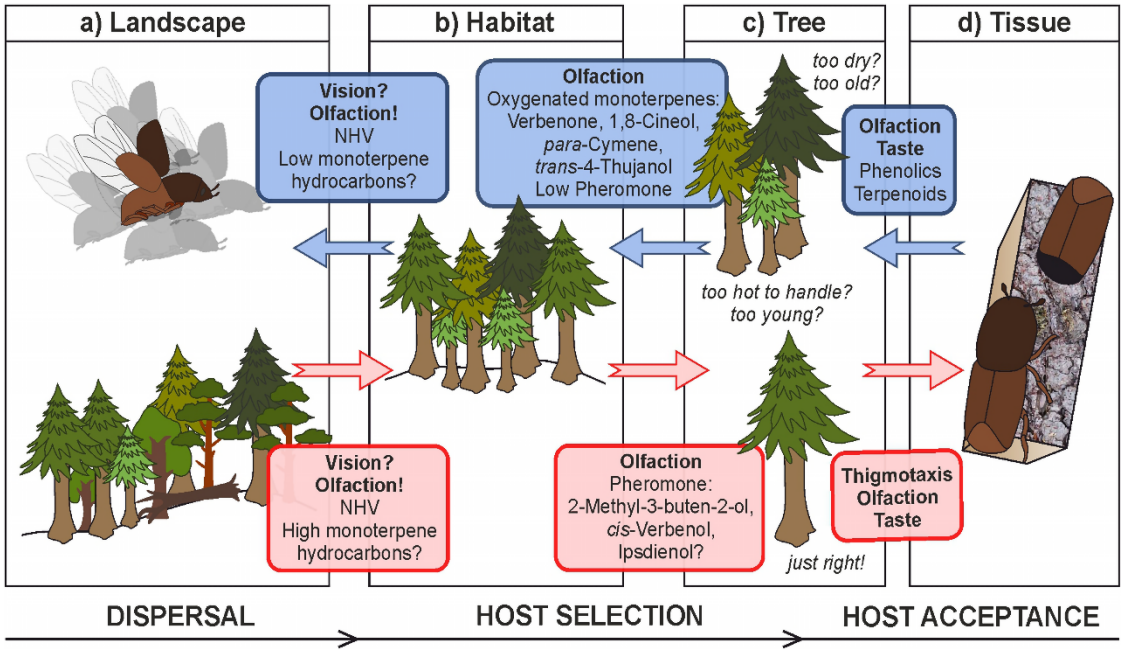

Figure 2: Bark beetle host selection overview.
This diagram illustrates the behavioral sequence of I. typographus *during host selection across different scales: a) landscape (dispersal), b) habitat, c) tree (both host selection), and d) tissue (host acceptance). The sequence is influenced by both positive cues (indicated by light blue arrows and boxes) and negative cues (indicated by red arrows and boxes). The focus is on pioneering male beetles, whose rapid production of pheromones and non-host volatiles (NHV) guides the aggregation of both males and females on the host tree. The chemical cues are listed by compound names, highlighting their role in guiding the bark beetles through a sequence of steps, which are driven by visual, chemo-sensory, and thigmotactic signals. (Source: Netherer et al., 2021)*

1.3. *Ips typographus* life stages in the context of pheromone biosynthesis.

The complete metamorphosis of *I. typographus* includes four developmental stages: egg, larva, pupa, and adult. The duration of each stage in the life cycle depends on various factors, such as climate, habitat conditions, and available food sources (Annila, 1969). The only developmental stage that occurs outside of the bark is the adult beetles.

There are differences between male and female adult beetles in their life stages. In the context of pheromone production, the focus is primarily on males (Birgersson et al., 1984). When adult male beetles emerge from the bark and begin to fly, their flight

muscle activates the enzymatic system, indicating the importance of this life stage for certain pheromone mechanism studies (Ivarsson et al., 1995).

Upon landing on a selected tree, the males search the bark surface and begin chewing to challenge the tree's defenses. At this stage, they produce a trace amount of pheromone, with the primary pheromone production occurring once they successfully bore into the bark (Schlyter and Löfqvist, 1986). This pheromone attracts conspecific beetles, both males and females, to the tree. Female beetles are then drawn to the boring holes created by the pioneer males, where they attempt to enter and locate the males, who, in the meantime, have constructed a nuptial chamber. When a female bark beetle enters the bark successfully, the male and female beetles mate in the mating chamber (Paynter et al., 1990). Typically, one male *I. typographus* will be associated with two or three females and have two generations per year (Felicijan et al., 2015).

Past research in *I. typographus* pheromone primarily focused on adult males, specifically emerged beetles (pioneers in finding suitable hosts) and those in mating chambers (Birgersson et al., 1984; Byers et al., 1989) (Figure 3). Trace amounts of 2-methyl-3-buten-2-ol and *cis*-verbenol were identified in flying beetles and higher concentrations of these compounds were found in males while boring into host trees. Later, Ipsdienol was detected in males from mating chambers along with females (Birgersson et al., 1984). In the later stages of an attack, increasing amounts of verbenone were identified in the entrance holes when the tree's resources were depleted. Verbenone is presumably converted from the pheromone compound *cis*-verbenol by the beetle's gut microbiome (Brand et al., 1976; Hunt and Borden, 1990) and acts as an anti-aggregation signal, indicating food depletion in the attacked tree (Leufvén et al., 1984).

However, recent studies in other bark beetle species have highlighted the importance of juvenile life stages, including larvae and pupae, in pheromone biosynthesis research. Notably, *cis*-verbenol was identified in earlier stages, presumably as a detoxification

byproduct, which may later serve as a precursor for pheromone production in adult male beetles (Chiu et al., 2017).

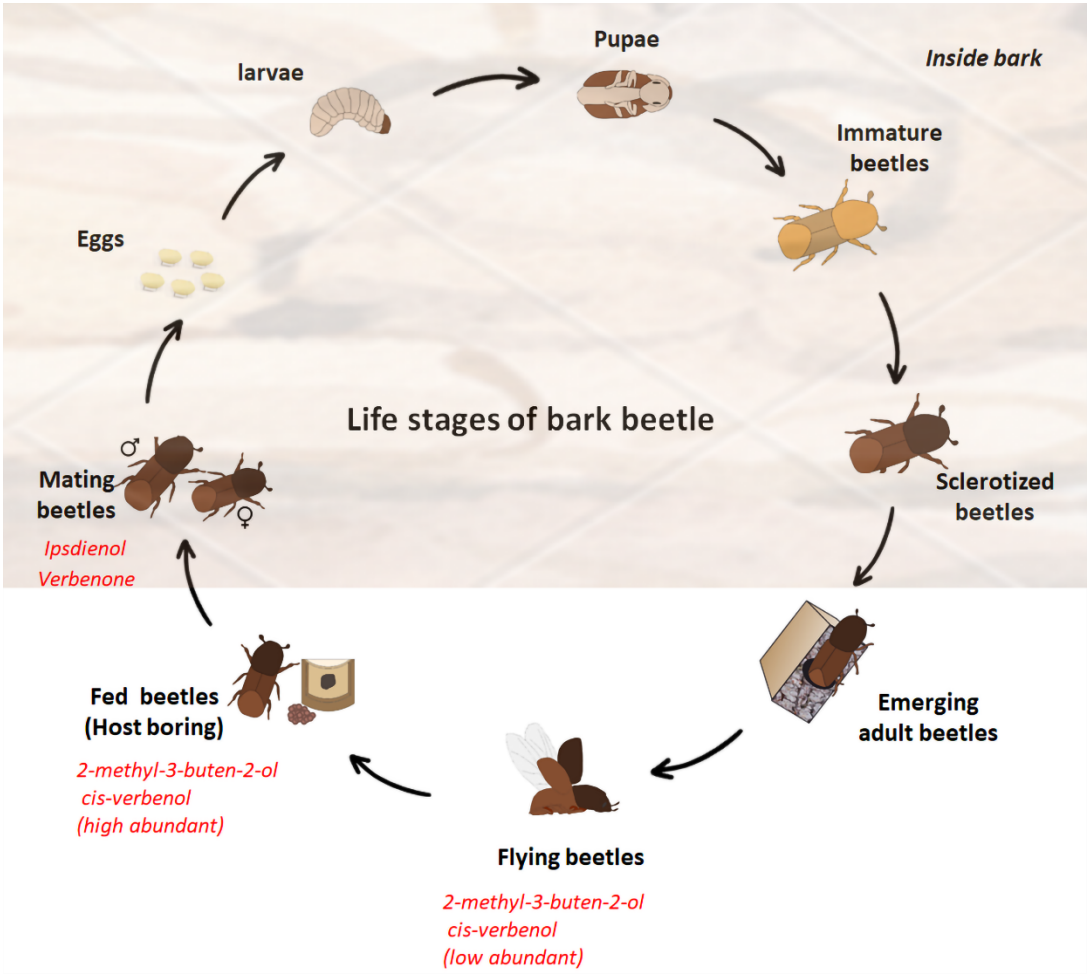

Figure 3: Life stages of European Bark beetle, Ips typographus*.*
The life stages inside the tree bark are shown in the shaded region. (Source: Recreated from Ramakrishnan et al., 2022a.) The pheromone compounds known from existing research findings are mentioned in red font for the corresponding life stages.

Thus, pheromone biosynthesis research in bark beetles across different life stages is crucial to understanding the bark beetle's fitness and success (Birgersson et al., 1984; Aw et al., 2010). The pheromone production is regulated in response to immediate environmental and life conditions. For example, they can switch pheromone production off when the pheromone concentration becomes too high due to the presence of too many males, thereby controlling the attraction of additional bark beetles (Pureswaran et al., 2000).

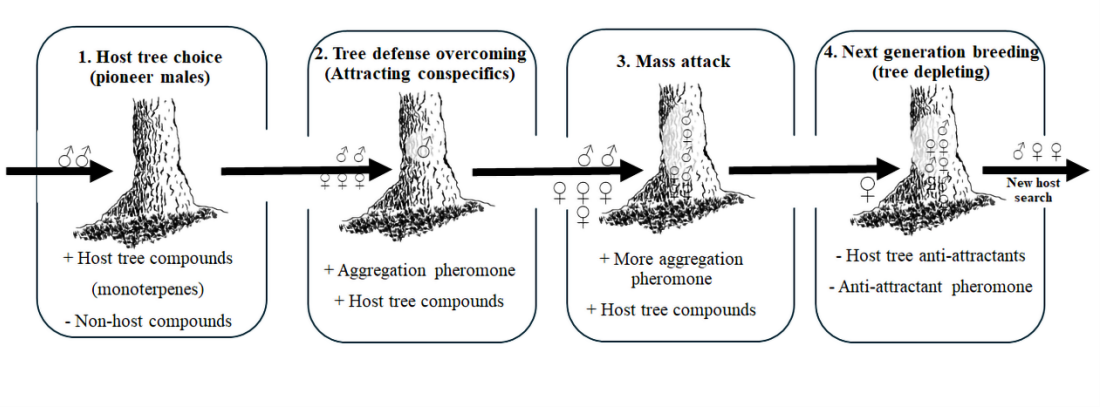

Figure 4. Attack dynamics of I. typographus *on its natural host, Norway spruce,* P. abies*.*
Description: ***Step 1:*** *Pioneer male locates the host tree using the host and non-host compounds.* ***Step 2:*** *Male I. typographus releases an aggregation pheromone blend, including MB (2-Methyl-3-buten-2-ol) and cV (*cis*-Verbenol) along with host compounds and symbiotic fungal volatile organic compounds (VOCs).* ***Step 3:*** *The chemical cue attracts more conspecific beetles to the host tree and more aggregation pheromones are released by the newly attracted conspecific beetles.* ***Step 4:*** *The tree defence is depleted completely with low resin flow and the release of other compounds such as anti-attractants to repel further conspecific beetles. (Recreated from Byers, 1989).*

1.4 Pheromones biosynthesis in bark beetles.

The mechanism of pheromone production in various bark beetle species has been extensively studied over the decades (Gray, 2002; Seybold et al., 2003; Blomquist et al., 2010; Wermelinger, 2019). These pathways have co-evolved with tree defence detoxification mechanisms to facilitate successful host attacks (Chiu et al., 2018). Bark beetles synthesize pheromones either *de novo* from basic metabolites or by modifying carbon skeleton precursors sequestered from host trees (pinene, myrcene). For most species, the gut tissue is the primary site of pheromone biosynthesis, with pheromones being released through faeces known as wooden frass (Silverstein et al., 1966; Hall et al., 2002).

Early studies analyzed compound production by exposing bark beetles to labelled and unlabelled precursors, providing evidence for proposed biosynthetic mechanisms. These findings paved the way for transcriptomic and genomic research to identify enzymes and corresponding genes involved in pheromone production. Advances in affordable, high-quality sequencing technologies and bioinformatics now support

interdisciplinary studies of biosynthesis (Venter et al., 2004; Powell et al., 2021). Despite these advancements, functional characterization of genes responsible for key biosynthetic steps has been achieved in only a few instances.

1.4.1. Compositions and structures of *Ips typographus* pheromone.

The structural repertoire of biologically active pheromone compounds in genus *Ips*, where *I. typographus* belongs, is relatively limited, primarily consisting of oxygenated hemi- or monoterpenes (Kohnle et al., 1988). These compounds are volatile and structurally resemble the defence compounds (resin) found in their host conifer trees, like myrcene and α-pinene (Figure 5).

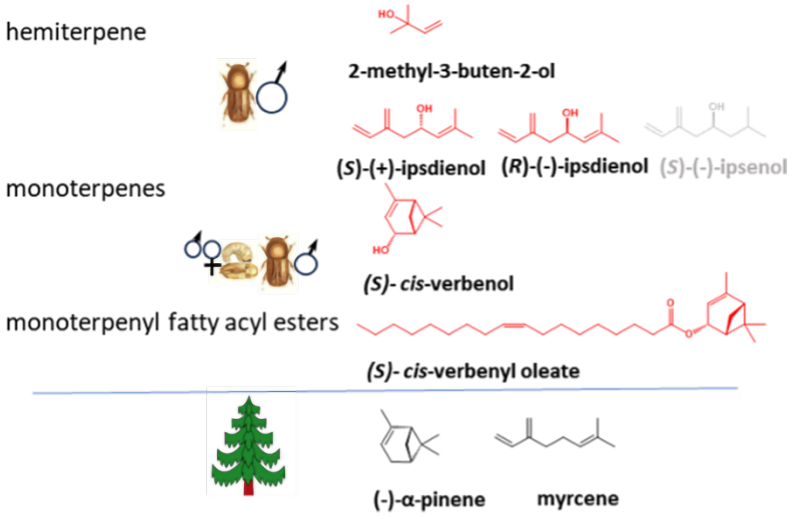

Figure 5: Structures of pheromone components and its precursors in I. typographus*.*
The structure of bark beetle pheromone, pheromone conjugates, and relative tree precursors are shown from top to bottom (Recreated from Birgersson et al., 1984; Chiu et al. 2018).

Similar to most *Ips* species, *I. typographus* also produces ipsdienol and traces of ipsenol (Birgersson et al.,,1984), compounds unique to this bark beetle family (Seybold et al., 1995a; Tillman et al., 1998). These two compounds were identified along with aggregation pheromones, 2-methyl-3-buten-2-ol and *cis*-verbenol (Bakke A., 1976, Figure 5). In the pheromone blend of the Central European population, the ratio of these compounds was 2-methyl-3-buten-2-ol: *cis*-verbenol: ipsdienol at 10:1:0.1 (Lanne et al., 1989). Among the pheromone compounds of *I. typographus*, only ipsdienol occurs with a certain enantiomeric ratio. The enantiomeric ratio of ipsdienol

in the Central European population of *I. typographus* has been reported as (*S*-):(*R*-) 5:95 (Dickens et al., 1981).

1.4.2. The role of the mevalonate pathway in pheromone biosynthesis.

The listed structures of bark beetle pheromones belong to the isoprenoids/terpenoids group, exclusively produced in animals via the mevalonate pathway. Unlike plants, which can also utilize the Rohmer pathway, also known as the 2-C-methyl-D-erythritol 4-phosphate/1-deoxy-D-xylulose 5-phosphate (MEP/DOXP) pathway (Martin D., et al., 2003).

The initial evidence of the involvement of the mevalonate pathway in the *de novo* production of pheromones in *Ips* species was provided by Ivarsson et al. (1993). They demonstrated that the inhibitor of the mevalonate pathway, compactin (Nakamura and Abeles, 1985), decreased the formation of ipsdienol and *E*-myrcenol in *Ips duplicatus* males. Subsequent direct evidence for the mevalonate pathway was provided after the incorporation of basic precursor ^{14}C-mevalonolactone into ipsdienol and ipsenol in *I. pini* and *I. paraconfusus* males (Seybold et al., 1995b).

The mevalonate pathway initiates with the condensation of two activated acetate units to form acetoacetyl CoA, catalyzed by *acetoacetyl-coenzyme A thiolase* (AACT). Subsequently, a third acetyl CoA molecule alkylates acetoacetyl-CoA, leading to the production of hydroxymethylglutaryl-CoA. This reaction is facilitated by *hydroxymethylglutaryl-synthase* (HMG-S). Hydroxymethylglutaryl-CoA is then reduced by *hydroxymethylglutaryl-reductase* (HMG-R) to yield mevalonic acid, which undergoes phosphorylation in two successive steps mediated by *mevalonate-kinase* (MK) and *phosphomevalonate-kinase* (PMK), resulting in the formation of mevalonate diphosphate. Following decarboxylation by *mevalonate 5-diphosphate decarboxylase* (MPDC), the first fundamental building block of isoprenoids, isopentenyl diphosphate (IPP), is generated. IPP can undergo controllable isomerization by *isopentenyl-diphosphate isomerase* (IPPI) to dimethylallyl diphosphate (DMAPP), the second building block of isoprenoids (Figure 6).

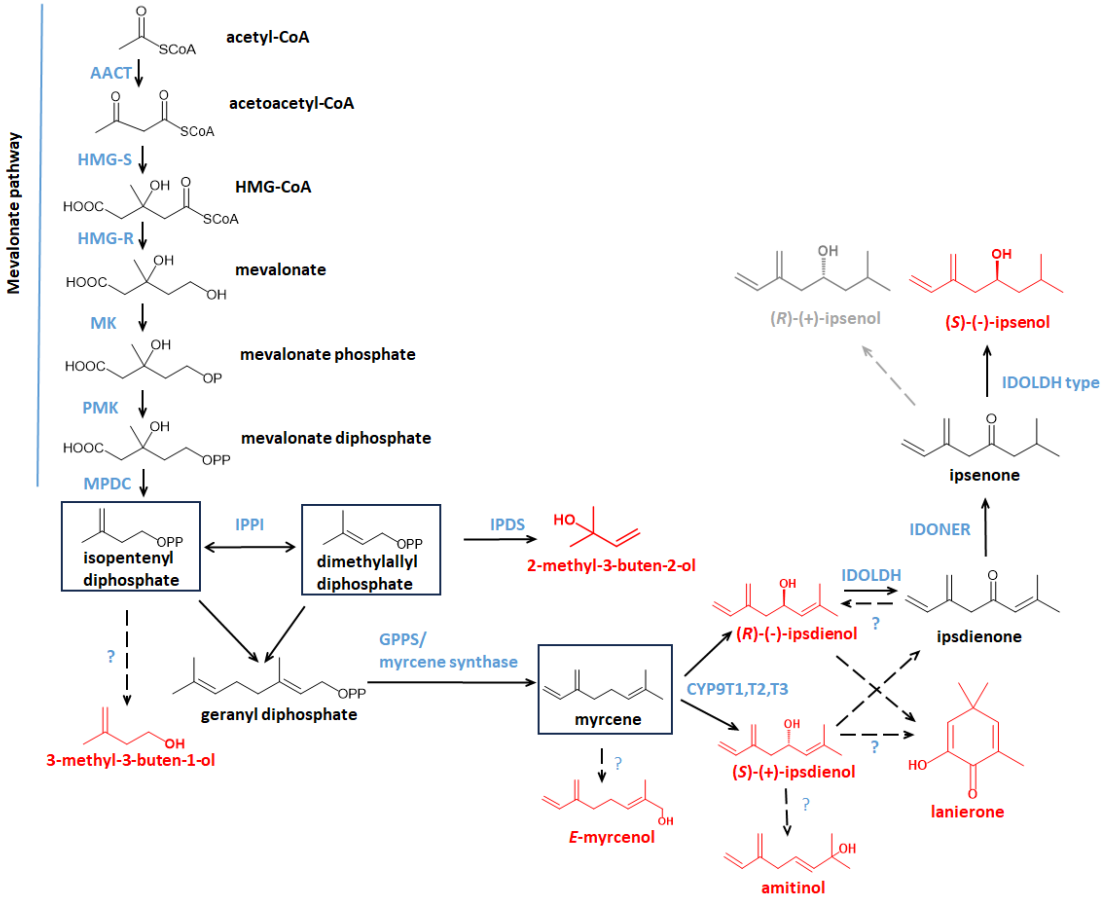

Figure 6: De novo *pheromone biosynthesis via mevalonate pathway in gut tissue of* I. typographus.
The abbreviations of the pathway genes are described as follows: acetoacetyl-CoA thiolase (AACT), 3-hydroxy-3methyl glutaryl Co-A synthase (HMG-S), 3-hydroxy-3methyl glutaryl Co-A reductase (HMG-R), mevolnate-3-kinase (MK), phosphomevalonate kinase (PMK), isopentenyl-di-phosphate isomerase (IPPI), isoprenoid-di-phosphate synthase (IPDS), geranyl diphosphate synthase (GPPS), Cytochrome P450 9 like (CYP9T1, T2, T3), ipsdienol dehydrogenase (IDOLDH), ipsdienone reductase (IDONER) (Source: modified from Ramakrishnan et al., 2022a).

Unlike many other insects, *Ips* bark beetles have a unique ability to synthesize the monoterpene myrcene *de novo* in their gut through the mevalonate pathway. Myrcene is synthesized from the basic isoprenoid units, isopentenyl diphosphate (IPP), and dimethylallyl diphosphate (DMAPP). These units catalytically condense to form geranyl

diphosphate (GPP), which is then dephosphorylated and, myrcene is produced in a single step. This reaction is catalyzed by the enzyme *geranyl diphosphate/myrcene synthase* (GPPS), which is unique to animals and was first described in *I. pini* (Gilg et al., 2005).

1.4.3. Regulation of mevalonate pathway genes.

The transcription of certain genes in the mevalonate pathway is influenced by various factors such as sex, juvenile hormone levels (specifically JH III treatment), and the feeding behaviors of male beetles. These genes can regulate the final production of the pheromone. Targeting these genes can be an effective strategy for influencing pheromone production at the genetic level.

The first of these regulatory genes discovered in bark beetles was the *3-hydroxy-3-methylglutaryl-CoA reductase* (HMG-R) in the gut of *I. pini*, which contributes to ipsdienol synthesis. This gene was found to be upregulated following JH III treatment (Tillman et al., 1998, 2004). Subsequently, other genes such as HMGS and GPPS were also analyzed and identified for higher expression in *I. pini* males after 32 hours of feeding on logs (Bearfield et al., 2009).

Interestingly, when comparing the regulation of HMG-R by JH III in two species from the bark beetle *grandicolis* subgeneric group, it was observed that the HMG-R transcript level was stimulated in *I. paraconfusus*, but not in *Ips confusus* (Bearfield et al., 2009). This suggests the presence of interspecific differences in the hormonal regulation of pheromone biosynthesis, which could contribute to species-specificity in their pheromone mixtures (Tillman et al., 2004; Tittiger et al., 1999).

1.4.4. Biosynthesis of ipsdienol and ipsenol.

Ipsdienol is synthesized from myrcene (either sequestered from trees or synthesized *de novo* from bark beetle), by hydroxylating enzymes belonging to the Cytochrome P450 (CYP450) (Hall et al., 2002; Tittiger & Blomquist, 2017; Blomquist et al., 2021). The enzyme CYP9T1, a member of this family, has been specifically characterised for its role in ipsdienol production in *I. paraconfusus* (Huber et al., 2007). Additionally, the enzymes CYP9T2 and CYP9T3, which share 94% amino acid identity with CYP9T1, have

been identified and characterized in *I. pini* (Sandstrom et al., 2006; Keeling et al., 2006; Song et al., 2013) and *I. confusus* (Sandstrom et al., 2008). However, the enantiomeric ratios of ipsdienol produced by these enzymes are still uncertain.

A downstream step in the biosynthesis of ipsenol involves the conversion of ipsdienol to ipsenol (Figure 6), a process observed in nearly all *Ips* species. This hypothesis was initially tested through experiments that used ipsdienol as a precursor for ipsenol production. In these experiments, unlabelled ipsdienol was either topically applied or administered as a vapor to *Ips* species such as *I. paraconfusus* (Hughes, 1974) and *I. pini* (Lu, 1999; Ivarsson et al., 1997) to verify its conversion to ipsenol. In *Ips cembrae*, only the (-)-enantiomer of ipsdienol was utilized for ipsenol synthesis, indicating a high degree of chiral selectivity (Renwick & Dickens, 1979). Furthermore, deuterium-labelled ipsdienol was converted to labelled ipsenol in *I. paraconfusus* (Fish et al., 1979).

The precise mechanism of this conversion was later elucidated, involving the oxidation of ipsdienol to the corresponding ketone, ipsdienone, followed by hydrogenation to ipsenone, and subsequent dehydrogenation to ipsenol (Fish et al., 1984; Byers, 2012). The enzyme *ipsdienol dehydrogenase* (IDOLDH) catalyzes the dehydrogenation of ipsdienol to ipsdienone. This enzyme has been functionally characterized in *I. pini* (Figueroa-Teran et al., 2012) and specifically converts the (4*R*) -(-)-ipsdienol enantiomer to ipsdienone, without reacting with (4*S*) -(+)-ipsdienol (Figueroa-Teran et al., 2016). This enantiomeric specificity likely influences the varying ratios of (4*R*) -(−)- and (4*S*) -(+)-ipsdienol in different *Ips* species and even within different populations of the same species (Sandstrom et al., 2008).

Moreover, the same enzyme, IDOLDH, or a homologous enzyme, catalyzes the terminal enantioselective hydrogenation of ipsenone to form (4*S*) -(−)-ipsenol (Figueroa-Teran et al., 2012; Figueroa-Teran et al., 2016). The final step in ipsenol biosynthesis, which involves the conversion of ipsdienone to ipsenone by reducing a carbon-carbon double bond, is catalyzed by the enzyme *ipsdienone reductase*

(IDONER). This enzyme was recently identified and functionally characterized in the gut of *I. confusus* (Fisher et al., 2021). The substrate kinetics and enantioselectivity of IDOLDH and IDONER, which catalyze the terminal conversion of ipsdienol to ipsenol, play a key role in regulating the variability of ipsenol production. However, the regulation of these enzymes' functions remains poorly understood, and further research is needed to unravel the complexity of their roles.

1.4.5. Biosynthesis of 2-methyl-3-buten-2-ol.

The highly volatile hemiterpene 2-methyl-3-buten-2-ol is the main component of the pheromone produced by *I. typographus*, occurring alongside *cis*-verbenol in a 10:1 ratio. For a long time, the biosynthesis of 2-methyl-3-buten-2-ol in the insect was unknown. The first evidence for the *de novo* origin of 2-methyl-3-buten-2-ol in *I. typographus* was provided by Lanne et al. (1989), who demonstrated the incorporation of radioactive carbon-14-labeled mevalonate into the structure of this molecule when injected into male beetles.

1.4.6. Biosynthesis of *cis/trans*-verbenol.

Many *Ips* species use the cyclic hydroxylated monoterpene (*S*)-*cis*-verbenol (Figure 7) as a key component of their aggregation pheromone (Vanderwel & Oehlschlager, 1984). However, neither *cis*-verbenol nor its isomer, *trans*-verbenol, is synthesized *de novo* within the beetle's body. Instead, these bark beetles sequester the precursor *α*-pinene from their host conifers and enzymatically introduce the hydroxyl group using cytochrome P450 enzymes, which function in oxidoreduction processes (Renwick et al., 1976; Figure 7).

The hydroxylation of terpene hydrocarbons by bark beetles is recognized as a detoxification mechanism for otherwise toxic compounds, and pheromone production in these beetles may have evolved as a byproduct of this detoxification process (Chiu et al., 2019a; Blomquist et al., 2021).

In *Ips* species, the production of behaviorally active *cis*-verbenol or male-specific *trans*-verbenol depends on the enantiomeric composition of *α*-pinene. A labelling study

demonstrated that *I. paraconfusus* males produce *cis*-verbenol from the (−)-enantiomer of *α*-pinene and *trans*-verbenol from the (+)-enantiomer (Renwick et al., 1976). This enantiomer-specific production was later confirmed in *I. typographus* (Klimetzek & Francke, 1980; Lindström et al., 1989).

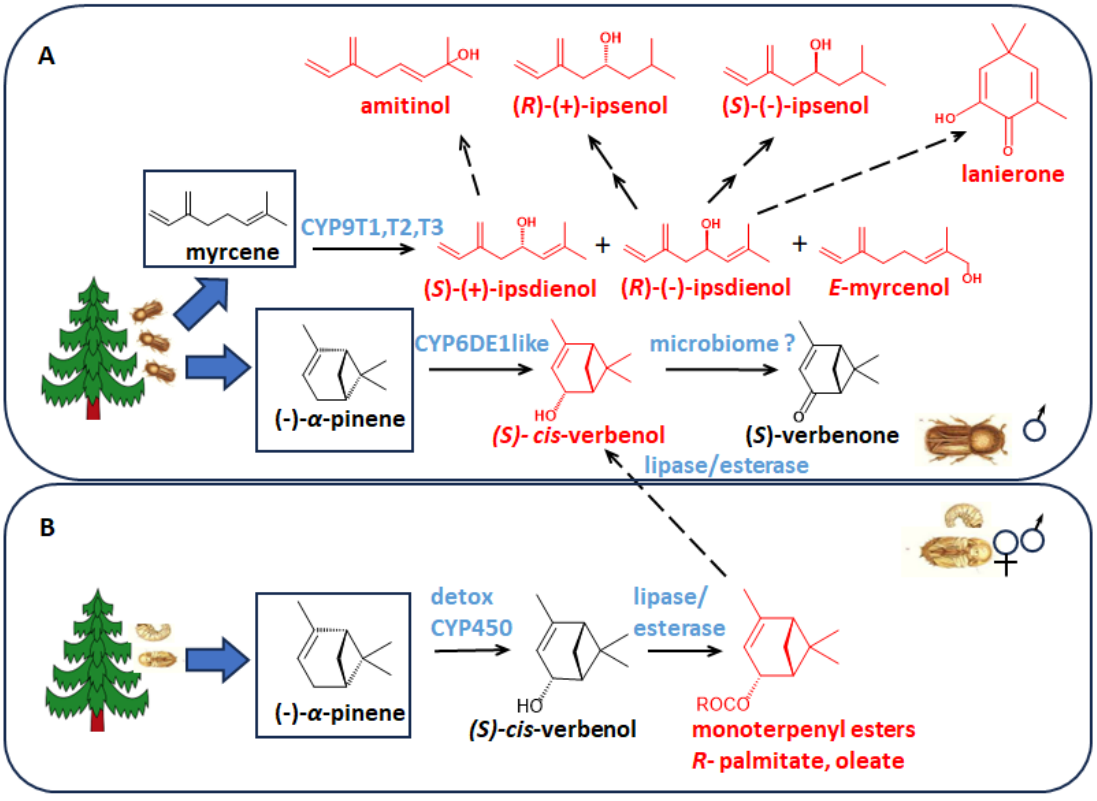

Figure 7:*The hypothesized biosynthetic origin of verbenol storage in bark beetles.*

Biosynthetic pathways of pheromone compounds via the hydroxylation of α- pinene and myrcene sequestered from the host tree. The formation and hydrolysis of verbenyl fatty acid esters as putative pheromone cis-verbenol precursors (Source: Modified from Ramakrishnan et al., 2022a).

Another theory proposed that the symbiotic intestinal microbiome might be involved in *cis*-verbenol production, given its role in monoterpene detoxification. However, this theory was dismissed when antibiotic treatment did not impede the bark beetle's ability to convert host-derived *α*-pinene to verbenol (Byers & Woods, 1981), and later research confirmed the beetles' own enzymatic system was responsible for verbenol synthesis.

The hydroxylation of *α*-pinene is catalyzed by the cytochrome P450 enzyme family, which is known for its broad substrate specificity. This enzyme family plays a key role in various oxidative reactions in bark beetle metabolism, including the detoxification of toxic host terpenes (Qiu et al., 2012; Chiu et al., 2019a). Both pheromone biosynthesis and detoxification processes occur in the bark beetles' gut, complicating the identification of specific enzymes involved in pheromone biosynthesis. Genes encoding these CYP450 enzymes have been identified in the guts of *I. hauseri* (Fang et al., 2021), as well as in other bark beetle species (Chiu et al., 2019a, 2019b). The functions and significance of these genes have been extensively reviewed in the context of bark beetle biology (Huber et al., 2007; Fang et al., 2021; Blomquist et al., 2021).

1.4.7. Verbenyl fatty acid esters as putative pheromone precursors.

After analyzing extracts from bark beetle bodies by GC-MS, large amounts of high molecular weight compounds with mass spectra similar to monoterpenes were detected and later identified as monoterpenyl fatty acid esters (Chiu et al., 2018). The highest concentrations of these esters were found in the fat bodies of young, pre-sclerotized beetles of both sexes that had fed on trees before emerging.

In adult *Ips* bark beetles, these compounds were specifically found in males. Notably, the content of *cis*-verbenol fatty acid esters decreased in males who were actively producing pheromones.

1.4.8. Biosynthesis of verbenone as anti-attractant terminating the attack.

Verbenone is a ketone derived from the oxidation of verbenol and acts as an anti-attractant for many bark beetle species (Frühbrodt et al., 2024). However, verbenone is not classified as a pheromone and typically co-occurs with *cis*-verbenol (Figure 7). The content of verbenone increases during the later developmental stages of bark beetles, particularly at the end of the attack phase, when the host tree is heavily colonized by fungi, nutrient-depleted, and decomposing.

Several studies have shown that bark beetles' gut microbiota including fungi, yeast, and bacteria along with external symbionts, can convert verbenol to verbenone (Hunt & Borden, 1990; Birgersson et al., 1984; Schlyter et al., 1987). Since this type of oxidation is common among microbes, this conversion alone cannot be considered definitive proof of a specific source for verbenone. Moreover, no bark beetle enzyme has yet been identified for this specific function.

1.4.9. Endo- and exosymbiotic microbiome involvement in *Ips* bark beetle pheromone production.

As explained above, bark beetle pheromone compounds are either synthesized de novo within the bark beetle's body or derived from tree precursors that are converted by beetle enzymes (Blomquist et al., 2010; Lanne et al., 1989; Renwick et al., 1976). An intriguing aspect of this system is the involvement of symbiotic organisms and microbes in the complex communication among bark beetles (Brand et al., 1975; Chakraborty et al., 2020). Symbiotic gut microbes may play a direct or indirect role in pheromone production, as demonstrated in male *I. paraconfusus*, where the ingestion of antibiotics inhibited the production of their pheromones, ipsenol and ipsdienol (Byers & Wood, 1981).

Several labelling experiments have shown that bark beetle-associated gut microbiomes can produce bark beetle pheromones (Brand et al., 1975; Brand et al., 1976; Byers & Wood, 1981). Recent findings reveal that external fungi associated with bark beetles, such as *Grosmannia penicillata* and *Endoconidiophora polonica*, can synthesize specific pheromone compounds like 2-methyl-3-buten-2-ol (Zhao et al., 2015) and brevicomins (Zhao et al., 2019). Additionally, the volatile compounds produced by ophiostomatoid fungi contain mixtures whose roles in bark beetle communication are not entirely understood, but these compounds significantly influence bark beetle behavior (Kandasamy et al., 2019; Kandasamy et al., 2023; Moliterno et al., 2023). The production of pheromone-like compounds by these fungi may enhance their role in facilitating bark beetle colonization of host trees (Jirošová et al., 2022).

1.5 Juvenile hormone regulation in bark beetles.

Hormonal regulation plays a crucial role in many morphological and behavioral changes in the class Insecta (Smykal et al., 2014). Specifically, morphological changes such as body development, reproduction, parental care, mating behavior, moulting, growth, and diapause are all hormonally regulated (Jindra et al., 2013). The two primary classes of insect hormones are ecdysteroids and juvenile hormones (Miyakawa et al., 2018). In the context of pheromone biosynthesis in Coleoptera, juvenile hormone III (JH III) is the most extensively studied (Tillman et al., 1998; Keeling et al., 2016). The main function of these hormones is to maintain juvenile characteristics and prevent premature metamorphosis (Goodman and Cusson, 2012).

JH III is synthesized in the exocrine gland known as the corpus allatum and is transported through the hemolymph to its target receptors via binding proteins (Jindra and Bittova, 2020). This hormone has been widely used to study various gene families involved in insect growth, metamorphosis, and social behavior (Riddiford et al., 2001; Trumbo, 2018). Insect larvae initially contain high levels of JH III, which are subsequently reduced as the larvae undergo metamorphosis into pupae (Treiblmayr et al., 2006).

During the pre-metamorphic stages, JH III has been studied for its influence on the development of larval muscles and the prothoracic glands that produce ecdysteroids. It also plays a role in restructuring gut development, fat body, and epidermis in various insect species (Riddiford, 2012; Jindra et al., 2013). In adult insects, JH III influences multiple aspects, including pheromone production (Tillman et al., 2004), social behavior (Trumbo, 2018), caste determination (Cristino et al., 2006), aggression and display (Emlen et al., 2006), migration (Zhu et al., 2009), and neuronal remodelling (Leinwand and Scott, 2021).

In bark beetles, the effects of juvenile hormone III (JH III) have primarily been studied in relation to the induction of pheromone biosynthesis. Many pheromone compounds, such as ipsenol and ipsdienol, which are known exclusively from *Ips* species, are

regulated by JH III (Hall et al., 2002). When the bark beetles bore into the host tree, JH III is released from the endocrine gland, initiating a series of hormonal signalling processes that lead to the production of aggregation pheromone components in male beetles.

In controlled laboratory conditions, pheromone biosynthesis induction can be achieved by topically applying JH III to the bark beetle abdomen (Byers and Birgersson, 1990; Ivarsson et al., 1993; Seybold et al., 1995b; Tillman et al., 1998). This method triggers the *de novo* synthesis of pheromone compounds while avoiding potential interference with the metabolic pathways involved in the digestion of ingested phloem tissues. Pheromone induction using JH III has been demonstrated in bark beetles such as *I. pini*, *I. hauseri*, *Dendroctonus ponderosae* (Nardi et al. 2002; Tillman et al. 2004; Fang et al., 2021). However, certain *Ips* species, such as *I. confusus* and *Ips grandicollis*, have been reported to be unresponsive to JH III-induced pheromone induction (Tillman et al., 2004; Bearfield et al., 2009). It is essential to explore the regulation of specific enzymes following the induction of JH III at a molecular level. This can be achieved through RNA biology techniques, such as gene and protein expression analysis, which are the focus of this research.

1.6 Molecular techniques for the discovery of biosynthetic genes.

Molecular research on various bark beetle species (Coleoptera) has so far resulted in 12 genome sequencing studies, with the recently sequenced *I. typographus* genome playing a crucial role in understanding many fundamental mechanisms of the organism (Powell et al., 2021). To further advance molecular pathway research, high-throughput RNA-oriented methodologies with precise analysis are essential (Stark et al., 2019). Genome-annotated RNA and corresponding enzyme analysis enhance molecular studies by enabling targeted research efforts. These approaches have been applied to challenging research areas, such as clinical pathology detection and the development of species-specific biopesticides, yielding important solutions (Ernst et al., 2016; Roy et al., 2017). RNA-based methods have also led to the development of pest control strategies targeting functional genes (Lancaster et al., 2018).

Recent technological advancements have made it possible to obtain whole transcriptomes of model organisms with high-quality data, a feat that was not feasible just a few years ago (Wang et al., 2009). However, selecting the appropriate RNA sequencing (RNA-seq.) method for analyzing differential gene expression (DGE) remains a critical aspect of research (Cloonan et al., 2008). For instance, short-read sequencing library preparation involves numerous steps, increasing the potential for bias, while long-read or direct RNA sequencing library preparation involves fewer steps, but achieving high-quality RNA is often challenging.

The standard RNA-seq. workflow begins with RNA extraction, followed by mRNA enrichment or ribosomal RNA depletion, cDNA synthesis, and the preparation of an adaptor-ligated sequencing library (Figure 8a, Stark et al., 2019). The library is then sequenced to a read depth of several million reads per sample on high-throughput platforms. In Illumina sequencing, individual cDNA molecules are clustered on a flow cell for sequencing by synthesis using 3' blocked labelled nucleotides. During each round of sequencing, the growing DNA strand is imaged to detect which of the four fluorophores has been incorporated, generating reads of 50–500 bp. In Pacific Biosciences sequencing, individual molecules are loaded into a sequencing chip where they bind to a polymerase immobilized at the bottom of a nano well, generating reads of up to 50 kb. In Oxford Nanopore sequencing, individual molecules are attached to motor proteins during adaptor ligation, and the motor protein controls the translocation of the RNA strand through the nanopore, causing changes in current that are processed to generate sequencing reads of 1–10 kb (Figure 8b).

The final steps involve computational analysis, including aligning and/or assembling the sequencing reads to transcriptome and quantifying reads that overlap transcripts, filtering and normalizing between samples, and statistically modelling significant changes in the expression levels of individual genes and/or transcripts between sample groups (Stark et al., 2019).

Choosing the appropriate RNA sequencing methods depends on the specific research requirements (Sparks et al., 2017). Many methods are currently in use, with a particular focus on identifying functional pathway analyses for bark beetle research (Tillman et al., 1998; Fisher et al., 2021).

Gene functional characterization proves the role of encoded enzymes in the pheromone biosynthetic steps:

Upon completing the gene sequencing analysis using the methods mentioned above, it is essential to validate and confirm the functions of the identified key genes. Molecular techniques such as protein engineering, where enzymes are expressed in living cells (e.g., bacteria or insect cells), followed by enzyme assays using specific substrates, can be used to confirm gene functions (Lancaster et al., 2018; Frick et al., 2013). Another approach is RNA *interference* (RNA*i*), which involves silencing the target gene and then examining the resulting protein and its products in living organisms (Joga et al., 2016).

These methods are particularly useful for identifying the functions of biosynthetic genes responsible for producing crucial components of aggregation pheromones, offering a promising strategy for pest management. The practical application of gene silencing will be discussed in the next chapter.

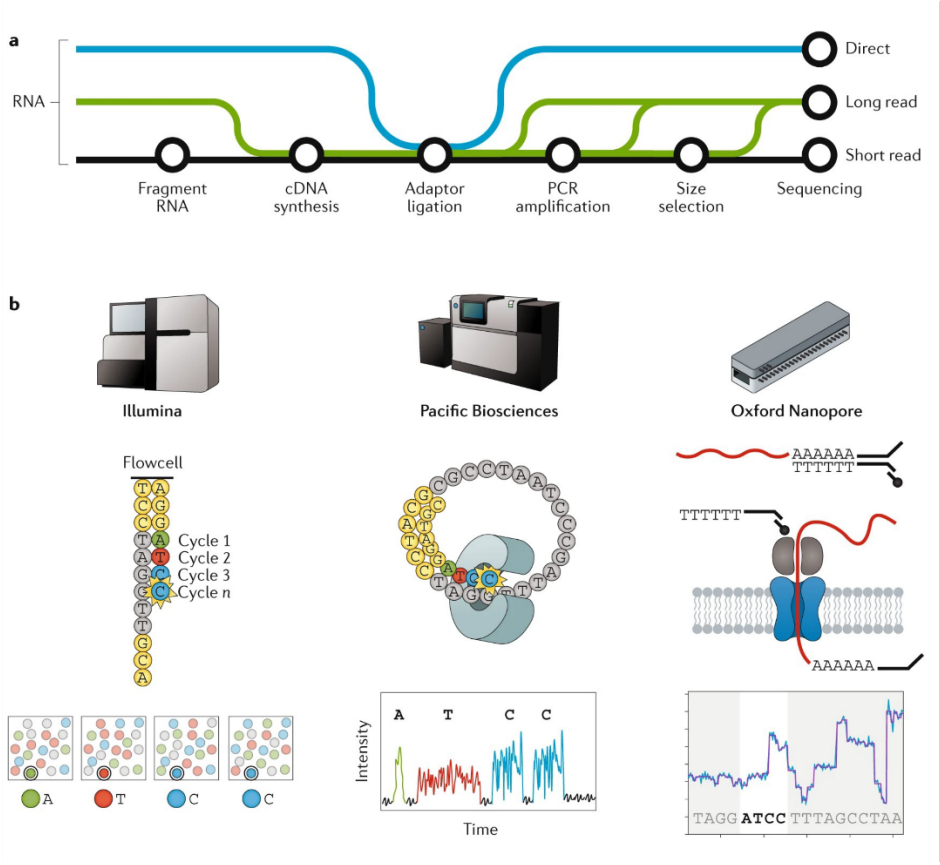

Figure 8: Overview of library preparation methods for different RNA-sequencing methods. Methods are categorized as short-read sequencing (black), long-read cDNA sequencing (green), or long-read direct RNA-seq. (blue). b: Overview is shown of the three main sequencing technologies for RNA-seq. from left to right, Illumina (Fluorophore labelling), Pacific Biosciences (enzyme immobilization chips), and Oxford nanopore (using motor proteins) for respective methods mentioned. (modified from Source: Stark et al., 2019)

1.7 Integrated Pest Management (IPM) of bark beetle.

The impact of bark beetle infestations on conifer forests in Europe, North America, and, more recently, Asia has caused significant ecological and economic crises. Traditional methods for managing bark beetle outbreaks, which remain the most effective so far, include early identification of infested trees (Kautz et al., 2013) and the timely removal or treatment of these trees with insecticides to prevent further spread (Hlásny et al., 2022). However, recent bark beetle outbreaks, driven by climate change and rising temperatures, have led to exponential increases in bark beetle populations (Lubojácký et al., 2022), rendering traditional management methods insufficient (Bentz

et al., 2010). This situation has prompted scientists and foresters to develop new control measures through Integrated Pest Management (IPM) (Lorio et al., 1982). IPM strategies aim to combine multiple approaches to forest protection, incorporating new methods based on scientific findings while maintaining ecological balance and minimizing or eliminating impacts on non-target insect populations, a significant departure from the use of non-selective insecticides (Kogan, 1998).

The use of bark beetle aggregation pheromones is a key component of this approach in forest protection. When the initial findings on aggregation pheromones were reported, there was significant optimism about their potential as baits in pheromone traps to reduce bark beetle population density a strategy known as the "trap and kill" method. Early research suggested that this approach could reduce *I. typographus* infestations by over 30% (Birgersson et al., 1984). However, subsequent studies have shown that the method has limited success (Galko et al., 2016). The primary issue with using pheromones in the trap-and-kill strategy is the spillover effect, where the high concentration of pheromones attracts bark beetles to the traps but also causes them to aggregate and attack nearby trees (Kuhn et al., 2022).

As a result, in current forest management practices, bark beetle pheromones are primarily used for monitoring purposes. This approach allows foresters to track the spatial and temporal distribution of bark beetle activity and to implement appropriate forest management strategies, including early detection and control of infestations, as well as the sanitation of already-infested trees (Šramel et al., 2021). Additionally, pheromone blends can be used in combination with other protective measures, such as trap trees or poisoned trap trees, to enhance their attractiveness (Wermelinger, 2004; Hlásny et al., 2019).

2. HYPOTHESES AND OBJECTIVES.

Hypotheses.

Hypothesis 1: In European spruce bark beetles, ***Ips typographus***, the aggregation pheromone compounds **2-methyl-3-buten-2-ol** and **ipsdienol** are synthesized *de novo* in the key life stages of male beetles' gut via the mevalonate pathway.

Hypothesis 2: The alternative source of ***cis*-verbenol** is its release from stored fatty acid esters in the fat body of *I. typographus*, along with the conversion of *α*-pinene sequestered from spruce trees.

Hypothesis 3: Juvenile hormone III (JH III) induces *de novo* pheromone biosynthesis and influences the detoxification metabolism of *I. typographus*.

Specific objectives 1.

1. To compare the production of pheromone compounds, their precursors, and related metabolites between sexes and across key life stages of *I. typographus*, with a specific focus on feeding males that produce pheromones.

2. To compare the expression of gene transcripts that encode key enzymes catalyzing the identified pheromone metabolite biosynthesis in sexes and across key life stages of *I. typographus*.

3. Based on the findings, to propose the biosynthetic pathways of 2-methyl-3-buten-2-ol, ipsdienol, and *cis*-verbenol, including their genetic underpinnings, and identify *I. typographus*-specific genes involved in these pathways.

Specific objectives 2.

1. To study the regulatory effects of JH III in the biosynthesis of pheromones metabolites and associated precursors in *I. typographus*.

2. To identify genes and enzymes linked to aggregation pheromone biosynthesis and study their regulation after treatment JH III on *I. typographus*.

3. To investigate the impact of JH III on the detoxification mechanism related to the formation of pheromone components in *I. typographus*.

3. SUMMARY OF WORK METHODOLOGY.

To test the above-mentioned objectives, we equipped the following methodologies involving analytical and molecular methods. The detailed methods are explained in this chapter.

3.1 *Ips typographus* rearing conditions in the laboratory.

Picea abies tree logs naturally infested by *I. typographus* (F0 generation) were obtained from plots near Kostelec nad Černými lesy, the Czech Republic. These infested logs left were kept under controlled laboratory conditions (70% humidity, 24°C,16:8 h day/night period, and ventilated plastic containers of 56x39x28 cm/45 l volume) until the wild F0 bark beetle generation emerged.

Subsequently, fresh spruce logs (approximately 50 cm in length) were infested with the collected F0 bark beetles (150 bark beetles per log) and maintained under the same laboratory conditions to establish the F1 generation. Over four weeks of incubation period, bark beetles of key life stages from the F1 generation were collected. The **key life stages** include larvae, pupae, immature beetles (golden-colored teneral beetles with soft cuticles), sclerotized beetles (beetles with dark cuticles and haven't left the breeding log), emerged beetles (beetles emerged from the breeding logs), flying beetles (emerged beetles with 24 hours of flight activity), fed beetles (males and females feeding separately on fresh spruce logs for 24 hours) and mated beetles (male introduced first in a fresh spruce log, followed by female beetle after 24 hours, with both beetles collected from mating chambers after 48 hours). The collected bark beetles were sorted by life stages, sex, and external morphological characteristics (following Schlyter & Cederholm, 1981) (except for larvae and pupae). For hormone **treatment with juvenile hormone III** (JH III), adult emerged beetles were sorted by sex and used for the treatments**.** Acetone (0.5 µl; control) and 10 µg of JH III (0.5 µl of 20 µg/µl JH III in acetone) were applied topically on the abdomen of bark beetles. After treatment, bark beetles were kept under laboratory conditions for 8 hours, then frozen in liquid nitrogen and stored at -80̊ C for further processing. Before analysis, the **guts**

from the bark beetles were dissected (excluding larvae and pupae). In this experiment "**beetle body"** refers to the remaining tissue with the fat bodies after the gut, elytra, and wings were removed.

3.2. Metabolomic analysis.

3.2.1. Gas chromatograph coupled to mass spectrometer (GC-MS) analysis.

Dissected guts from the frozen bark beetles were immediately submerged in 2 ml analytical vials containing cold pentane (for life stages research) or hexane (for JH III research) at a concentration of 10 guts per 100 µl. The bark beetle body was placed in a separate vial with chloroform (10 beetle bodies per 1000 µl of chloroform)

The extracted compounds were separated, identified, and quantified using a GC-MS system, Agilent 7890B (Agilent Technologies, Palo Alto, CA, USA) employing a time-of-flight mass analyzer, Pegasus 4D (LECO, St. Joseph, MI, USA). One microliter of the extract was injected into a cold PTV injector (20°C) in split 10:1 mode. After injection, the inlet was heated to 275 °C at a rate of 8 °C/s. Separation was conducted on an HP-5MS UI capillary column (30 m, 0.25 mm i.d., 0.25 µm film thickness) from Agilent. The GC oven temperature program was set as follows: 40 °C for 1 minute; followed by a ramp of 10°C/min to 210°C, then 20°C/min to 320°C, where it was held for 6 minutes. The total GC run time was 29.5 minutes. Ions (ionization energy of 70eV) were collected in a mass range of 35-500Da at a frequency of 10 Hz.

For the separation and quantification of compounds in bark beetle body extracts, two-dimensional comprehensive gas chromatography was employed using the same instrument. In this case, the injection was performed in split mode (100:1) and the secondary GC and modulator were programmed with temperature offsets of 5°C and 15 °C to the first dimension GC oven, respectively. A BPX-50 column (SGE, Australia, 1.5 m, 0.1 mm i.d, 0.1 µm film thickness) was used for two-dimensional separation. A modulation period of 5 seconds was maintained throughout the analysis. The temperature program was as follows: 40°C for 1.7 minutes ramped at 10 °C/min to

210°C, then at 20 °C/min to 320°C where it was held for 15 minutes. The total GC run time was 39.2 minutes.

Automated spectral deconvolution and peak detection were performed using ChromaTOF software (LECO, St. Joseph, MI, USA). In target compound analysis, the peak areas of unique ions from the mass spectrum were used for quantification. Linear calibration curves were constructed using responses from calibration mixtures diluted from standards. Bark beetle body extracts were specifically targeted and quantified for fatty acid esters, verbenyl oleate and myrtenyl oleate using artificially synthesized external calibration standards (Chiu et al., 2018).

In non-target analysis, a peak alignment tool was used to compare and align all chromatographic signals with a signal-to-noise ratio (S/N) higher than 25 across all gut extract samples. A non-target search in the bark beetle body extracts was performed using S/N=threshold of 50. The data were then cleaned, normalized (using constant raw sum), and analyzed using principal component analysis (PCA) and partial least squares-discriminant analysis (PLS-DA) in SIMCA 15 software (Sartorius Stedim Data Analytics AB, Malmö, Sweden). For the tentative identification of compounds, mass spectra were compared at the National Institute of Standards and Technology (NIST 2017) library. For identity confirmation, retention indices from NIST or retention times of corresponding standards were used.

3.2.2 Ultra-high-performance liquid chromatography-electrospray ionization -high-resolution tandem mass spectrometry (UHPLC-ESI-HRMS/MS) analysis.

We performed two extraction methods to target both polar and non-polar compounds. For non-polar extraction, dissected guts (5 guts per sample) were collected in ethyl acetate (5 µl per gut) and stored at -80°C until analysis. The solvent without the gut tissue was used to extract the non-polar fraction. For polar extraction, the remaining solvent was evaporated using a gentle stream of nitrogen, and the residual tissue was extracted (7 ml per gut) with a methanol/water/acetic acid mixture (70/30/0.5 v/v) containing $^{13}C_2$-myristic acid (1 µg/ml) as an internal standard. The tissue was then sonicated on ice for 5 minutes, disrupted with a pre-chilled Eppendorf

tip, and sonicated for an additional 5 minutes. The samples were then centrifuged at 4000 RPM for 3 minutes and the supernatant was transferred to a new vial with a 100 µl glass insert for further analysis. Both polar and non-polar fractions of the gut extracts were analyzed using UHPLC-HRMS/MS.

The UHPLC-ESI-HRMS/MS analysis was performed on an Ultimate 3000 series RSLC system (Dionex) coupled with a Q-Exactive HF-X mass spectrometer (Thermo Fisher Scientific, Waltham, USA). Water (solvent A) and acetonitrile (solvent B), both containing 0.1% (v/v) formic acid (LC-MS grade, Sigma Aldrich, Steinheim, Germany), were used as the binary solvent system. After injecting 10 µl extract, chromatographic separation was carried out at a constant flow rate of 300 µl/min using an Acclaim C18 column (150 × 2.1mm, 2.2 µm; Dionex, Borgenteich, Germany). The solvent gradients were as follows: 0.5–100% solvent B over 15 minutes, 100% B for 5 minutes, followed by a rapid decrease to 0.5% B over 0.1 minutes, and held at 0.5% B for 5 minutes.

Ionization in the heated electrospray ionization (HESI) source was achieved with a cone voltage of 4.2 kV, a capillary voltage of 35 V, and a capillary temperature of 300°C in positive ion mode, and 3.3 kV, 35 V, and 320°C in negative ion mode. Mass spectra were recorded in both positive and negative ion modes over an m/z range of 80–800. Data-dependent acquisition using the TOP5 routine was employed, with one survey scan at 60,000 mass resolution (FWHM) followed by five Collision-induced dissociation (CID) scans at 7,500 resolutions, collected every 0.3 seconds. CID of quadrupole-selected precursors (0.8 Da mass window) was performed in a collision cell at a normalized collision energy of 30 eV.

For compound identification, pairs of accurate masses of precursor ions and their CID fragments, along with retention time values, were interpreted using XCALIBUR software (Thermo Fisher Scientific, Waltham, USA). Metabolite identification was performed by comparing samples and statistical evaluation using MetaboAnalyst 2.0. The high-resolution LC-MS raw spectra were centroided and converted to mzXML format using MS Convert (ProteoWizard 3.0.18324). Data processing was conducted in

R Studio v1.1.463 using the Bioconductor XCMS package v3.4.2, which provided algorithms for peak detection, deconvolution, alignment, and gap filling.

The resulting peak list was uploaded to MetaboAnalyst 4.0 (Chong et al., 2018), a web-based tool for metabolomics data processing, statistical analysis, and functional interpretation. Missing values were estimated using the k-nearest neighbour method, and data filtering was applied by removing non-informative variables with near-constant values across conditions based on their interquartile ranges (IQR). Data were then auto scaled. Out of 3020 detected mass features, those relevant to Principal Component Analysis (PCA) and Partial Least Square Discriminant Analysis (PLS-DA) were retained for further investigation.

To identify candidate metabolites, individual mass features contributing to class separation were characterized using univariate and multivariate statistical tests, including PLS-DA variable importance, t-tests, and Random Forest analysis. Alongside retention time, accurate mass, and MS/MS spectra, the resulting information was cross-referenced with existing literature and databases. MS/MS spectra were also centroided and imported into the Global Natural Products Social Molecular Networking (GNPS) platform for spectral matching and molecular networking (Wang et al., 2016).

3.3. Differential gene expression (DGE) analysis.

Gut tissue was dissected and placed in an RNA later solution. For each biological sample, 10 guts were pooled, and four technical replicates were prepared for each biological replicate. RNA extraction was completed using the preoptimized protocol (Roy et al., 2017; Sellamuthu et al., 2022). The quality and quantity of the extracted RNA were evaluated using agarose gel and Qubit, respectively. Integrity was determined using the 2100 Bioanalyzer system (Agilent Technologies, Inc). Pure RNA samples (RIN>7) were sent for sequencing to the NoVo gene sequencing company in China. Sequencing was completed with NOVAseq6000 (PE150, 30 million raw reads).

RNA (1 µg) was used for cDNA synthesis using the M-MLV reverse transcriptase kit following the manufacturer's protocol and stored at −20°C for downstream analysis.

3.3.1 RNA sequencing (RNA-seq.) analysis.

Gene expression from the RNA-seq. data was quantified using CLC workbench and standardized via a pre-optimized setting for mapping exon regions exclusively with genome reference (Powell et al., 2021). Later, a TPM algorithm was used to correct the sequence dataset biases and variation in transcript sizes using correct estimates for relative expression levels. Finally, empirical differential gene expression (DGE) analysis was performed using the recommended parameters (Roy et al. 2017). For DGE analysis, a false discovery rate (FDR) corrected p-value of less than 0.05, and a fold change threshold of ±4 was used to determine significance.

Genes that are differentially expressed were annotated using the "cloud blast" with functional features using a "Blasto2GO plug-in" in CLC Genomic Workbench. A nucleotide blast was performed against the arthropod database with an E-value cut-off 1.0E-10. Both annexe and GO slim were used to improve the GO term identification further by crossing the three GO categories (biological process, molecular function, and cellular component) to search for name similarities, GO term, and enzyme relationships within KEGG (Kyoto Encyclopedia of Genes and Genomes) pathway database.

3.3.2 Quantitative-RealTime PCR (qRT-PCR) analysis:

Total RNA was extracted from male gut tissue samples to validate the RNA sequencing data. Twenty genes, including eight genes from the mevalonate pathway, nine genes from CYP450, and three gene esterases were selected for qRT-PCR based on the differential expression level and specific functions. Primers were designed using IDT`s primer design software (www.idtdna.com). cDNA was synthesized using an M-MLV reverse transcriptase kit following the manufacturer's protocol. qRT-PCR was performed using SYBR™ Green PCR master mix (Applied Biosystems, USA) under the following parameters: 95°C for 3 min, 40 cycles of 95°C for 3 s, 60°C for 34 s (Roy et al.

2017). A melting curve was generated to ensure single-product amplification and eliminate the possibility of primer dimers and nonspecific amplicons. The relative expression levels of the target genes were calculated using the $2^{-\Delta\Delta Ct}$ method, with the housekeeping genes ribosomal proteins *RbPL6* and *RbPS18* used as references for normalization (Ramakrishnan et al., 2022b). Four biological replicates were analyzed, each with four technical replicates.

3.4. Differential protein expression (DPE) analysis.

Guts from frozen bark beetles were dissected under dry ice, and four biological replicates of each treatment were used for protein extraction and analysis. Each biological replicate contained tissue of three individual guts. Protein extraction was followed with the optimized protocol from Cox et al., 2014. The protein extracts were lysed in a cold buffer containing 50 mM Tris-HCl, pH 7.5, 1 mM EDTA, 150 mM NaCl, 1% N-octyl glycoside, and 0.1% sodium deoxycholate. The buffer, along with the protease inhibitor mixture (Roche), was incubated for 15 min on ice. Lysates were cleared by centrifugation, and after precipitation with chloroform/methanol, proteins were resuspended in 6 m urea, 2 m thiourea, 10 mM HEPES, pH 8.0, and proceeded for digestion. The samples were homogenized and lysed by boiling at 95°C for 10 min in 100 mM TEAB (triethylammonium bicarbonate) containing 2% SDC (sodium deoxycholate), 40 mM chloroacetamide, and 10 mM Tris-2-carboxyethyl phosphine. Subsequently, the samples were subjected to sonication using a Bandelin Sonoplus Mini 20, equipped with an MS 1.5 probe (Cox et al., 2014). Obtained proteins were measured for concentration using a standard protein assay kit (Thermo Fisher Scientific, USA) and about 30 µg of protein per sample was used for MS sample preparation.

SP3 beads were used for sample processing. Five µl of SP3 beads were mixed with 30 µg protein in a lysis buffer and made up to 50 µl with TEAB (100 mM). Protein binding was induced by adding ethanol to a final concentration of 60% (vol/vol). The samples were thoroughly mixed and incubated at 24 °C for 5 min. After SP3 was bound to the proteins, the tubes were placed on a magnetic rack, and the remaining unbound

supernatant was discarded. Using 180 µl of 80% ethanol, beads were washed twice. After washing, samples were digested with trypsin (trypsin/protein ratio 1/30) and reconstituted in 100 mM TEAB at 37°C overnight. Digested samples were acidified using trifluoro acetic acid for 1% final concentration. Finally, peptides were desalted using in-house stage tips packed with C18 disks (Empore) (Rappsilber et al., 2007).

3.4.1 NanoLiquid Chromatography (nLC)-MS/MS analysis.

nLC-MS/MS analysis was performed with nano-reversed-phase columns (EASY-Spray column, 50 cm × 75 µm ID, PepMap C18, 2 µm particles, 100 µm pore size). In this analysis, mobile phase buffer A (0.1% formic acid in water) and mobile phase buffer B (acetonitrile and 0.1% formic acid) were used. Samples were loaded in a trap column of C18 PepMap100, 5 µm particle size, 300 µm x 5 mm from Thermo Scientific. About 4 min at 18 µl/min loading buffer with water, 2% acetonitrile, and 0.1% trifluoroacetic acid were used for loading. Peptides were eluted with a mobile phase B gradient of 4–35% over 120 min. The eluted peptide cations were converted into gas-phase ions by electrospray ionization. A Thermo Orbitrap Fusion (Q-OT-qIT, Thermo Scientific) was used for the analysis. Survey scans of peptide precursors from 350–1400 m/z were performed using an Orbitrap at 120 K resolution (200 m/z) with a 5 × 105 ion count target. Tandem MS was isolated at 1,5 using a quadrupole, HCD fragmentation with a normalized collision energy of 30, and rapid scan analysis in the ion trap. The second mass spectral ion count target was set to 104, and the maximum injection time was 35 ms. Precursors with charge states two to six were strictly sampled and the selected precursor and its isotopes were included in the dynamic exclusion duration of 30 s with 10-ppm tolerance. Monoisotopic precursor selection was performed, and the instrument was run in 2 s cycles speed mode (Hebert et al., 2014).

All data were analyzed and quantified using MaxQuant software (version 2.0.2.0) (Cox and Mann, 2008). The FDR was limited to 1% for both full proteins and small peptides. The peptide lengths of the seven amino acids are specified. An MS/MS spectral search was performed using the Andromeda search engine against the *I. typographus* genome

database. The C-termini of Arg and Lys were set for enzyme specificity, allowing the cleavage of proline bonds with a maximum of two missed cleavages. Cysteine dithiomethylation was selected as the fixed modification. Various modifications were considered with N- N-terminal protein acetylation and methionine oxidation. Matches between the run features from MaxQuant were used to transfer the identified peaks to other LC-MS/MS systems. Runs based on masses and retention times (with a maximum deviation of 0.7 min) were also considered for quantification. A label-free MaxQuant algorithm was used for quantification (Cox et al., 2014). Data analysis was performed using Perseus 1.6.15.0 (Tyanova et al., 2016).

3.5 Statistics.

Statistical analysis of quantified data was performed using a one-way analysis of variance (ANOVA) and Fisher (LSD) test with a 95% confidence interval in the XLSTAT-Student 2020 licensed version and TIBCO Statistics (USA, 2021). UHPLC-HRMS-MS data analysis was performed using MetaboAnalyst 4.0. G -MS data were cleaned for residua of analysis, normalized (constant raw sum), and evaluated using principal component analysis (PCA) in the SIMCA 17 software (Sartorius Stedim Data Analytics AB, Malmö, Sweden). The data from transcriptome and proteome was normalized using CLC workbench 21.0.5 (QIAGEN Aarhus, Denmark) and MaxQuant software (version 2.0.2.0), respectively, for significant data ($P< 0.05$).

4. RESULT SYNTHESIS.

This synthesis consolidates data from four key articles to elucidate the biochemical mechanisms behind pheromone production in the European spruce bark beetle, *I. typographus*. The research focuses on the biosynthesis of aggregation pheromones 2-methyl-3-buten-2-ol, ipsdienol, and *cis*-verbenol exploring their biosynthesis, genetic and hormonal regulation, and variation across life stages and sexes. It also examines the role of juvenile hormone III (JH III) in these processes, the research provides a comprehensive overview of how *I. typographus* produces and manages its aggregation signals. The subsequent sections will present detailed results and findings from these studies, addressing the objectives.

4.1. Publication 1: Metabolomics and transcriptomics of pheromone biosynthesis in an aggressive forest pest *Ips typographus*.

Ramakrishnan R., Hradecký J., Roy A., Kalinová B., Mendezes C. R., Synek J., Bláha J., Svatoš A., Jirošová A. 2022a. Insect Biochemistry and Molecular Biology, 2022a. https://doi.org/10.1016/j.ibmb.2021.103680*

Summary of this article:

This article investigates the biosynthesis of aggregation pheromones in key life stages of *I. typographus* (Figure 3, Chapter 1.3.) by analyzing changes in pheromone-related metabolite production and the underlying genetic mechanisms, addressing objective 1 outlined earlier (Chapter 2).

We conducted metabolomic and transcriptomic analyses on gut tissues from various life stages of *I. typographus*, with a particular focus on pheromone-producing feeding males. Comparative analyses were performed between the key life stages, as well as between sexes, to identify upregulated metabolites and gene transcripts related to pheromone biosynthesis. Additionally, similar analyses were conducted on extracts from body tissues (including fat bodies), to target verbenyl fatty acid esters, conjugates of *cis*-verbenol, and other pheromone-related metabolites and genes.

The aggregation pheromones 2-methyl-3-buten-2-ol, *cis*-verbenol, and ipsdienol were identified and quantified across key stages of adult males, with peak production of 2-methyl-3-buten-2-ol and *cis*-verbenol observed in males while feeding on logs and ipsdienol in the mating chamber. Notably, *cis*-verbenol was also detected in both male and female beetle guts during immature life stages (golden beetles that had not yet emerged from the bark). This finding suggests that in immature bark beetles, *cis*-verbenol is a detoxification product of pinene consumed in wood and probably has not communication function.

Furthermore, verbenyl fatty acid esters were identified in the fat bodies of both sexes during these immature life stages, but in adult beetles, they were found exclusively in males. In feeding males, who release pheromones, the content of these esters slightly decreased, suggesting that these conjugates serve as storage molecules from which adult males release *cis*-verbenol during the calling phase. This represents a new concept in *Ips* species.

DGE analysis identified candidate genes potentially involved in the biosynthesis of these pheromones and related compounds. Notably, genes in the mevalonate pathway, proposed to be involved in the synthesis of 2-methyl-3-buten-2-ol and ipsdienol (Figure 6, Chapter 1.4.3.), were highly expressed exclusively in the guts of fed males, along with the insect-specific isoprenyl-di-phosphate synthase gene Ityp09271, which is involved in the final step of 2-methyl-3-buten-2-ol biosynthesis. Additionally, the putative cytochrome P450 gene, CYP6DE1-like, linked to *cis/trans*-verbenol synthesis, was also expressed in the guts of fed males (Figure 7, Chapter 1.4.7.). Additionally, the esterase gene (Ityp11977), which may regulate verbenyl fatty acid synthesis, was identified in the immature male gut (Figure 7, Chapter 1.4.7.).

The study provided evidence that in *I. typographus* 2-methyl-3-buten-2-ol and ipsdienol are synthesized *de novo* in male beetles via the mevalonate pathway, with terminal modification steps (Figure 6, Chapter 1.4.3.) c*is*-Verbenol, with pheromone communication function, is synthesized through the hydroxylation of pinene by adult

males and, potentially, by the release from verbenyl fatty acid esters when needed to support pheromone production. (Figure 7, Chapter 1.4.7.)

4.1.1. Comparative analysis of metabolites profiles and contents in various life stages of *I. typographus.*

4.1.1.1. Non-targeted and targeted GC-MS analysis of *I. typographus* gut extracts.

Highlights: *The non-targeted analysis showed separation of the fed male beetles (due to 2-methyl-3-buten-2-ol) and immature male beetles (due to* cis*-verbenol and myrtenol) and the targeted analysis revealed that 2-methyl-3-buten-2-ol and* cis*-verbenol are produced by fed male beetles, while* cis*-verbenol was also detected in both sexes of immature beetles. Ipsdienol was found only in mated males.*

To identify key pheromone components, gut extracts from various life stages of *I. typographus* were analyzed using GC-MS, followed by principal component analysis (PCA) with a relative score plot. The PCA score plot accounted for over 75% of the variability in the dataset and showed a clear separation between fed male guts and immature male gut extracts. The separation of fed males was primarily influenced by 2-methyl-3-buten-2-ol, while *cis*-verbenol and myrtenol were the most significant variables for immature males. Other life stages did not form distinct clusters (Figure 9).

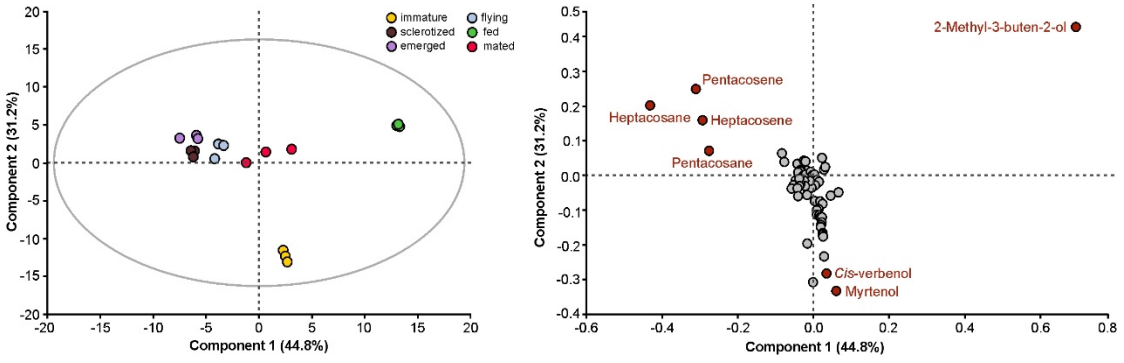

Figure 9: GC-MS Metabolomics: PCA of Gut Extracts from I. typographus *male beetles across key life stages.*
The PCA plot on the left depicts the distribution of male gut extracts across key life stages, while the plot on the right identifies the corresponding compounds within the respective quadrants from the analysis.

Further quantification of the active pheromone compounds 2-methyl-3-buten-2-ol, *cis*-verbenol, ipsdienol, and verbenone was conducted in guts of the key life-stage, with

concentrations ranging from trace amounts to a maximum of 250 ng/gut (Figure 10). As expected, the aggregation pheromone 2-methyl-3-buten-2-ol was detected only in fed male beetles with the highest concentration of 238 ng/gut. A trace amounts (5-6 ng/gut) of 2-methyl-3-buten-2-ol were found in males after emerging and in females after mating. The other aggregation pheromone, *cis*-verbenol, was quantified at 16-23 ng/gut in immature beetles of both sexes. After the sclerotized stage, *cis*-verbenol disappeared and then reappeared in later stages exclusively in males, showing high levels during flying, feeding, and mating. A similar pattern was observed for the anti-attractant verbenone (the ketone of verbenol), although its levels were lower (<5 ng/gut). Ipsdienol, typically found in mated beetles, was detected in trace amounts (<1 ng/gut) in mated male guts (Figure 10).

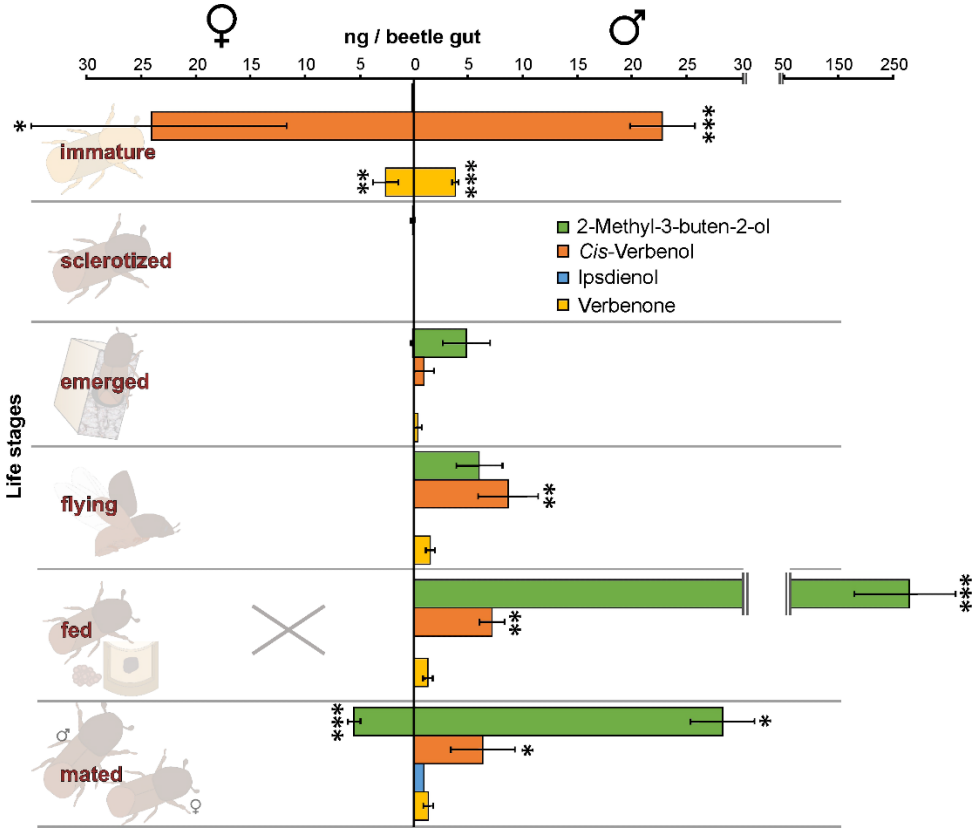

Figure 10: GC-MS quantification of active pheromone compounds.
*Data was analyzed from gut tissue of I. typographus different life stages. Statistics: One-way ANOVA with Fisher (LSD) test with a 95% confidence interval with the Sclerotized stage as a control group. *** represents P<0.001, ** represents P<0.01, * represents P<0.05. X in Fig. indicates that the stage was not analyzed.*

4.1.1.2. Non-targeted and targeted GC-MS analysis of extracts from *I. typographus* body corps containing fat body.

Highlights: *The non-targeted GC-MS analysis showed separation of the larvae stage (due to ethyl hexadecanoate. The separation of immature beetles and pupae was due to the fatty acid esters, verbenyl and myrtenyl oleates, and further quantification revealed that verbenyl oleates remained exclusively in adult males. The balance between verbenyl oleate as a conjugate and* cis*-verbenol across male life stages suggests that in fed males, the verbenyl oleate breaks into* cis*-verbenol and methyl oleate.*

The metabolomic profiles of the extracts of the bark beetle corpses (containing fat bodies) from different life stages, including larvae and pupae, were compared. We aimed to compare semi-polar compounds, present mainly in the fat body, with relevancy to pheromone biosynthesis. The PCA plot shows a distinct separation of larvae from other life stages (Figure 11). This separation was associated with ethyl hexadecanoate. The pupae and immature beetles were clustered together. The cluster corresponded with monoterpenyl fatty acid esters, especially with verbenyl and myrtenyl oleate (Figure 11).

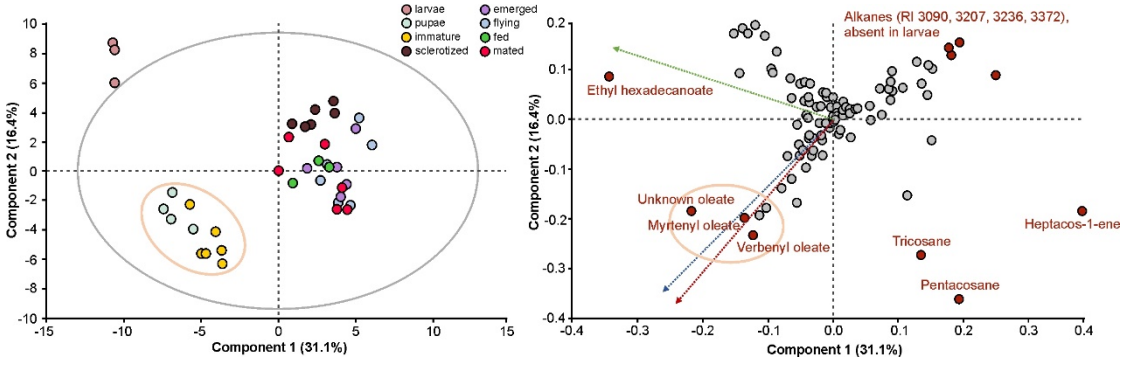

Figure 11: GC-MS Metabolomics Analysis: PCA of bark beetle body extracts across I. typographus *key life stages.*
The PCA plot on the left illustrates the distribution of various life stages of bark beetles, while the plot on the right highlights the corresponding compounds. The analysis was conducted on tissue samples from the male beetle body.

We quantified verbenyl oleate and myrtenyl oleate, as representatives of fatty acid esters in the beetle body from key life stages, including larvae and pupae (Figure 12). Verbenyl oleate and myrtenyl oleate were quantified in trace amounts (app. 50 ng/mg of the body) in larvae and up to 475 ng/mg pupae. Verbenyl oleate was quantified up

to 1604 ng/mg of the male beetle body and 1424 ng/mg of the female beetle body of immature life stage. Later, verbenyl oleate was found only in the body of mature male life stages (sclerotized, emerged, flying, fed, and mated), ranging 50-200 ng/mg of beetle body. Furthermore, myrtenyl oleate was also quantified in larvae (17 ng/mg of the body) and pupae (511 ng/mg of the body). In the immature stage, myrtenyl oleate levels were higher in males (519 ng/mg of the body) than in females (221 ng/mg of the body). Later, myrtenyl oleate could not be found in certain mature stages of both sexes (sclerotized, emerged, and flying). Interestingly, myrtenyl oleate reappeared in a fed and mated male beetle body with traces amount (25-26 ng/mg of the body). (Figure 12).

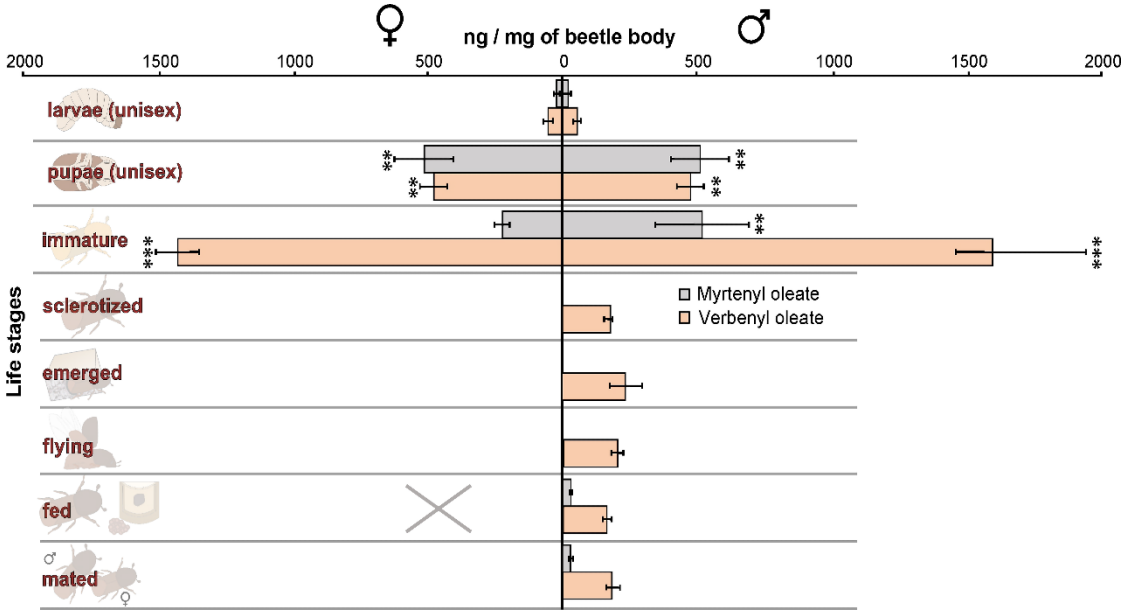

Figure 12: GC-MS quantification of myrtenyl and verbenyl oleate in the body of I. typographus *from the beetle body of* I. typographus *different life stages male and female beetles at different life stages. Statistics: One-way ANOVA with Fisher (LSD) test with 95% confidence interval with Sclerotized stage as a control group. *** represents P<0.001, ** represents P<0.01, * represents P<0.05. X in Fig. indicates that the stage was not analyzed.*

The relative abundance of verbenyl oleate, methyl oleate (proposed byproduct from verbenyl oleate), and *cis*-verbenol among different life stages of male beetle extract from the gut and beetle body are presented as a percentage. The results showed a correlation between the quantity of the three compounds with a change across the key life stages. The immature stage showed high levels of verbenyl oleate and *cis*-

verbenol, with less than 10% of methyl oleate. Importantly, in the fed beetles, where *cis*-verbenol pheromone is produced, the percentage of vebenyl oleate as a putative precursor decreased (<5% abundance), and the percentage of methyl oleate and *cis*-verbenol as putative products increased. A similar pattern was also found in mated beetles (Figure 13).

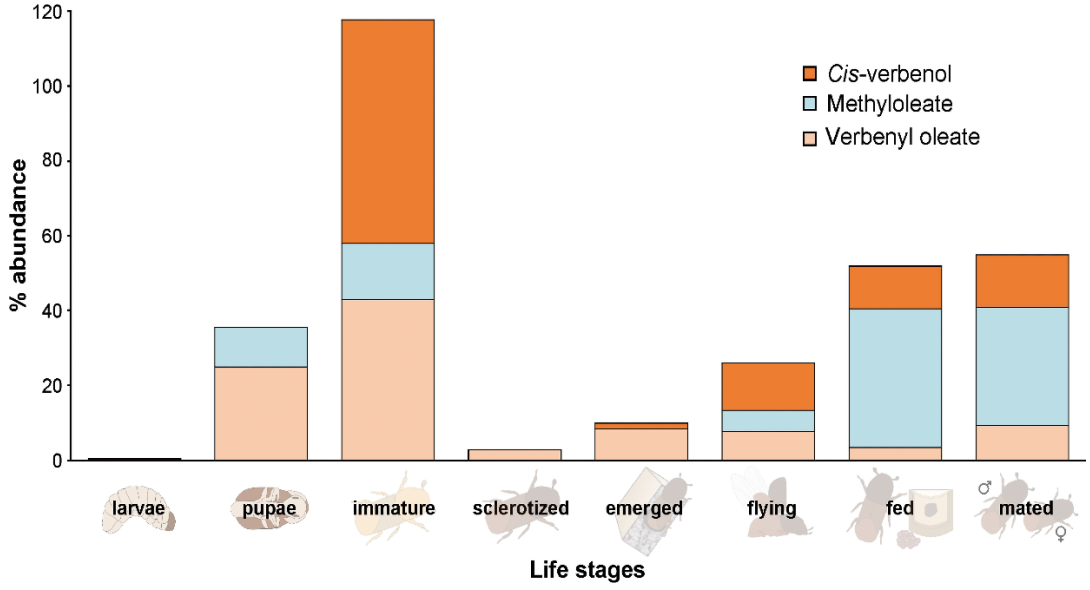

Figure 13: Relative abundance of cis-verbenol and relevant oleates from I. typographus *gut.*

Percentage abundance was calculated as a ratio of quantified compounds at individual life stages to the sum of quantified compounds at key life stages of male beetles, obtained from GC-MS quantification data.

4.1.1.3. Targeted HPLC-MSMS analysis of extracts from *I. typographus* guts.

Highlights: *In gut extracts, upstream precursors of the mevalonate pathway (mevalonate-5-phosphate, isopentenyl diphosphate, and dimethylallyl diphosphate) were found, likely involved in the biosynthesis of 2-methyl-3-buten-2-ol and ipsdienol.*

While tracing potential precursors of 2-methyl-3-buten-2-ol, we checked for isopentenyl diphosphate (IPP) and /or dimethylallyl diphosphate (DMAPP). It was detected as a minor peak with Rt 4.73 min at m/z 244.99760, and corresponding molecular formulae $C_5H_{11}O_7P_2$ (M-H)- and delta -0.704 mmu were calculated. CID spectra and Rt correspond to an authentic standard, and the CID spectrum is characterized by intense m/z 78.9578 PO3- ion. Under the chromatographic conditions, we could not separate a mixture of authentic IPP and DMAPP standards,

and the peak is assigned as a mixture of both compounds. However, peak intensity was too low to obtain reliable integration data, and other isobaric compounds were co-eluted in this retention time window contaminating the mass spectra. However, upstream IPP/DMAPP intermediate, mevalonate-5-phosphate (Rt 9.2 min, m/z 227.0323 $C_6H_{12}PO_7$ delta -0.312 mmu; with MS/MS fragments at m/z 78.9581 (PO_3) and 98.9687 (H_2PO_4) characteristic for monophosphate), was more abundant, providing better data. Mevalonate-5-phosphate abundance peaks were found in the male gut. The compound appeared with high abundance in the flying stage and its abundance reduced in the fed stage. Later, mevalonate-5-phosphate reappeared in the mated stage. A similar pattern was observed in the female with a low significance (Figure 14). The UHPLC/HR MS-MS data also detected the verbenyl and myrtenyl oleates as minor peaks at m/z 417.37227, $C_{28}H_{49}O_2$ and corresponding diglycosides detected at m/z 445.20761. Due to the unavailability of authentic standards, we couldn't quantify them. However, the presence of peaks and CID spectra indicate that these compounds are likely oxidative products of *α*-pinene like myrtenol and *cis/trans* verbenol.

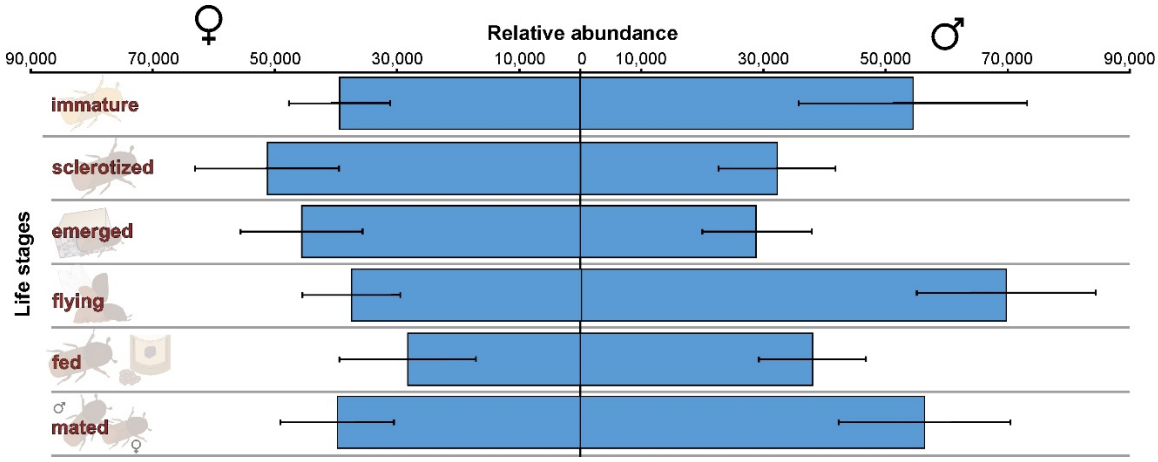

Figure 14: Intensity of putatively identified mevalonate-5-phoshate, m/z 227.0323 from I. typographus *gut tissues at key life stages.*
Gut extracts were analysed using an UPLC-ESI-MS/MS instrument in negative ion mode with TOP 5 scanning with one precursor ion scan and 5 MS/MS scans. Bars represent the standard error of the mean, N = 3

4.1.2. Comparative analysis of gene expressions encoding enzymes that catalyze key pheromone biosynthesis across key life stages of *I. typographus.*

4.1.2.1. Differential gene expression (DGE) analysis from gut tissue of *I. typographus*.

Highlights: *The differentially expressed profiles of genes in the gut of immature males and fed males showed significant differences in many gene families.*

To further evaluate the expression profiles of genes associated with the biosynthesis of key pheromone components 2-methyl-3-buten-2-ol and *cis*-verbenol, we chose the gut tissue from two important stages (immature male and fed male) of the bark beetle for RNA-sequencing analysis. Followed by a validation of the obtained expression pattern using a quantitative Real Time-PCR. Among a total of 23937 annotated genes in the *I. typographus* genome, the expression of 11657 genes were upregulated in the fed male gut, and 7484 genes were upregulated in the immature male gut (shown as a heat map of Publication 1, Ramakrishnan et al., 2022a).

4.1.2.2. Expression analysis of mevalonate pathway genes in *I. typographus* gut.

Highlights: *Mevalonate pathway genes were upregulated in pheromone-producing life stages of adult males. A novel isoprenoid-di-phosphate synthase (IPDS) proposed in the terminal biosynthetic step of* 2-methyl-3-buten-2-ol *was upregulated exclusively in fed male beetle guts. Besides IPDS, another two IPDS (GPPS) were also identified with their relative expression pattern in fed male beetle guts.*

It is known that mevalonate is involved in 2-methyl-3-buten-2-ol synthesis (Lanne et al. 1989); moreover, our UHPLC-HRMS/MS analysis revealed the presence of mevalonate-5-phosphate (a mevalonate pathway intermediate) at key life stages in *I. typographus*. Therefore, we targeted the mevalonate pathway genes (contig numbers from the *I. typographus* genome are given in brackets next to gene names). Interestingly, five of the targeted genes showed upregulated expression in the fed stage; these included genes encoding *isoprenoid-di-phosphate synthase* (IPDS) (Ityp09271), *isopentyl-di-phosphate isomerase* (IPPI) (Ityp04875), *3-hydroxy-3-methyl glutaryl co-enzyme A reductase* (HMG-R) (Ityp17150), *3-hydroxy-3-methyl glutaryl Co-enzyme A synthase* (HMG-S) (Ityp09137), and *phosphomevalonate kinase* (PMK) (Ityp06045) (Figure 15).

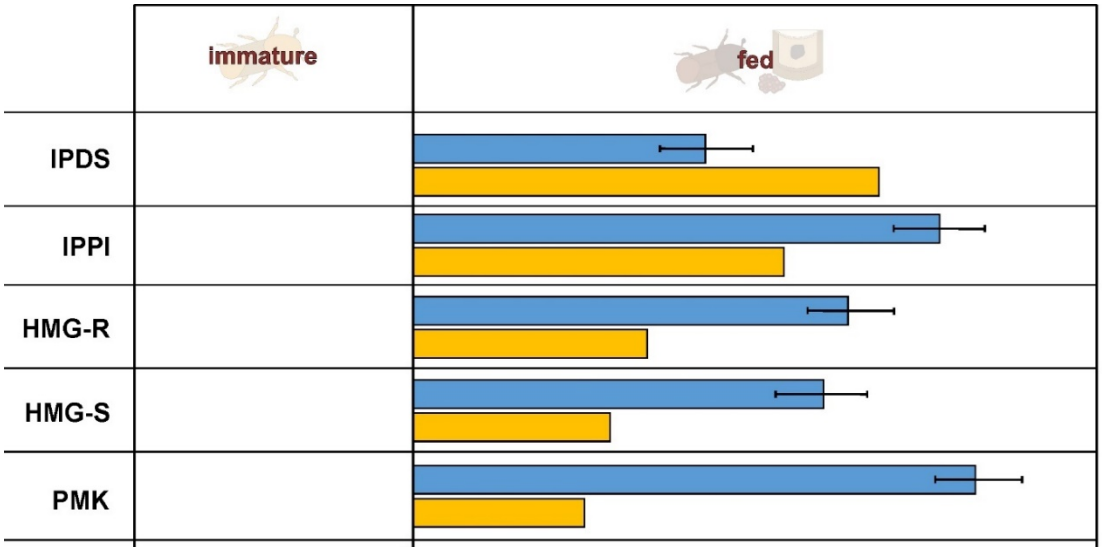

Figure 15: Relative expression of mevalonate pathway gene from I. typographus *gut.*

The expression pattern was determined from RNA-seq. and qRT-PCR data. Tissue: fed male gut vs immature male gut. Yellow: log fold change values from RNA-seq. data. Blue: log fold change values from qRT-PCR data. Error bars indicate standard error.

Further expression analysis using qRT-PCR was performed for the five key mevalonate pathway genes from the gut tissue of *I. typographus* at different life stages (Figure 15). We calculated the relative expression of the genes at five mature male stages (sclerotized, emerged, flying, fed, and mated) with the immature stage used as a reference. Four genes, IPPI (Ityp04875), HMG-R (Ityp17150), HMG-S (Ityp09137), and PMK (Ityp06045), showed similar expression patterns in the emerged, flying, and fed male gut. On the other hand, IPDS (Ityp09271) expression showed a significant upregulation ($p \leq 0.05$) in the fed male gut only. This gene was moderately expressed in the sclerotized, emerged, and flying stages and downregulated in the mated male gut (Figure 16).

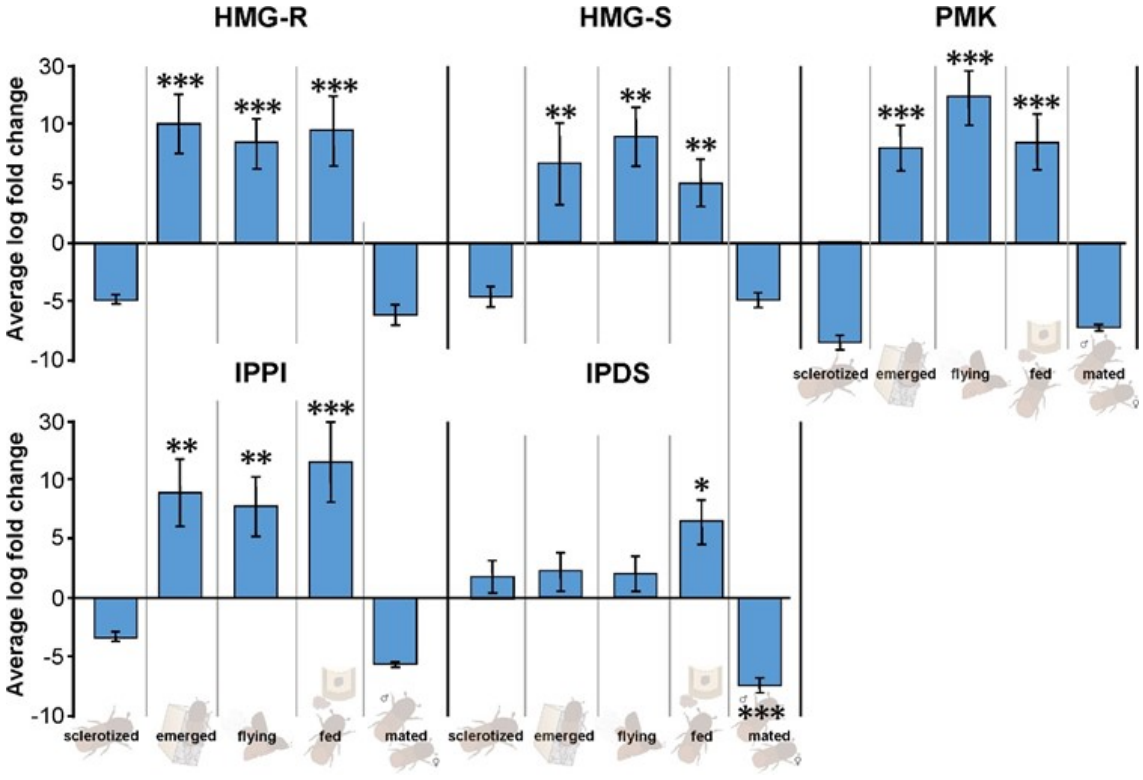

Figure 16: Relative expression of mevalonate pathway genes in I. typographus *life stages.*

*The expression was from male gut tissue determined by qRT-PCR. Statistics: One-way ANOVA with Fisher (LSD) test with a 95% confidence interval with the Sclerotized stage as a control group. *** represents P<0.001, ** represents P<0.01, * represents P<0.05. N=4.*

Along with the identified IPDS gene family (Ityp09271), two isomers of GPP/Myrcene synthase genes Ityp17873, and Ityp17861 also showed moderately upregulated in the fed stage (Figure 17).

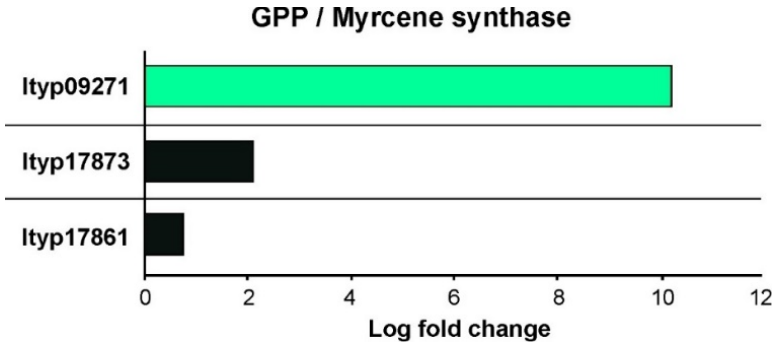

Figure 17: Relative expression of GPP/myrcene synthase from RNA-seq data.
Expression showed in fed male gut compared to immature male gut. Green: Proposed IPDS candidate for 2-methyl-3-buten-2-ol synthesis. Black: isomers proposed for possible geranyl-di-phosphate synthase (GPPS) function.

4.1.2.3. Expression analysis of cytochrome P450 (CYP450) genes in *I. typographus* gut

Highlights: *Nine CYP450 gene candidates were selected for comparative analysis to examine differential expression in the immature male beetle gut compared to the fed male beetle gut. Of these, five candidates were chosen for expression analysis in the mated male gut compared to the sclerotized beetle gut. Two candidates are likely involved in catalyzing* cis/trans-*verbenol production in immature beetles as part of a detoxification process, two may participate in myrcene hydroxylation to ipsdienol, one is implicated in hydrocarbon synthesis, and two are suggested to catalyze the production of pheromone* cis-*verbenol in feeding adult male beetles.*

We focused on the cytochrome P450 (CYP450) gene families, known for their diverse functions, including the biosynthesis of the pheromone compound verbenol and ipsdienol. In the gut tissue of fed and immature males, over 56 CYP450 genes were differentially expressed, 24 genes were upregulated, and 32 genes were downregulated in the fed male gut. A neighbour-joining phylogenetic tree was

constructed based on sequence similarity with a functionally characterized gene from *D. ponderosae*. Sequences were obtained from the NCBI database and analyzed using the MEGA X program to elucidate the evolutionary relationships of CYP450 genes. The phylogenetic tree revealed seven subgroups of identified CYP450 genes (Figure 18A). These clusters included candidates with names such as CYP450-6 like, CYP450-4 like, and CYP450 9e2 like, along with a few uncertain CYP450 genes (Ramakrishnan et al., 2022b).

Potential candidates were chosen based on sequence similarity from functionally known genes from other bark beetle species. The CYP450 candidate Ityp0496 (C1) and Ityp03903 (C2) similar to the *trans*-verbenol synthesizing gene CYP6DE1 (a1-like) and Ityp03140 (C3) and Ityp03230 (C4) similar to the detoxification gene CYP6DE3 (a2-like) from *D. ponderosae* were chosen. The gene candidates Ityp03153 (C5), Ityp03146 (C6), and Ityp01834 (C7) showed similarity to CYP-9T1/T2, involved in ipsdienol synthesis in other *Ips* species. The gene candidates Ityp04142 (C8) and Ityp04140 (C9) were chosen for similarity to CYP4G55/56, in hydrocarbon synthesis from *Ips* species.

In the fed male beetle gut, C1 and C2 were moderately upregulated, whereas C3 and C4 were downregulated (Figure 18B). Expression analysis in the mated male gut, compared with the sclerotized beetle gut revealed upregulated expression of C5 and C7 in the mated male gut, a life stage where ipsdienol pheromone synthesis is expected. C8 showed upregulated expression in the sclerotized stage, the life stage during which long-chain hydrocarbons were identified (Figure 18C). The expression pattern confirms the proposed candidates for relevant functions in certain life stages of *I. typographus*.

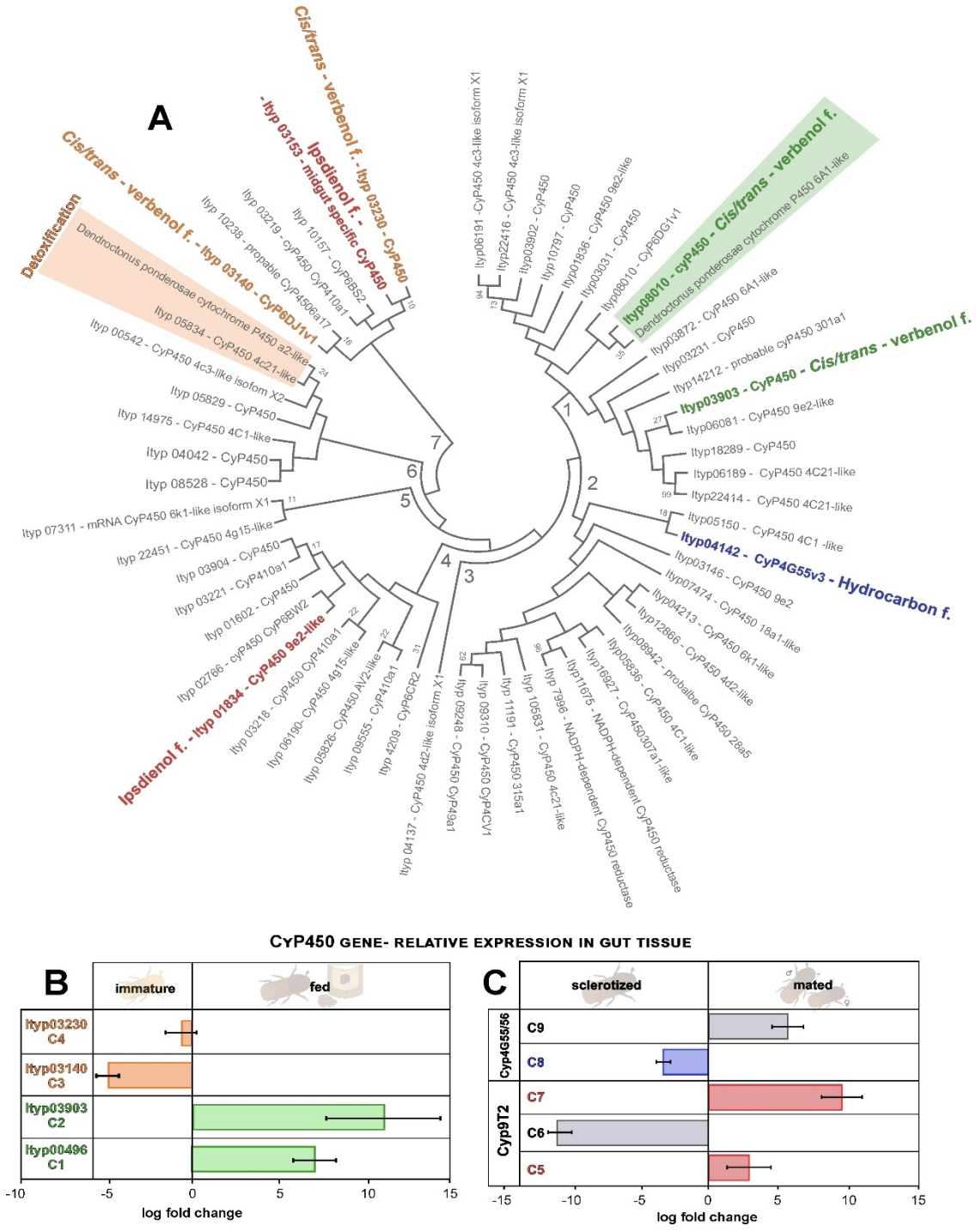

Figure 18: Phylogenetic clustering CYP450 from I. typographus *gut.*
Mega X, bootstrap 100 times. A) The highlighted region indicates genes with known functions. B & C: Relative expression of genes of the CYP450 family, as determined by qRT-PCR. C1-C4 (functionally proposed for cis/trans verbenol synthesis): Tissues compared: Immature male gut vs fed male gut. C5-C7: A sequence like CYP9T2 (functionally known for ipsdienol synthesis from myrcene). C8 and C9: A sequence like CYP4G55/56 (functionally known for hydrocarbon synthesis). Tissues compared: mated male gut vs sclerotized beetle gut.

4.1.2.4. Expression analysis of esterase/lipase potentially involved in verbenyl fatty acid estres formation in *I. typographus* gut.

Highlights: *Through comparative analysis of overexpressed genes in the immature male gut versus the fed male gut, three esterases were selected. One esterase is suggested to function in the esterification of verbenyl fatty acid esters in immature male beetle guts, while another is likely involved in their hydrolysis in fed male beetle guts.*

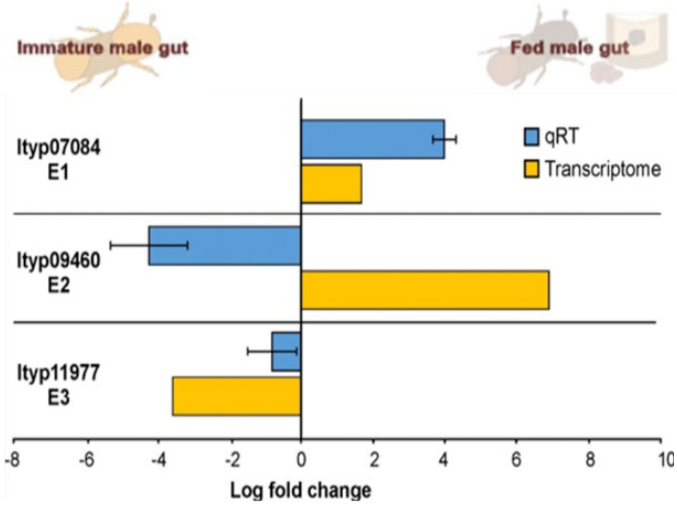

Figure 19: Relative expression of esterase gene family from I. typographus *gut.*
Tissue: fed male gut vs immature male gut. Yellow: log fold change values from RNA-seq. Blue: log fold change from qRT-PCR. The error bar indicates standard error. N=4.

In addition to the above-mentioned genes, we also chose three esterase gene candidates E1 (Ityp_7084), E2 (Ityp_9460), and E3 (Ityp_11977), that showed similarity to an Esterase (BT127766.1) in *D. ponderosae*. This esterase is expected to play a role in fatty acid ester storage. E1 expression was upregulated in the fed male gut and E3 expression was upregulated in the immature male gut. Although the qRT-PCR result of E2 showed an expression pattern opposite to that of the RNA-seq. data, the expression patterns of E1 and E3 were consistent both analysis (Figure 19).

Based on the findings from this publication, we concluded that the proposed candidate genes from the three respective families are promising for future research. In particular, the mevalonate pathway genes related to 2-methyl-3-buten-2-ol and the abundance of *cis*-verbenol in earlier life stages, along with its potential storage

mechanism with the help of CYP450 and esterase gene candidates point to important future research directions.

My contribution.

I reared the bark beetles in the laboratory, collected all their life stages, and separated them by sex. I dissected the gut tissue and participated in metabolomic data analysis. Additionally, I performed RNA extraction from the gut tissue, synthesized a cDNA library, and used it for further gene expression studies using qRT-PCR. I designed the primers for the genes analyzed in this study and conducted the statistical analysis of the collected data. I compiled all the data and prepared the main draft, which I then shared with co-authors for further revision. I also contributed to proofreading the final draft.

4.2. Publication 2: Metabolome and transcriptome-related dataset for pheromone biosynthesis in an aggressive forest pest *Ips typographus*.

Ramakrishnan R., Roy A., Kai M., Svatoš A., Jirošova A*. *Data in Brief. 2022b.* *https://doi.org/10.1016/j.dib.2022.107912*

Summary of this article: This data article presents crucial information related to the biosynthesis of aggregation pheromones in key life stages of *I. typographus* (Figure 3, Chapter 1.3.), that was not covered in a previous publication (Ramakrishnan et al., 2022a). Metabolomic and transcriptomic analyses of gut tissue from significant life stages of *I. typographus* revealed a diverse array of metabolites and gene families beyond those involved in pheromone biosynthesis. Notably, metabolomic data obtained through UHPLC–HR-MS/MS analysis provided detailed insights into metabolites across different life stages, using two measurement modes. This data has been made available in a Dryad database.

The data acquisition methods, which utilized bioinformatics tools such as GNPS and SIRIUS, offer valuable guidance for similar future analyses and the development of bioinformatics tools for high-throughput metabolomics. Additionally, the optimization of standard housekeeping genes using relative algorithms addresses gaps in the analysis of quantitative real-time PCR. This publication also reports on the expression patterns of gene sub-classes within the cytochrome P450 family, which are involved in detoxification processes in the gut tissue across various bark beetle life stages. Overall, this research provides essential knowledge about metabolite changes during *I. typographus* life stages, laying a foundation for future studies that build on these findings.

4.2.1. Additional data for non-targeted HPLC-MS/MS analysis of gut extracts from key life stages of *I. typographus.*

In UHPLC-HR MS/MS metabolomic analysis, we obtained data for several polar metabolites, while examining compounds related to pheromone biosynthesis. In the untargeted analysis, both positive and negative ion modes were run for the mass range

from m/z 80 to m/z 800. Typically, ca 3000 mass features and automatically selected for CID fragmentation using the TOP5 instrument algorithms setting. Several hundred (500-600) MS/MS spectra were collected in an individual run. These mass data were used for compound identification using the GNPS network engine (Wang et al., 2016), and obtained library hits were manually evaluated and modified wherever needed. One hundred forty-six compounds were identified in positive ion mode and sixty-one compounds in negative mode. They belonged to diverse structural classes. Amino acids/peptides were abundant in positive mode data. In the negative mode, phenylpropanoids were the most abundant class. Metabolites in individual life stages were well separated both in positive and negative ion modes. Though several compounds responsible for PLSDA data separations were detected, pheromone biosynthesis-related compounds could not be identified (Figure 20).

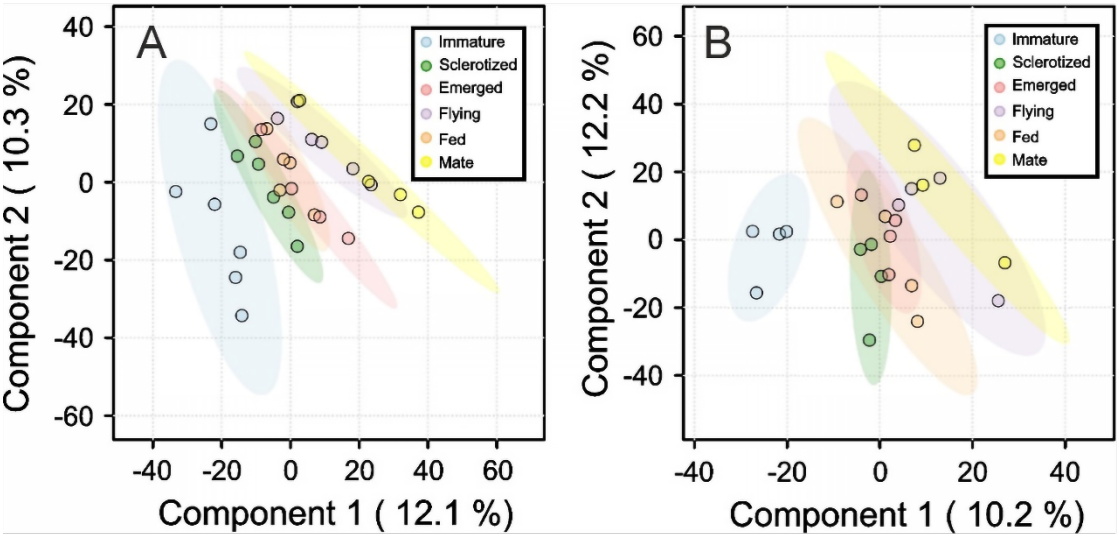

Figure 20: Partial least squares-discriminant analysis (PLS-DA) of UHPLC-HR- MS/MS data. Data analyzed metabolites from gut extracts of I. typographus *male beetle – different life stages. PLS-DA was performed using MetaboAnalist 5.0 (Pang et al. 2021), an online tool for streamlined metabolomics data analysis. The colored areas represent 95% of the confidence interval. A: positive ion mode. B: negative ion mode.*

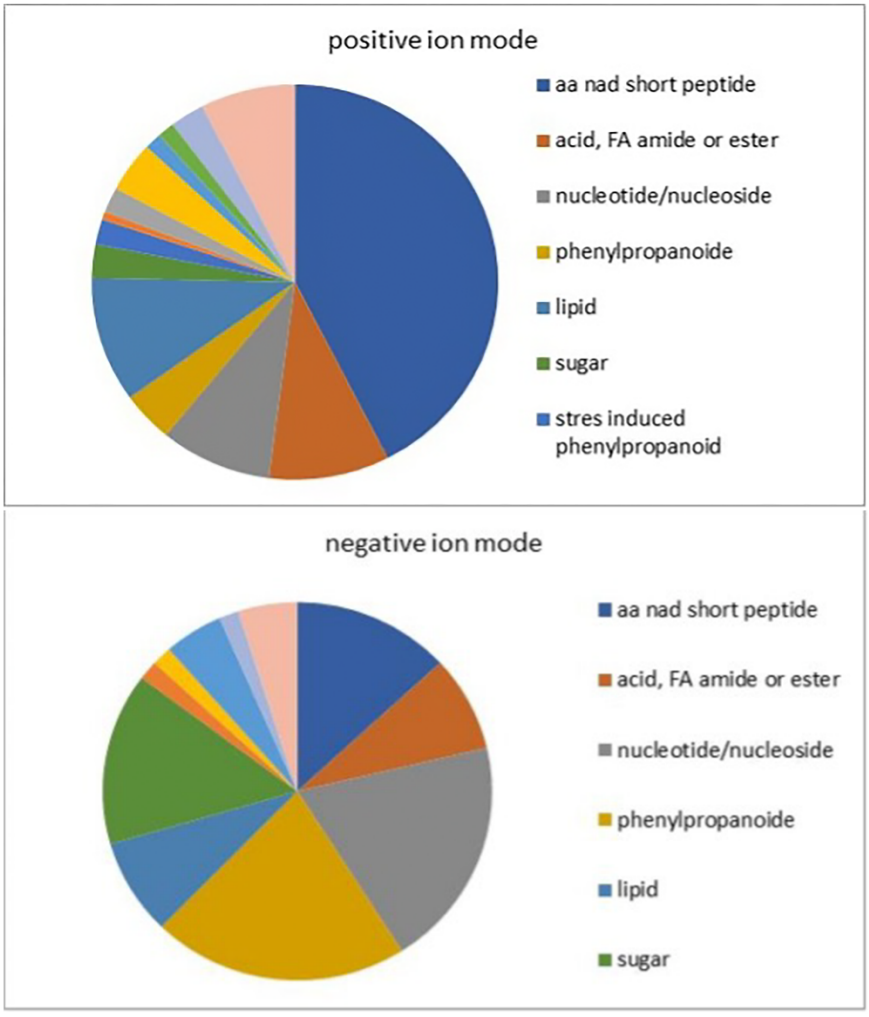

Figure 21: Chart of metabolite classes from UHPLC-HR-MS/MS data.
With positive and negative ion mode using data dereplication in GNPS and manually edited with Sirius data annotations. The chart shows the components aa: amino acid, acid, FA: fatty acid amide, ester, nucleotides, phenylpropanoid, lipid, and sugar in the respective proportions.

This data set was also provided in the form of a table in both positive and negative ion mode (in the full text available in supplements). Particularly, the data obtained can answer questions such as detoxification, regulatory and beetle development mechanisms of *I. typographus* This study also showed the abundance of certain components such as short peptides in positive mode and components such as sugars and phenylpropanoids were relatively segregated in negative modes which are key

information to understand the mechanism in bark beetle at certain life stages (Figure 21). The compounds identified were provided in a elaborated table from the publication (Ramakrishnan et al., 2022b Table 1).

4.2.2. Additional data for comparative gene expressions analysis in key life stages of *I. typographus.*

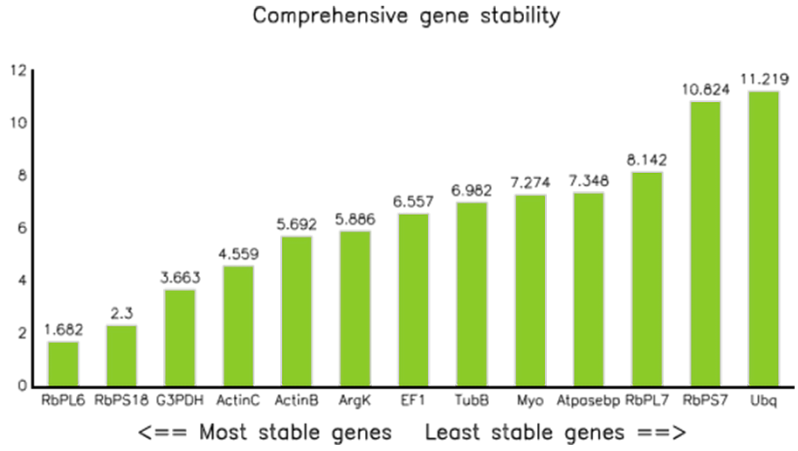

Figure 22: Housekeeping gene validation for gene expression studies in I. typographus *gut. The Validation was performed using algorithms of geNorm, NormFinder, BestKeeper, and ΔCT methods. The Gene names from left to right: Ribosomal proteinL6 (RbPL6), Ribosomal protein S18 (RbPS18), glyceraldehyde-3-phosphate dehydrogenase (G3PDH), Actin-C, Actin- β, arginine kinase isoform X1(ArgK), elongation factor 1α (EF-1), Tubulin beta-1 chain (Tubβ), Myosin (Myo), V-type proton ATPase catalytic subunit A (Atpasebp), Ribosomal proteinL7 (RbPL7), Ribosomal proteinS7 (RbPS7) and ubiquitin C variant (Ubq).*

In context to gene expression analysis, thirteen stable genes were selected as the best housekeeping genes based on literature and RNA-sequencing data. These genes include ribosomal proteins and structural proteins such as actin, elongation factor, tubulin, and ubiquitin. By analyzing the expression patterns of these genes in the gut tissue of *I. typographus* at different life stages, we identified the most stable candidates as housekeeping genes to compare expressions from the gene of interest. The best housekeeping genes were ranked using four established algorithms (Figure 21; Sellamuthu et al., 2022).

Subsequently, we identified 52 candidate genes from the cytochrome P450 family in the gut of male *I. typographus*, a family known for its diverse functions. Although our

initial focus was on identifying the gene responsible for *cis*-verbenol production, the large number of identified genes led us to explore their detailed functional annotations using sequence similarity from the KEGG pathway database. The identified genes were categorized into seven subclasses, as shown below (Table 1) and the phylogenetic tree from publication 1 (Figure 18).

Table 1: Subclasses of Cytochrome P450 gene from I. typographus *male gut.*

The seven sub-classes of the gene family were represented in seven different colour-shaded areas.

Contigs	CyP names	Contigs	CyP names
	Cluster 1		**Cluster 4**
Ityp04042	CyP450	Ityp16927	CyP450 307a1-like
Ityp04209	CyP450 CYP6CR2	Ityp03219	CyP450 CYP410a1
Ityp03230	CyP450	Ityp03221	CyP450 CYP410a1
Ityp03231	CyP450	Ityp03218	CyP450 CYP410a1
Ityp03902	CyP450	Ityp09555	CyP450 CYP410a1
Ityp03903	CyP450	Ityp05831	CyP450 4c21-like
Ityp02766	CyP450 CYP6BW2	Ityp05829	CyP450
Ityp03904	CyP450	Ityp05826	CyP450 4V2-like
Ityp00496	CyP450	Ityp05834	CyP450 4c21-like
Ityp10157	CyP450 CYP6BS2	Ityp05836	CyP450 4C1-like
Ityp03140	CyP450 CYP6DJ1v1	Ityp22414	CyP450 4c21-like
Ityp08010	CyP450 CYP6DG1v1	Ityp06189	CyP450 4c21-like
Ityp03872	CyP450 6A1-like	Ityp22415	CyP450 4g15-like
	Cluster 2	Ityp06190	CyP450 4g15-like
Ityp06081	CyP450 9e2-like	Ityp22416	CyP450 4c3-like isoform X1
Ityp03146	CyP450 9e2	Ityp06191	CyP450 4c3-like isoform X1
Ityp03153	midgut-specific cy P450	Ityp17996	NADPH-dependent CyP450 re
Ityp01834	CyP450 9e2-like	Ityp11675	NADPH-dependent CyP450 re
	Cluster 3	Ityp04142	CYP450 CYP4G55v3
Ityp14212	probable cy P450 301a1,	Ityp12866	CyP450 4d2-like
Ityp11191	CyP450 315a1,	Ityp09310	CyP450 CYP4CV1
Ityp09248	CyP450 CYP49a1	Ityp04137	CyP450 4d2-like isoform X1
Ityp18289	CyP450	Ityp00542	CyP450 4c3-like isoform X2
Ityp03031	CyP450	Ityp14975	CyP450 4C1-like
Ityp08528	CyP450	Ityp05150	CyP450 4C1-like
		Ityp07474	CyP450 18a1-like
	Cluster 5		**Cluster 6**
Ityp08942	probable CyP450 28a5	Ityp07311	CyP450 6k1-like isoform X1
Ityp10238	probable CyP450 6a17	Ityp04213	CyP450 6k1-like
	Cluster 7	Ityp10797	CyP450
Ityp01602	CyP450	Ityp01836	CyP450 9e2-like

The publication was concluded with new insights beyond the traditional scope beyond pheromone research. Specifically, it highlighted changes in bark beetle metabolites and gene expression patterns across the key life stages of *I. typographus* that are related to many functions such as detoxification, hydrocarbon biosynthesis, and beetle development. The Housekeeping gene works is an essential work for the *I. typographus* gene expression analysis.

My contribution.

I reared the bark beetles in the laboratory, collected all their life stages, and separated them by sex. I dissected the gut tissue and provided samples for metabolomic data analysis. Additionally, I performed RNA extraction from the gut tissue and synthesized a cDNA library, which was used for housekeeping gene validation using qRT-PCR. I designed the primers for the genes analyzed in this study and conducted the statistical analysis of the collected data. I compiled all the data and prepared the main draft, which I then shared with co-authors for further revision. I also contributed to proofreading the final draft.

4.3. Publication 3: Juvenile Hormone III Induction Reveals Key Genes in General Metabolism, Pheromone Biosynthesis, and Detoxification in Eurasian Spruce Bark Beetle.

Ramakrishnan R., Roy A., Hradecký J., Kai M., Harant K., Svatoš A., Jirošová A. Frontiers in Forests and Global Change. 2024. http://doi.org/10.3389/ffgc.2023.1215813*

Summary of this article: In this article, we applied Juvenile Hormone III (JH III) and conducted a comparative analysis of metabolites (metabolomics), gene transcripts (transcriptomics), and proteins (proteomics) in both male and female *I. typographus* to address objectives 2 (Chapter 2).

Our findings revealed that numerous gene families were enriched following JH III treatment, including those associated with catalytic and oxidoreductase activity, esterases, phosphatases, and membrane transporters. We observed sex-specific enrichment, with reproduction-related and detoxification genes being upregulated in females, while metabolic regulation genes were more prominent in males. At the protein level, we confirmed the enrichment of metal ion binding and transferase enzymes in male beetles. Following JH III treatment, mevalonate pathway genes, including *isoprenyl diphosphate synthase* (IPDS), were upregulated 35-fold exclusively in males, indicating *de novo* biosynthesis of the pheromones 2-methyl-3-buten-2-ol and ipsdienol.

Additionally, cytochrome P450 genes, likely encoding enzymes involved in *cis*/*trans*-verbenol formation, detoxification, and ipsdienol biosynthesis, were upregulated more than 3-fold in the male gut. This increase in gene expression correlated with heightened production of the corresponding metabolites. Detoxification conjugates, such as verbenyl oleate in the bark beetle fat body and verbenyl diglycosides in the gut, were induced by JH III application, confirming the hormone's regulatory role in the formation of these conjugates. JH III induction also led to the upregulation of esterase and glycosyl hydrolase in the male gut. The esterase is proposed to release the pheromone *cis*-verbenol in adult males by breaking down verbenyl oleate. Metabolic

analyses showed a reduction in the abundance of verbenyl oleate in JH III-induced male beetles, correlating with increased esterase gene expression.

Overall, the data provide strong evidence of JH III's regulatory role in the expression of genes and enzymes related to fundamental beetle metabolism, pheromone biosynthesis, and detoxification in *I. typographus* bark beetles.

4.3.1. Comparative analysis of metabolites profiles and contents in *I. typographus* after JH III treatment.

4.3.1.1. Non-targeted and targeted GC-MS analysis of JH III treated *I. typographus* gut extracts.

Highlights: *The non-targeted analysis revealed that JH III treatment in male beetles resulted in the production of 2-methyl-3-buten-2-ol,* cis*-verbenol, and 2-phenylethanol. Quantification of these pheromones indicated their abundance following JH III treatment in* I. typographus*. Repeated quantification (excluding 2-methyl-3-buten-2-ol due to its dominance in the measurements) after JH III induction showed the abundant of* cis*-verbenol, phenylethanol, verbenone, myrtenol, and ipsdienol.*

To identify the specific pheromone components after JH III treatment in *I. typographus*, we used comprehensive two-dimensional gas chromatography to analyze gut extracts from both male and female beetles after the treatment.

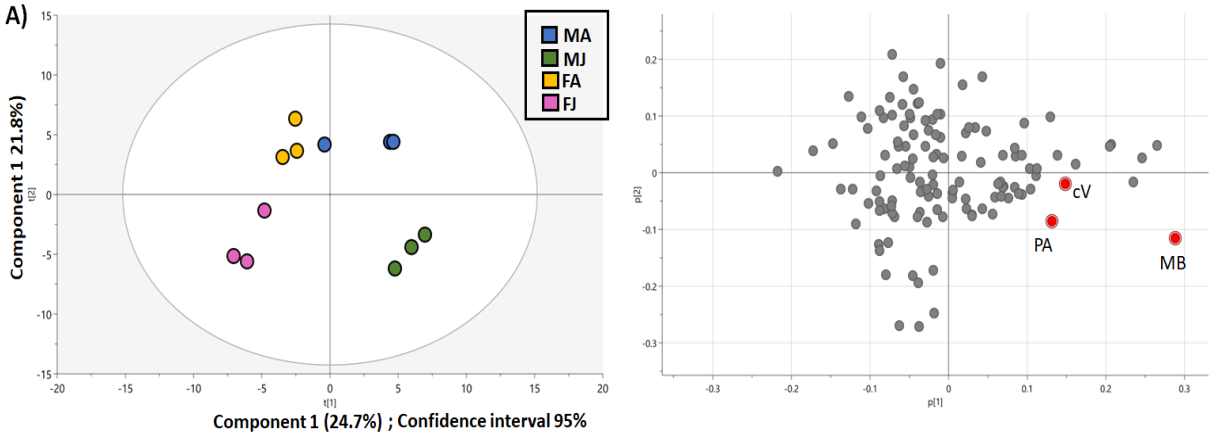

Figure 23*: GC-MS metabolomics: PCA of gut extracts from* I. typographus *after JHIII treatment.*

The key component responsible for separation are highlighted in red colour- PA- 2-Phenylethanol, MB- 2-methyl-3-buten-2-ol, and cV- cis-verbenol. Treatment: MA/FA- male/female acetone-treated bark beetle gut. MJ/FJ- Male/female JH III treated beetle gut.

The initial Principal Component Analysis (PCA) revealed a distinct separation of JH III-treated male gut samples from control samples treated with acetone. The first two components of the PCA plot accounted for 46.5% of the variance in the data (Figure 23). The primary compound responsible for this separation was identified as the main *I. typographus* aggregation pheromone component, 2-methyl-3-buten-2-ol. Additionally, compounds such as *cis*-verbenol and 2-phenylethanol (male-specific compound also known in other *Ips* species (Gries, 1990)), have contributed to this separation.

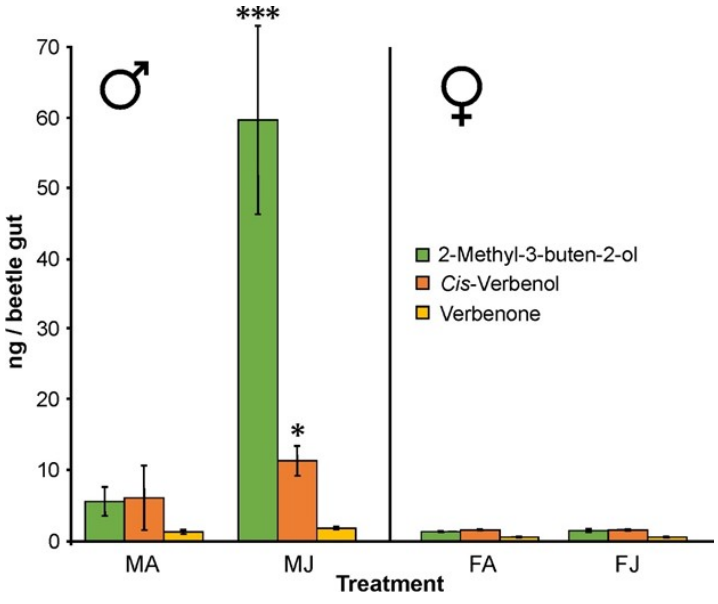

Figure 24: GC- MS Quantification from I. typographus *after JH III treatment.*
*Treatment: MA/FA- male/female acetone-treated beetle gut. MJ/FJ- Male/female JH III treated beetle gut. Statistics: One-way ANOVA with Fisher (LSD) test with 95% confidence interval. *** represents P<0.001, * represents P<0.05. N=3.*

Identified components were quantified and the 2-Methyl-3-buten-2-ol (60 ng/gut) levels were significantly higher in male beetles after JH III treatment compared to those after acetone treatment (control). Additionally, *cis*-verbenol (12-15 ng/gut) levels also increased, albeit with low significance, in male beetles after JH III treatment. Whereas female beetles produced a trace amount of these compounds in both JH III treated and control groups. Traces of verbenone (an oxidized product of *cis*-verbenol) were detected in the guts of both males and females with JH III treatments (Figure 24).

Along with *cis*-verbenol, we also detected other compounds, such as 2-phenylethanol, ipsdienol, and myrtenol, in the JH III-treated male gut. Male-specific compounds were individually quantified in the JH III treated and control guts, and the abundance of all compounds increased after the JH III treatment (Figure 25).

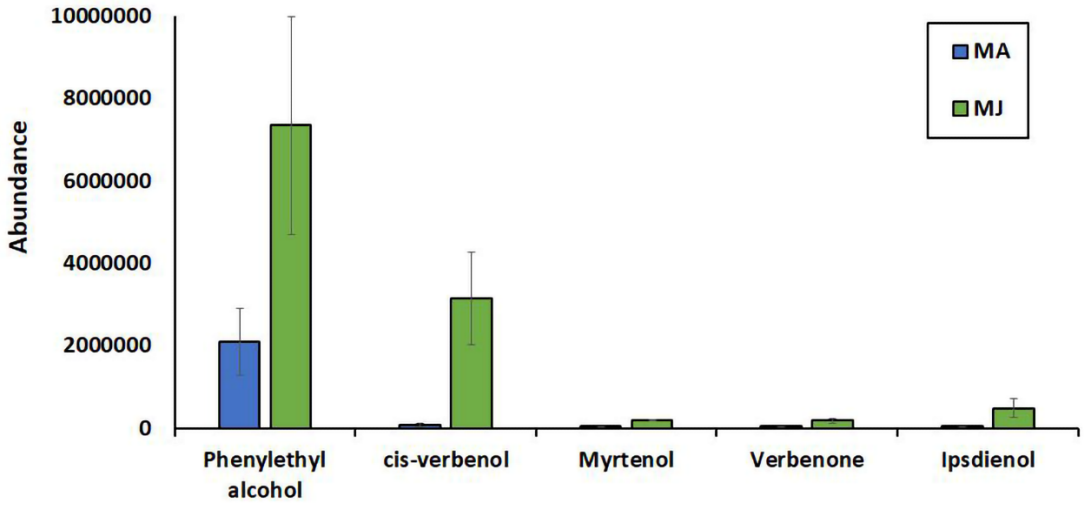

Figure 25: GC-MS – Compounds quantification from I. typographus *male gut after JH III*
MA- Males topically treated with acetone – control; MJ- Males topically treated with JH III – treatment The error bar indicates standard error. N=3.

4.3.1.2. Quantification of pheromone conjugates in JH III treated *I. typographus.*

Highlights: *Targeted quantification revealed that JH III treatment in* I. typographus *led to an increased abundance of verbenyl oleate and verbenyl diglycosides in the gut tissue. Additionally, verbenyl oleate was also detected in the beetle body following JH III treatment. These results indicate a significant increase in the production of these compounds after treatment.*

Using a targeted approach, the relative abundance of the pheromone precursor verbenyl oleate (as discussed in Publication 1) was identified in extracts from both the guts and beetle bodies (including the fat body) following JH III treatment (Figure 26). In female beetle body extracts, topical JH III treatment resulted in a 15-fold increase in verbenyl oleate levels compared to the control group. In contrast, male beetles already

exhibited the presence of this compound before treatment, with only a modest 1.5-fold increase after JH III application.

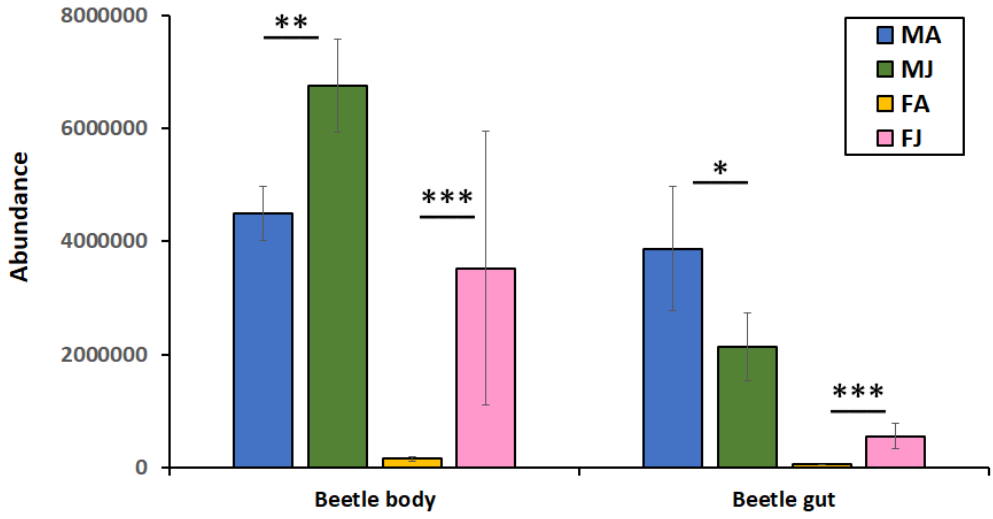

Figure 26: GC-MS data: Quantification of Pheromone precursors (Verbenyl oleate) from I. typographus *after JH III treatment.*
Relative abundance of Verbenyl oleate in the beetle body (left) and gut tissue (right) after JH III induction compared to the control.

In the targeted quantification of conjugates using GC-MS analysis, an increasing trend in conjugate levels was observed in the gut extracts of both male and female beetles, with a 15-fold increase in females. However, in male gut extracts, JH III treatment resulted in a significant 1.8-fold decrease in the relative abundance of verbenyl oleate compared to the control group. This reduction is likely due to the cleavage of these monoterpene conjugates, releasing the free pheromone *cis*-verbenol (Figure 26). As previously quantified, the absolute amount of verbenyl oleate in various bark beetle life stages was 250 ng/mg of beetle body weight (Ramakrishnan et al., 2022a). The content of free *cis*-verbenol in the guts of freshly emerged beetles was 5 ng per gut, which can be compared with the control bark beetles in this study.

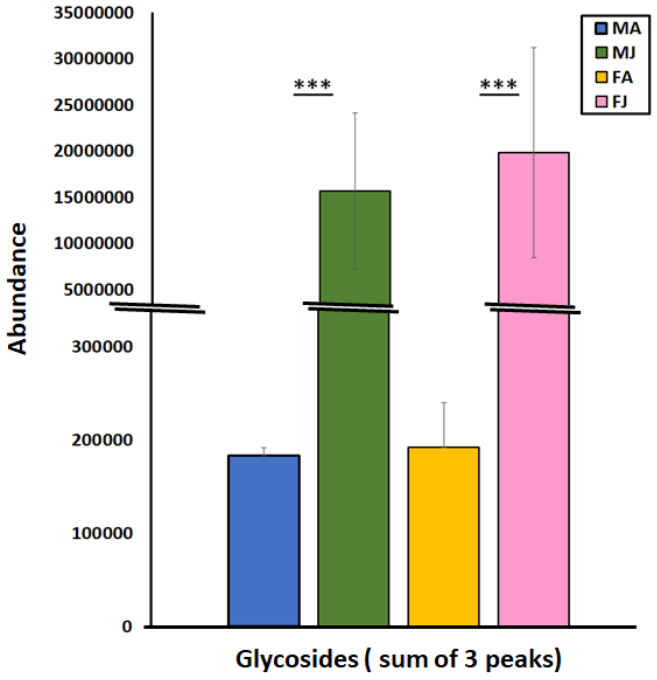

Figure 27: UHPLC-HR-MS/MS: the abundance of Verbenyl diglycosides from I. typographus *gut after JH III treatment.*
*MA- Males topically treated with acetone – control; MJ- Males topically treated with JH III – treatment, FA- Females topically treated with acetone – control, FJ- Females topically treated with JH III – treatment. Statistics: T-test with paired independent parameters. *** represents p < 0.001, N=3.*

In non-targeted analysis via UHPLC/HRMS, the total abundance of verbenyl diglycosides was calculated as the sum of the peak areas from the three individual verbenyl diglycoside peaks. After treatment with JH III in *I. typographus*, the total abundance of diglycosides content significantly increased in the guts of both sexes compared to the acetone-treated controls. There was no significant difference in the induction of these compounds by JH III between males and females (Figure 27). The actual amount of these compounds per beetle gut could not be determined due to the lack of standards.

4.3.2. Comparative analysis of expression of genes encoding enzymes catalyzing key pheromone biosynthesis reactions in *I. typographus* after JH III treatment.

Highlights: *The gene expression profiles in JH III treated male and female guts showed significant differences. JH III treated female beetles showed more gene numbers expressed, compared to JH III treated male beetles.*

To understand the molecular changes in *I. typographus* treated with JH III, we performed RNA sequencing and proteome analysis of the gut tissue following the JH III treatment.

Differential gene expression (DGE) analysis from the RNA sequencing data revealed a clear distinction between the gene sets of JH III-treated and control bark beetles, as shown in a principal component analysis (PCA) (Ramakrishnan et al., 2024, supplementary figure 2a). In male beetle gut tissue, JH III treatment resulted in the upregulation of 710 transcripts and the downregulation of 545 transcripts, as depicted in a Venn diagram (Figure 28A). In contrast, female gut tissue showed upregulation of 518 transcripts and downregulation of 456 transcripts. Across both male and female gut tissues, 5,155 transcripts were upregulated, while 4,595 were downregulated. Overall, the total number of genes upregulated in male beetle guts after treatment was higher (10,385 transcripts) compared to females (9,682 transcripts) (Figure 28A).

At the protein level, differential protein expression (DPE) analysis of JH III treated *I. typographus* gut tissue showed significant fold changes in the expression of numerous proteins. Although JH III treatment is traditionally associated with pheromone production in adult male beetles, the female beetle gut tissue exhibited a higher number of identified proteins after treatment 449 proteins in females compared to 229 proteins in males. Among the upregulated proteins, 79 were male-specific, 302 were female-specific, and 145 were detected in both male and female guts. For downregulated proteins, 68 were male-specific, 69 were female-specific, and 27 were detected in both sexes (Figure 28B).

Aiming to narrow down the upregulated genes from male gut tissue with possible functional significance, we compared the gene contig lists from the DGE and DPE analyses (Figure 28 C). Although the number of identified proteins was 100-fold lower

than the number of transcripts from the DGE analysis, the results of the comparison helped identify a unique set of gene contigs for further evaluation. The male gut tissue had 129 contigs from transcript and protein analysis (names are provided in Ramakrishnan et al., 2024, Supplementary Table 3A). The key mevalonate pathway genes *isoprenoid-di-phosphate synthase* (IPDS) (Ityp09271), *isopentyl-di-phosphate isomerase* (IPPI) (Ityp04875), *3-hydroxy-3-methyl glutaryl co-enzyme A reductase* (HMG-R) (Ityp17150), *3-hydroxy-3-methyl glutaryl Co-enzyme A synthase* (HMG-S) (Ityp09137), and *phosphomevalonate kinase* (PMK) (Ityp06045) were also upregulated. A similar pattern was observed for other gene families involved in hydrolase function, specifically those related to *glycosyl hydrolase* activity, which acts on glycosyl bonds (GO:0016798). We also identified *transferases*, including *acetyltransferase* and *UDP-glucuronosyltransferase*. Additionally, many ribosomal and membrane transporter contigs, such as *V-type ATPases*, were upregulated, and several genes with unknown functions were found among the male-specific upregulated gene contigs (Figure 28A &B).

In the female gut tissue, approximately 183 contigs were identified through transcript and protein comparative analysis (Figure 28C). Although the number of contigs identified in females was higher than in males, mevalonate pathway genes were not predominant among the candidates in females. However, another prenyl tranferase, *geranyl-di-phosphate synthase* (GPPS) (Ityp17861), was upregulated. Additionally, gene families such as glycine dehydrogenase, *ubiquitin carboxyl-terminal hydrolase*, and vitellogenin-like proteins, which likely play roles in detoxification and oocyte formation, were found to be upregulated. Similar to the males, many genes related to mitochondrial ribosomal proteins, elongation factors, binding proteins, and a large number of genes and proteins with unknown functions were also upregulated (Figure 28C).

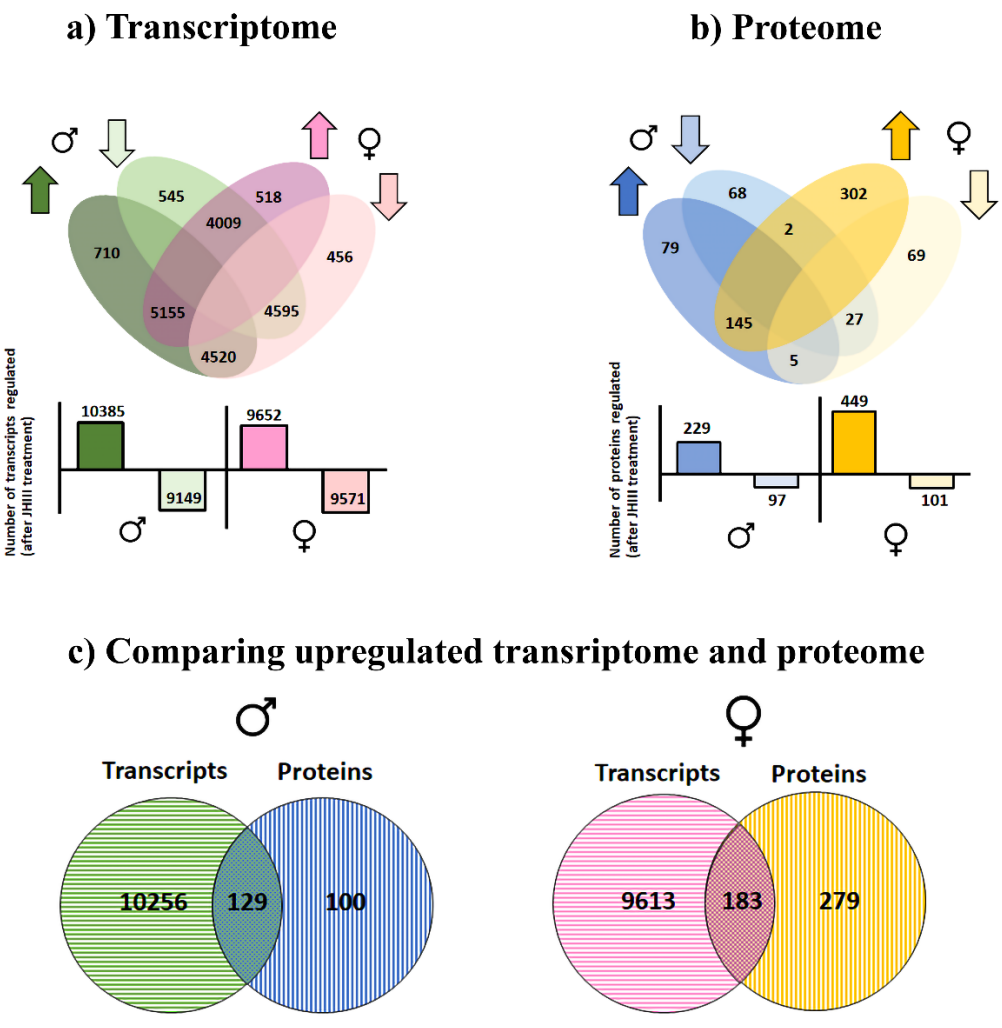

Figure 28: Transcriptome and proteome comparison of I. typographus *gut after JH III treatment. Gene regulation in* I. typographus *male and female gut tissue after JH III treatment. Up arrow – upregulation and down arrow – down-regulation. Green and blue represent male gut tissue. Pink and yellow represent female gut tissue. The graph below the Venn diagram represents the total number of transcripts and proteins regulated in both sexes after treatment. C) comparison of upregulated transcripts and proteins from males (left) and females (right) after treatment. The Jvenn platform was used for the comparison analysis.*

4.3.2.1. Regulation of Mevalonate pathway genes after JH III treatment.

Highlights: *In JH III-treated* I. typographus*, genes involved in the mevalonate pathway were upregulated. In addition, the male-specific enzyme IPDS (which is proposed for the terminal biosynthetic step of 2-methyl-3-buten-2-ol) was highly upregulated. Both HMG-S and IPPI were also significantly expressed at the protein level in the gut tissue of JH III-treated male beetles.*

Combining gene and protein expression along with qRT-PCR expression allowed a more comprehensive overview of the effect of JH III treatment and sex on the steps of the mevalonate pathway, which makes the *I. typographus* aggregation pheromones and pheromone precursors *de novo*. Upregulation of the mevalonate pathway key genes including PMK (Ityp06045), HMG-S (Ityp09137), HMG-R (Ityp17150), IPPI (Ityp04875), and IPDS (Ityp09271) were reported (Figure 29A). Though not all of these steps were identified at the protein level, the key steps involving HMG-S, IPPI, and IPDS were identified with upregulation. Notably, we found that the IPDS gene was upregulated by up to 35-fold in male gut tissue compared with that in female gut tissue after JH III treatment (Figure 29B). Besides the IPDS gene, HMG-S was also significantly upregulated in JH III-treated male gut tissue compared with that in treated females (Figure 29B). Additionally, we also found that IPPI was exclusively abundant in proteins from female gut tissue after treatment (Ramakrishnan et al., 2024, supplement figure 3).

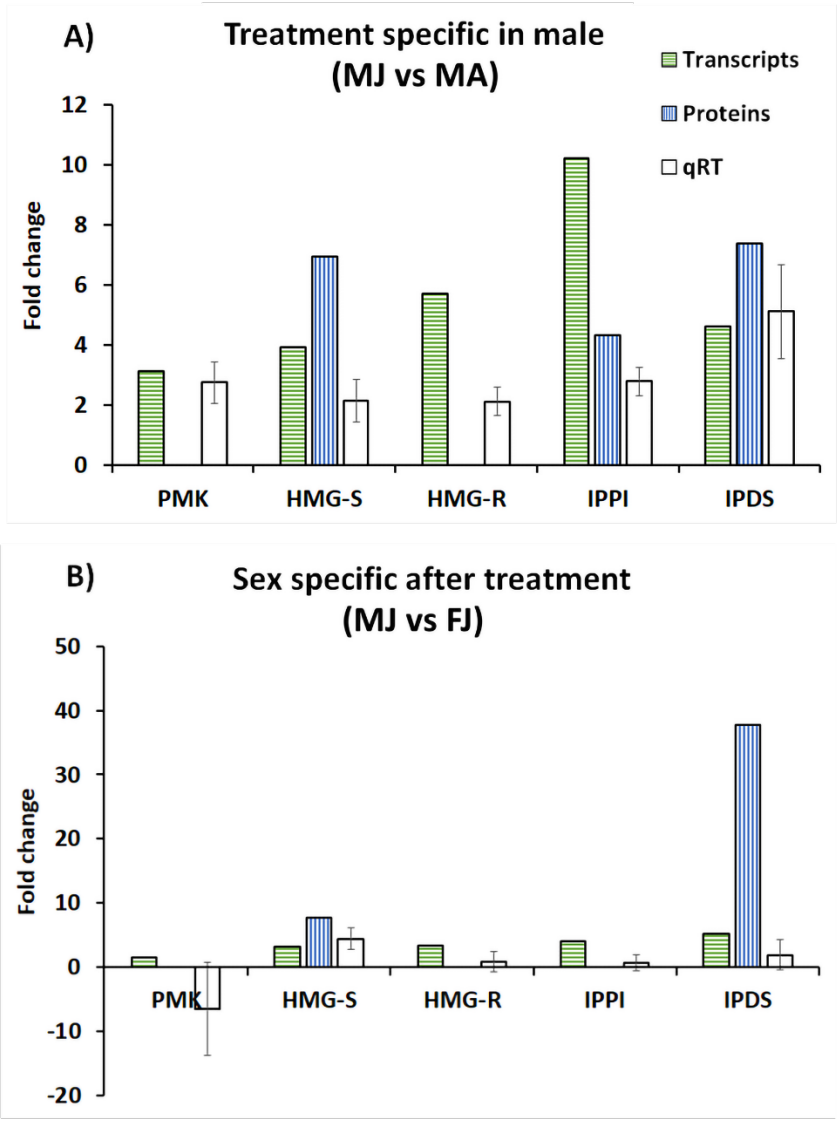

Figure 29: A: Mevalonate pathway genes expression in male I. typographus *after JH III treatment*

B: *Mevalonate pathway genes expression in JH III treated* I. typographus *male compared to female.* ***Gene names:*** *phosphomevalonate kinase (PMK), 3-hydroxy-3-methyl glutaryl coenzyme-A synthase (HMG-S), 3-hydroxy-3-methyl glutaryl coenzyme-A reductase (HMG-R), isopentyl-di-phosphate isomerase (IPPI), and isoprenoid-di-phosphate synthase (IPDS). The error bar indicates standard error. MA- Males topically treated with acetone – control; MJ- Males topically treated with JHIII – treatment, FA- Females topically treated with acetone – control, FJ – Females topically treated with JHIII – treatment. N=4.*

4.3.2.2. Regulation of Cytochrome P450 (CYP450) genes after JH III treatment.

Highlights: *In JH III-treated male* I. typographus*, genes from CYP450 which could be involved in* cis*-verbenol production and detoxification were upregulated after JHIII treatment. In addition, the CYP450 gene with sequence similarity to CYP9T1/T2, functionally proposed for myrcene hydroxylation to ipsdienol was highly expressed in the gut tissue of JHIII-treated males.*

A similar combined approach was taken to explore the regulation of CYP450 genes that are involved in the pheromone biosynthesis of *I. typographus* using RNA-Seq and qRT-PCR; no proteins of this family were detected in our proteomic investigation. CYP450 contigs showing differential expression patterns above a 2-fold change with a significant p-value ($P<0.05$) were confirmed by qRT-PCR analysis. Among the contigs previously proposed to be involved in pheromone biosynthesis (Ramakrishnan et al., 2022a), contigs Ityp3903 and Ityp0496 (proposed for verbenol synthesis), contigs Ityp3140 (proposed for detoxification), and Ityp3153 (proposed for ipsdienol) were all found to be upregulated genes in the JH III-treated male gut and are among the most highly upregulated genes measured in this study (Figure 30).

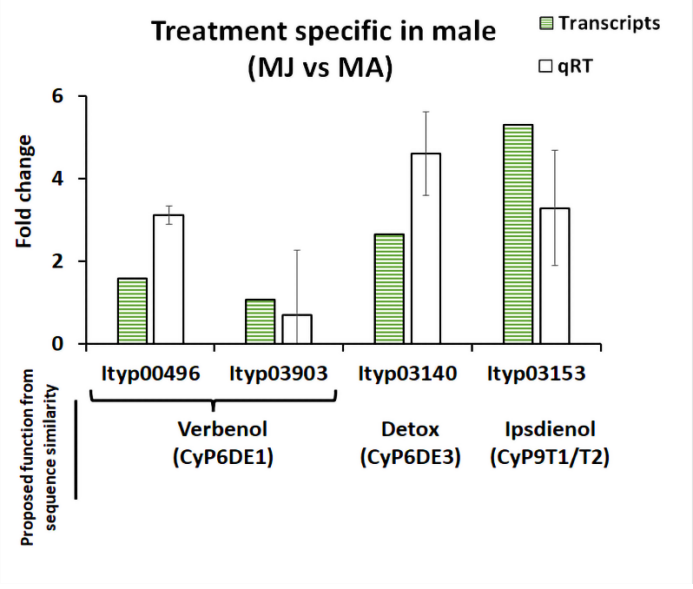

Figure 30: Cytochrome P450 genes expression pattern in I. typographus *after JH III treatment. Expression patterns are from transcriptome and qRT-PCR expression analysis from* I. typographus *male gut tissue after JH III treatment. The error bar indicates standard error. MA- Males topically treated with acetone – control; MJ- Males topically treated with JH III – treatment. N=4.*

4.3.2.3. Regulation of Esterase gene family after JH III treatment.

Highlights: *In JH III-treated* I. typographus *males, the esterase gene Ityp09460 was significantly expressed, which is proposed to be involved in the release of* cis*-verbenol from its conjugates. Additionally, the esterase gene Ityp11977, proposed for forming conjugates from* cis*-verbenol, was identified in both sexes.*

Among the esterase genes proposed for converting the stored verbenyl fatty acid ester from *cis*-verbenol, an esterase gene Ityp11977 (which occurred in the early life stage) was not significantly influenced by JH III treatment in males according to transcriptome and proteome analysis. However, another esterase contig, Ityp09460, presumed for *cis*-verbenol release from the stored fatty esters was upregulated in the protein analysis and qRT-PCR but downregulated in the RNA-Seq. (Figure 31A). In female gut tissue, none of these contigs were detected, except for Ityp11977 in qRT-PCR (Figure 31B).

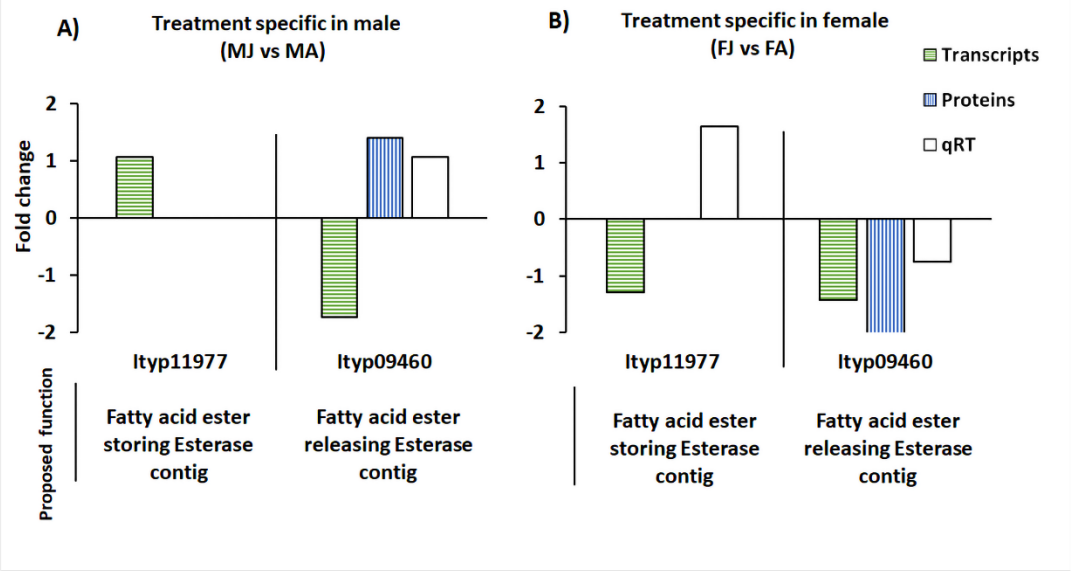

Figure 31: Esterase genes expression pattern in I. typographus *after JH III treatment. Expression patterns are from the transcriptome, proteome, and qRT-PCR analysis from* I. typographus *male and female gut tissue after JH III treatment. MA- Males topically treated with acetone – control; MJ- Males topically treated with JH III – treatment, FA- Females topically treated with acetone – control, FJ- Females topically treated with JH III – treatment. N=4.*

4.3.2.4 Regulation of glycosyl hydrolase gene family after JH III treatment.

Highlights: *In JH III-treated male* I. typographus*, a male-specific gene family, glycosylhydrolase, was identified as being highly expressed following JH III treatment. This gene family was targeted to investigate the abundance of verbenyl-di-glycoside in male gut tissue. Notably, after the mevalonate pathway genes, this glycosylhydrolase gene family was among the most prominently identified in all male-specific comparative analyses.*

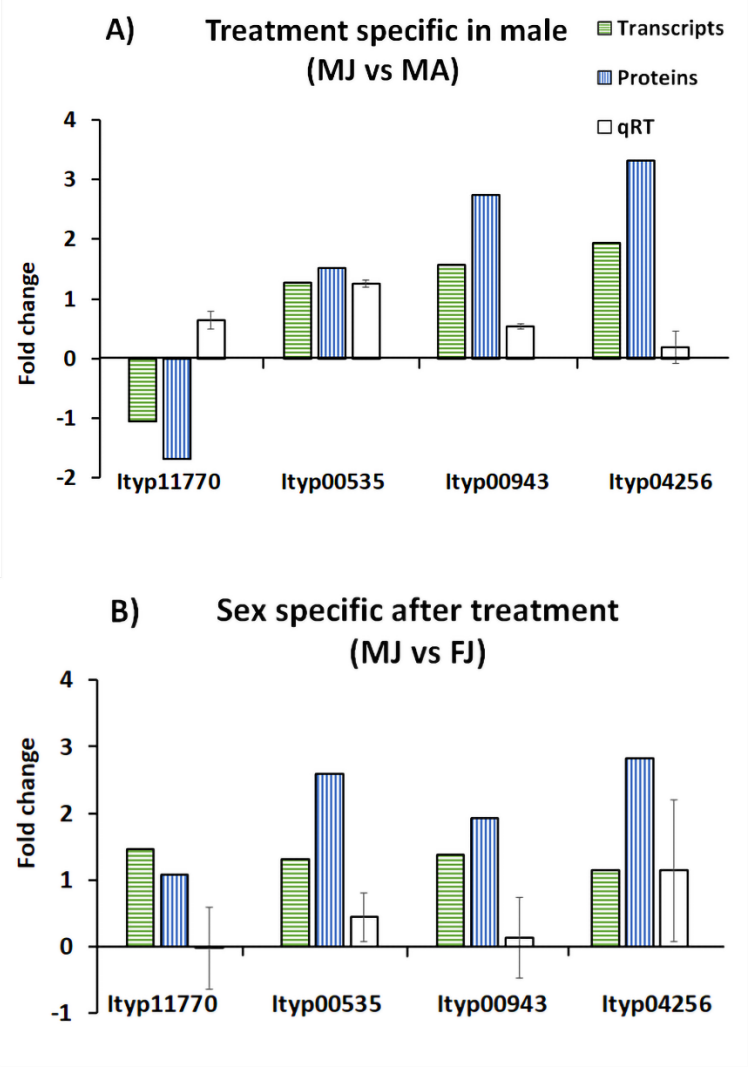

Figure 32: Glycosyl hydrolase genes expression pattern in I. typographus *after JH III treatment. Expression patterns are from transcripts, proteins, and qRT-PCR analysis. MA- Males topically treated with acetone – control; MJ- Males topically treated with JH III – treatment, FA- Females topically treated with acetone – control, FJ- Females topically treated with JH III – treatment. N=4. The error bar indicates standard error.*

When comparing DGE and DPE analyses in male gut tissue, a set of gene families known for glycosyl-hydrolase function was significantly upregulated after JH III treatment at both the transcript and protein levels with male specificity. Twelve gene contigs were detected from the glycosyl hydrolase family, four of which were significantly upregulated at the protein level, Ityp11770, Ityp00535, Ityp00943, and Ityp04256 (Figure 32).

Based on the findings from this publication, we concluded that the previously identified three gene families is reconfirmed in *I. typographus,* the context of JH III treatment, and hold promise for further gene characterization. Notably, the key gene in the production of 2-methyl-3-buten-2-ol, IPDS, was upregulated on both transcriptome and protein levels. The upregulation of *cis*-verbenol in the absence of tree-derived precursors suggests a storage and release mechanism facilitated by esterase gene candidates, along with CYP450 genes. Additionally, a new gene family, glycosyl hydrolase was identified, with key candidates highlighted for future research directions. Furthermore, we emphasized the important role of JH III in sex-specific pheromone studies, noting that female beetles are regulated for various functions as well.

My contribution.

I reared the bark beetles in the laboratory and separated them by sex for JH III treatment. I dissected the gut tissue and provided samples for metabolomic and RNA sequencing analyses. Additionally, I extracted RNA from the gut tissue and synthesized a cDNA library for gene expression analysis using qRT-PCR. I conducted the statistical analysis of the collected data, compiled the results, and prepared the main draft. I then shared the draft with co-authors for further revision and participated in proofreading the final version.

4.4. Publication 4: Aggregation Pheromones in the Bark Beetle genus *Ips*: Advances in Biosynthesis, Sensory Perception, and Forest Management Applications (Review article in manuscript format).

Ramakrishnan R., Shewale M. K., Strádal J., Hani U., Gershenzon J, Jirošová A.*

Summary of this article.

This review article summarizes the current understanding of *Ips* bark beetle aggregation pheromone production, olfactory perception, and their application in pest management, with a focus on the most economically important and extensively studied species, including *I. pini, I. typographus, I. duplicatus, I. cembrae, I. paraconfusus, I. confuses,* and *I. hauseri.* This article is connected to the introduction of this thesis chapter 1.4.

This review builds on information from previous studies and provides a comprehensive summary of findings related to pheromone composition, production mechanisms, pheromone perseverance, and their utilization in forest management. Furthermore, it highlights gaps in current knowledge and identifies areas in need of further research. The review bring a increased understanding of *Ips* aggregation pheromones communication, which offers new insights into the ecology of these species and suggests novel management strategies to reduce their economic impact and prevent bark beetle outbreaks.

4.4.1. Aggregation pheromone chemical composition and structural types in model *Ips* species.

Highlights: *This section compiles literature on pheromone composition of* I. pini, I. typographus, I. paraconfusus, I. confusus, I. hauseri, I. duplicatus*, and* I. cembrae. *and classifies the structures of biologically active compounds into different chemical classes*

In the majority of *Ips* species, the major pheromone components include ipsdienol and ipsenol, compounds exclusively produced by the bark beetle *Ips* genus. Some species also produce ipsdienol isomers such as amitinol or *E*-myrcenol, along with the derivative lanierone. Other identified active pheromone compounds are hemiterpenes like 2-methyl-3-buten-2-ol, 3-methyl-3-buten-1-ol, and the monoterpene *cis*-verbenol, originating from the host compound *α*-pinene (Figure 7, Chapter 1.4.6). This section discusses the structural similarity of the mentioned compounds and how the resulting pheromone blends are species-specific, driven by variations in the proportions of the mixtures and differences in enantiomeric composition.

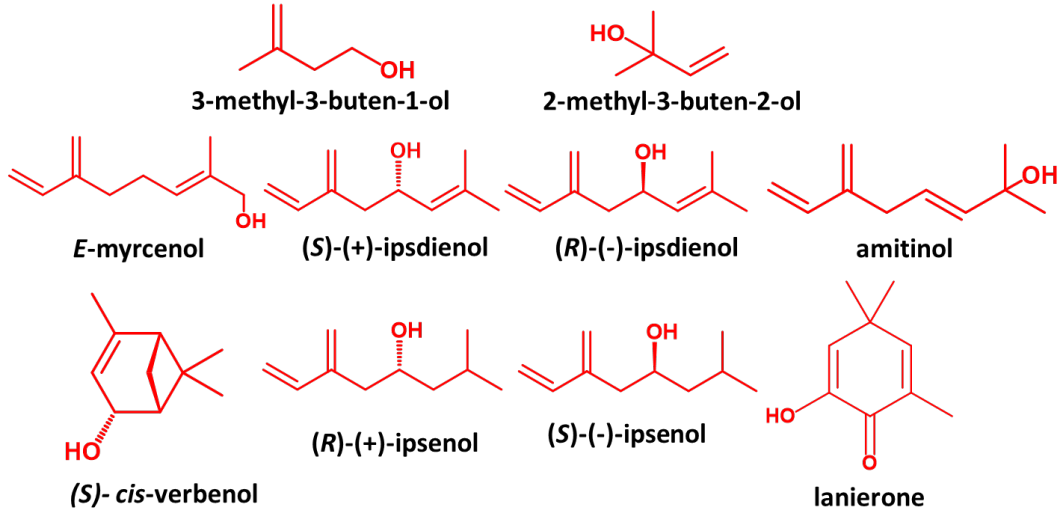

Figure 33: Summary of common male-specific components with pahromone activity shared by several Ips species.

Table 2: *Pheromone blends compositions, host trees and spatial distributions of selected* Ips *species. (Modified from Ramakrishnan et al., unpublished manuscript)*

Species	**Pheromone components**	**Enantiomeric ratio, if known**	**Host trees**	**Geographical distribution**
Ips typographus	2-methyl-3-buten-2-ol *cis*-verbenol ipsdienol Ipsenol **10:01:01** 2-methyl-3-buten-2-ol: *cis*-verbenol: ipsdienol	**95:5** *R*-(-)- :*S*-(+)-ipsdienol **100** (*S*)-*cis*-verbenol	Norway spruce (*Picea abies*)	Europe and Asia
Ips duplicatus	ipsdienol *E*-myrcenol **5:1** ipsdienol: *E*-myrcenol [45]	**50:50** *R*-(-)- :*S*-(+)-ipsdienol	Norway spruce (*Picea abies*)	Europe
Ips cembrae	ipsenol ipsdienol 3-methyl-3-buten-1-ol ~ **68:28: 4** ipsenol: ipsdienol: 3-methyl-3-buten-1-ol	**100** *S*-(-)-ipsenol **4:96** *R*-(-)- :*S*-(+)-ipsdienol	European larch (*Larix decidua*) and Japanese larch (*Larix kaempferi*)	Europe
Ips pini	ipsdienol lanierone ~**99:1** ipsdienol:lanierone	**35:65** *R*-(-)- :*S*-(+)-ipsdienol [39] **95:5** *R*-(-)- :*S*-(+)-ipsdienol†	Red pine (*Pinus resinosa*), Jack pine (*Pinus banksiana*), and White pine (*Pinus strobus*)	North America
Ips confusus	ipsenol ipsdienol **9:1** ipsenol: ipsdienol	**99** (*S*-(-)-ipsenol); **5:95** *R*-(-)- :*S*-(+)-ipsdienol	Pinon pine (~ *Pinus edulis*) and One-seed juniper (*Juniperus monosperma*)	North America
Ips paraconfusus	ipsenol ipsdienol *cis*-verbenol **1:0.1:1** ipsenol: *cis*-verbenol:ipsdienol	**100** (*S*)-(−)-*cis*-verbenol **99** (*S*-(-)-ipsenol) **10:90** *R*-(-)- :*S*-(+)-ipsdienol	Pinon pines (~ *Pinus edulis*) and timber tree *P. ponderosa, P. attenuata, P. contorta, P. coulteri, P. lambertiana, P. monticola, P. muricata, P. radiata and P. sabiniana.*	North America
Ips hauseri	ipsenol *cis*-verbenol **95:5**	**100** (*S*)-(−)-ipsenol **100** (*S*)-(−)-*cis*-verbenol	Schrenk spruce (*Picea schrenkiana* Fisch. & C.A. Mey.) and Siberian spruce (*Picea obovata* Ledeb.)	Central Asia

† The ratio varies for eastern and western populations of *I. pini* in the USA.

4.4.2. Pheromone production and biosynthetic mechanisms.

Highlights: *This subsection of the review details the mechanisms underlying pheromone biosynthesis, including genetic underpinnings and regulatory aspects.*

The content is partially compiled in the literature analysis section of this thesis, mainly in chapter 1.4.

4.4.3. Perception of pheromones by olfactory system.

Highlights: *This section focuses on how bark beetles perceive pheromones through their olfactory systems, particularly in the antennae, with details on sensilla and receptors characterized in model Ips bark beetles.*

Although the peripheral olfactory system in Coleoptera, particularly bark beetles, is less studied compared to Lepidoptera, extensive research has been conducted for example on the morphology of sensilla on the antennae and mouthparts of *Ips* species. This section listed several recent advances that have increased our understanding of the responses of *Ips* olfactory receptor neuron cells (ORN) located in beetle antenna to pheromone components because specific ORN classes have been identified for detecting bark beetle pheromones and their enantiomers.

4.4.4. Pheromone-Based Pest Management Strategies

Highlights: *This section reviews various ways of using pheromone for managing* Ips *bark beetles in forestry applications.*

The review section outlines the key facts about the distribution, economic significance, and preferred host trees of the model *Ips* species. It also provides a summary of recent management methods that use pheromones to control beetle populations. Additionally, future perspectives are discussed, focusing on the development of alternative pheromone-based approaches that could enhance forest pest management strategies, particularly for the most aggressive *Ips* species.

My contribution.

I contributed to this literature review by conceptualizing and researching pheromone biosynthesis in *Ips* species to address the identified research gap. Additionally, I participated in writing the chapters related to pheromone biosynthesis and assisted in developing other chapters and proofreading the final draft.

The full versions of the publications are included in the supplementary file.

5. DISCUSSION.

To address the key hypotheses 1 & 2 presented in Chapter 2, we thoroughly investigated the biosynthetic pathways of the three primary pheromone compounds 2-methyl-3-buten-2-ol, ipsdienol, and *cis*-verbenol in key life stages of *I. typographus* including their genetic basis.

5.1. Pheromone compounds 2-methyl-3-buten-2-ol, *cis*-verbenol, ipsdienol, and related metabolites were produced with variable courses between sexes and across key life stages of *I. typographus*.

In addressing objective 1.1, we confirmed that the aggregation pheromone blend in *I. typographus* consists of 2-methyl-3-buten-2-ol and *cis*-verbenol, both of which were abundantly present in the guts of fed males during colonization. This finding is consistent with earlier studies (Birgersson et al., 1984). Interestingly, we found that 2-methyl-3-buten-2-ol begins to appear in males immediately after they emerge from the colony, although its concentration at this early stage is likely too low to have a significant role in aggregation.

cis-Verbenol, presumed to be derived from the tree precursor *α*-pinene through feeding, as reported in other *Ips* species (Lindström, 1989; Lanne, 1989), was unexpectedly found in greater abundance during the immature stages of both sexes in *I. typographus*. This is a novel finding that has not been previously documented. During these immature stages, when beetles remain beneath the bark, *cis*-verbenol is likely a byproduct of *α*-pinene detoxification, rather than functioning as an aggregation pheromone. Interestingly, as the beetles matured, *cis*-verbenol content disappeared in females and persisted exclusively in mature males, the sex responsible for pheromone release. This observation aligns with its established role in conspecific aggregation (Schlyter et al., 1987), further supporting its functional significance in mature males.

Ipsdienol, a compound unique to *Ips* species and known to play a significant role in pheromone communication among *Ips* bark beetles (Seybold et al., 1995a; Tillman et al., 1998), was detected in *I. typographus*, though in only trace amounts. It was present in marginal quantities in the guts of mated males extracted from mating chambers. However, in *I. typographus*, ipsdienol does not appear to play a major role in overall pheromone function (Schlyter et al., 1987), suggesting its contribution to aggregation in this species is minimal.

To test hypothesis 2, *cis*-verbenol is released from stored fatty acid esters (Chiu et al., 2018), we identified and quantified monoterpenyl fatty acid esters, including verbenyl oleate and myrtenyl oleate, in the fat body of *I. typographus*. This finding aligns with similar results in *D. ponderosae*, where these esters were proposed as potential storage or detoxification conjugates for *trans*-verbenol (Chiu et al., 2018; Blomquist et al., 2021). Our study found that verbenyl oleate and myrtenyl oleate were abundant in immature beetles of both sexes, suggesting that these esters help immobilize monoterpene alcohol byproducts of detoxification during early developmental stages. However, as the beetles matured, verbenyl oleate synthesis persisted only in mature males, mirroring the occurrence pattern of *cis*-verbenol. Notably, we observed a slight reduction in verbenyl oleate content in fed, pheromone-producing males, while *cis*-verbenol levels increased. This suggests that *cis*-verbenol fatty acid esters, present in significant amounts in the fat body, may serve as an alternative reservoir of *cis*-verbenol for adult males. Such a mechanism could be crucial when bark beetles need to produce pheromones but are limited by the conversion of *cis*-verbenol from tree-derived *α*-pinene.

Additionally, other detoxification products, verbenyl, and myrtenyl diglycosides, were identified in the guts of *I. typographus* for the first time. However, their quantity and potential role in pheromone biosynthesis need to be further elucidated.

The analytical approach in this study also detected upstream intermediates of the mevalonate pathway in extracts from the bark beetles' guts, specifically mevalonate-

5-phosphate, dimethylallyl diphosphate, and isopentenyl diphosphate increased in relevant life stages. This provides supporting evidence for the *de novo* biosynthesis of 2-methyl-3-buten-2-ol and ipsdienol via the mevalonate pathway in *I. typographus* males suggested in a preliminary study by Lanne et al. (1989). Additionally, the elevated levels of mevalonate-5-phosphate during the flying stage further support previous findings on the activation of flight muscles driving *de novo* pheromone biosynthesis in other *Ips* species (Ivarsson et al., 1993).

5.2. Mechanism of pheromone production in key life stages and sexes of *I. typographus* involving specific gene families from the mevalonate pathway, cytochrome P450, and esterase.

The objective 1.2 was to explore the genetic basis and provide further evidence for the proposed mechanism of pheromone compound production in key life stages of *I. typographus*.

The mevalonate pathway genes PMK (Ityp06045), HMG-S (Ityp09137), HMG-R (Ityp17150), and IPPI (Ityp04875) were found to upregulate during key pheromone-producing life stages of mature male *I. typographus*. Similar upregulation of mevalonate pathway genes has been reported in other *Ips* species, such as *I. pini* (Keeling et al., 2004) and *I. hauseri* (Fang et al., 2021), but primarily in the context of ipsdienol biosynthesis.

In *I. typographus*, we propose that the upregulation of these genes first time supports the *de novo* biosynthesis of 2-methyl-3-buten-2-ol, the primary component of their aggregation pheromone, as suggested by Lanne et al. (1989).

Interestingly, within *I. typographus* guts of fed males during colonization, we observed substantial overexpression of a putative *isoprenoid-diphosphate synthase* gene (IPDS, Ityp09271), alongside the abundance of 2-methyl-3-buten-2-ol, the key aggregation pheromone. This observation leads us to hypothesize that this specific IPDS may function as a hemiterpenoid prenyl transferase, playing a critical role in the terminal

step of hemiterpene synthesis (refer to Figure 6 for the detailed mevalonate pathway). To date, hemiterpene synthesis has not been described in insects, further underscoring the novelty of our observations.

Based on the upregulation of IPDS, we propose that this enzyme may catalyze the terminal step of 2-methyl-3-buten-2-ol synthesis by converting dimethylallyl diphosphate (DMADP) through a carbocation intermediate, a mechanism that has been documented in plant systems (Fisher, 2000). The identification of this pathway in *I. typographus* suggests that this *IPDS* enzyme may be a hemiterpenoid prenyl transferase responsible for facilitating hemiterpene production in the insect.

We also identified other *prenyltransferase* in *I. typographus* males (Ityp17873, Ityp17861) that were probably involved in ipsdienol synthesis. These sequences correspond to the *GPPS*/*myrcene synthase* previously implicated in pheromone biosynthesis in *Ips* bark beetles, catalyzing the conversion of isopentenyl diphosphate (IPDP) and dimethylallyl diphosphate (DMAPP) into the monoterpene, myrcene (Gilg et al., 2005; Gilg et al., 2009). Notably, this enzyme uniquely produces two different products, GPP and myrcene, unlike most prenyltransferases that generate a single product. The gene encoding this enzyme has been functionally characterized (Gilg et al., 2009). The specific role of another ortholog of *GPPS* (Ityp17861) which we identified in females, remains uncharacterized and requires further investigation.

To confirm the biosynthesis of *cis*-verbenol in *I. typographus* via the oxidation of oxidation of *α*-pinene (Renwick et al., 1976), we screened and analyzed cytochrome P450 (CYP450) genes in the gut of fed males and other life stages. In *I. typographus*, we identified 56 CYP450 genes expressed in gut tissues, out of a total of 84 CYP450 genes present in the beetle genome (Powell et al., 2021). Among the identified CYP450 genes, two candidate genes, Ityp3903 and Ityp0496, were selected from the gut tissue of fed male beetles due to their sequence similarity to CYP6DE1, a functionally characterized gene in *D. ponderosae* known for hydroxylation of *α*-pinene to produce the pheromonal *trans*-verbenol (Chiu et al., 2019b). We propose that these genes may

perform a similar function in *I. typographus*, catalyzing the production of *cis*-verbenol. Additionally, another two candidate genes, Ityp3140 and Ityp3230 aligned with CYP6DE3, knwon for detoxification role in *D. ponderosae* (Nadeau et al., 2017). We propose that these genes may serve a similar detoxification function in *I. typographus* (Ramakrishnan et al., 2022a).

Since most CYP450 genes are multifunctional, distinguishing between their roles in pheromone biosynthesis and detoxification is challenging. This complexity is compounded by the fact that beetle survival also depends on the detoxification of host tree monoterpenes (Reid and Purcell, 2011; Naseer et al., 2023). In the guts of mated males where ipsdienol occurs, we identified two more CYP450 contigs, Ityp1834 and Ityp3153, with sequence similarity to CYP9T1 and CYP9T2, which are linked to ipsdienol biosynthesis through the hydroxylation of myrcene as reported in *I. pini* (Song et al., 2013). Recent studies have proposed CYP450 enzymes, such as CYP6 and CYP9, as candidates for the production of verbenol and ipsdienol in other *Ips* species, including *I. hauseri* (Fang et al., 2021). However, despite the identification of these potential candidates from the multifunctional CYP450 gene family across various *Ips* species, functional validation of the reported genes remains unexplored.

To investigate hypothesis 2, which suggests that verbenol is also released from stored verbenyl fatty acid esters, as proposed for *D. ponderosae* by Chiu et al. (2018), we searched for key esterase and lipase genes in the guts of fed males and immature males of *I. typographus*.

In *I. typographus*, we identified three esterase gene candidates, Ityp7084, Ityp9460, and Ityp11977 which share sequence similarity with the esterase gene in *D. ponderosae* (Bernier et al., 2020) and exhibit correlated expression with the identified verbenyl fatty esters in immature beetles. Since esterication is a reversible process, we propose that Ityp7084 and Ityp9460 may be involved in releasing *cis*-verbenol, while Ityp11977 may function in storing *cis*-verbenol as fatty acid esters.

5.3. Genetic underpinning of the proposed pathways based on the findings.

The outcome of objective 1.3 is the derivation of two biosynthetic pathways (Figure 6 and Figure 7) for the three listed pheromone components and their precursors in *I. typographus*. The modification we propose, based on our findings, deviates from previously published pathways in other *Ips* bark beetles (Bearfield et al., 2009; Chiu et al., 2018).

The biosynthesis of 2-methyl-3-buten-2-ol from the isoprenoid pathway, catalyzed by IPDS, is a modification proposed based on our findings (Figure 6). Additionally, our research proposes that *cis*-verbenol is converted into monoterpenyl fatty acid esters in immature beetles by an ester-synthesizing esterase. In feeding males, these esters are then hydrolyzed by another specific esterase, releasing the pheromone. The proposed pathway includes these esterases, modifying the classical *cis*-verbenol biosynthesis pathway from *α*-pinene (Figure 7).

5.4. Regulatory effects of JH III on the biosynthesis of pheromones metabolites and associated precursors in *I. typographus.*

To evaluate hypothesis 3 and objective 2.1 regarding the regulatory effects of Juvenile Hormone III (JH III) on *I. typographus*, we treated the beetles with JH III to induce pheromone biosynthesis and associated precursors in this bark beetle. The regulation of JH III in bark beetles was specifically chosen to study gene families while avoiding biases from wood digestion and detoxification processes that occur after feeding. This method has not yet been applied to *I. typographus,* and we were the first to attempt it.

The JH III treatment on *I. typographus* strongly increased the *de novo* synthesis of 2-methyl-3-buten-2-ol and ipsdienol, consistent with findings from *I. pini* (Seybold and Tittiger, 2003). Generally, the production of *cis*-verbenol in *Ips* species is induced by feeding on the host tree (Lindström et al., 1989). In JH III treatment of *I. typographus*,

cis-verbenol was also mildly increased, which aligns with recent findings in *I. hauseri* (Fang et al., 2021).

Early biosynthetic studies questioned whether verbenol could be produced *de novo* from synthesized pinene or was exclusively acquired from tree-derived *α*-pinene. This hypothesis was later refuted in *I. duplicatus* when the inhibition of the mevalonate pathway by compactin blocked only ipsdienol production, without affecting *cis*-verbenol production (Ivarsson et al., 1993). From our findings, the slight decrease in the content of verbenyl fatty acid esters in JH III-treated male *I. typographus* correlated with an increase in free *cis*-verbenol. Since pinene is not produced *de novo*, and *cis*-verbenol was detected after JH III treatment, this supports hypothesis 2, suggesting that *cis*-verbenol is also synthesized via verbenyl fatty acid esters mediated biosynthesis, alongside *de novo*-synthesized compounds. This similar trend was observed in female beetles of JH III treated *D. ponderosae*, which produces the pheromone, *trans*-verbenol (Chiu et al., 2018). The gene candidates which could be involved in this biosynthesis are discussed in the next chapter.

JH III also induced the production of other compounds in *I. typographus* with unknown or different biological activity, which were previously identified as male-specific in gut and headspace (Birgersson et al., 1984). The content of verbenone (the oxidized product of verbenol, known as an anti-attractant for *I. typographus*) was also increased by JH III treatment, similar to observations in *I. hauseri* (Fang et al., 2021). This upregulation reflects an increase in the content of its precursor, *cis*-verbenol. Additionally, the male-specific compounds 2-phenylethanol and myrtenol were upregulated in the guts of JH III-treated *I. typographus* males, consistent with earlier findings by Birgersson et al. (1984). However, the biological functions of these two compounds remain unknown.

5.5. Genes and enzymes linked to aggregation pheromone biosynthesis and study of their regulation by JH III treatment on *I. typographus*.

To test objective 2.2, we compared the gene and protein expression patterns to identify pheromone biosynthetic genes and enzymes regulated after JH III treatment in male and female *I. typographus*.

Following JH III treatment in male *I. typographus*, mevalonate pathway genes reported in chapter 5.2, were significantly expressed. This has been previously observed in other *Ips* species, though primarily in the context of ipsdienol production (Keeling et al., 2006). In *I. typographus*, a hemiterpene synthase, IPDS, was upregulated at both the gene and protein levels, which correlated with increased levels of 2-methyl-3-buten-2-ol in treated males, further supporting the role of mevalonate pathway genes in the *de novo* biosynthesis of this hemiterpene. Additionally, the regulatory genes of the mevalonate pathway, HMG-R, and HMG-S, were notably affected by hormonal regulation in *I. typographus* (Bearfield et al., 2009). However, the hormonal stimulation of this pathway may vary between *Ips* species. For example, in *I. paraconfusus*, HMG-R was also shown to be stimulated by JH III, but not in *I. confusus* (Tillman et al., 2004).

Since *cis*-verbenol is induced in *I. typographus* after JH III treatment and CYP450 is a potential gene in synthesizing the compound, we examined the previously proposed gene candidates discussed in Chapter 5.2 for their expression in verbenol-producing male beetles. CYP6450 genes suspected of being involved in verbenol production were reported to be induced by JH III in *I. hauseri* (Fang et al., 2021). This was unexpected, as previous hypotheses suggested that JH III primarily triggers the *de novo* production of pheromonal components (Seybold and Tittiger, 2003). Thus, the finding in *I. typographus* that the candidate genes proposed for *cis*-verbenol synthesis were only minimally induced following JH III treatment aligns with these earlier hypotheses. Interestingly, the candidate genes proposed for detoxification were more highly expressed after JHIII treatment in *I. typographus*, suggesting that JH III may also influence monoterpene detoxification in this species.

Notably, moreover, the CYP450 gene proposed for ipsdienol biosynthesis from myrcene (Sandstrom et al., 2006), as discussed in Chapter 5.2, was significantly induced in *I. typographus* after JH III treatment.

As our findings from the CYP450 gene family studies indicate their minimal involvement in *cis*-verbenol biosynthesis following JH III treatment in *I. typographus*, we further investigated esterases that could support the verbenyl fatty ester storage and release hypothesis. Specifically, we searched for previously identified esterase candidates involved in pheromone storage and release in *I. typographus* after JH III treatment (Chapter 5.2). However, among the listed candidates, we identified only one esterase that is implicated in the storage of verbenyl fatty acid esters in the gut tissue of *I. typographus* after JH III treatment. This finding corresponded with an increase in verbenyl fatty acid ester conjugates in the guts of both sexes following JH III treatments (Chapter 5.4). Since the concept of pheromone storage is newly explored in this thesis for *Ips* species, the identified genes, and this topic merit further investigation.

5.6. Impact of JH III on detoxification mechanism related to the formation of pheromone components in *I. typographus.*

To investigate objective 2.3, we examined the impact of JH III on *I. typographus* detoxification mechanism related to the formation of pheromone components (verbenyl conjugates).

As mentioned in earlier chapters (5.1; 5.5), JH III induction also influences detoxification mechanisms in *I. typographus*. We identified verbenyl diglycosides as detoxification compounds from our research on the key life stages of *I. typographus* (Chapter 5.1). Consequently, we further investigated the presence of these compounds in *I. typographus* after JH III treatment. We found that the content of verbenyl diglycosides was significantly increased in both sexes after JH III treatment.

Based on these findings, we targeted the gene family of glycosyl hydrolases, suspected to be involved in the release of verbenol from verbenyl diglycosides. These conjugates may also serve as storage molecules for verbenol in pheromone-producing males.

Although this gene family was expressed exclusively in the male gut of *I. typographus* after JH III treatment, its expression did not correlate with the occurrence of verbenyl diglycosides in both sexes after JH III treatment. Due to the low quantity of verbenyl diglycosides and the lack of alignment of its content with hydrolase activity, we reject the hypothesis that these conjugates serve as the source of *cis*-verbenol in adult males. Instead, we propose that they function as detoxification products of monoterpenes.

Nevertheless, alongside the effects of JH III on the upregulation of verbenyl fatty acid esters, detoxification-related cytochromes, and verbenyl diglycosides, we conclude that JH III significantly regulates detoxification processes in *I. typographus*. This topic is deserving of further detailed research.

The findings from this thesis support hypotheses 1, 2, and 3, with the specific objectives providing an in-depth understanding of the molecular and metabolite changes related to aggregation pheromone production in the European spruce bark beetles, *I. typographus.*

6. LIMITATIONS AND RECOMMENDATIONS FOR FUTURE DEVELOPMENT OF THE RESEARCH FIELD.

Although this study covers many aspects of pheromone biosynthesis in the bark beetle *Ips typographus*, there are certain limitations. While several potential gene candidates were identified based on relative abundance and their correlation with analytical results, further functional validation of these genes is necessary to support our findings. The logical next step is to research the functional expression of these gene candidates using both *in vivo* and *in vitro* model systems.

The mevalonate pathway genes, HMG-S and IPDS, from *I. typographus* should be functionally validated using established expression systems. *In vitro* assays can be performed by cloning these target genes into bacterial expression vectors, such as pDEST15, to produce N-terminal His-tag fusion proteins in *Escherichia coli*. The concept of pheromone *cis*-verbenol storage and release mechanisms in *Ips* species have been reported for the first time, a topic worth further detailed exploration in the proposed gene families. The identified gene candidates for *cis*-verbenol biosynthesis, including cytochrome P450 and esterase genes need functional validation, which can be carried out in insect cell lines like *Spodoptera frugiperda* (*Sf9*). Expression vectors such as pFastBac and pENTR4 are recommended for use in insect or mammalian cell lines. This approach will aid in characterizing genes/enzymes with specific functions through substrate-specific enzyme assays with the targeted end products (Lancaster et al., 2018; Frick et al., 2013).

For enzyme assays, substrates labelled with radioactive isotopes, including monoterpene enantiomers like (+/-) α-pinene, (+/-) β-pinene, and (+/-) limonene, can be used with necessary variations. This methodology will provide novel insights through established analytical techniques and significantly advance research on pheromone biosynthesis in bark beetles.

7. PRACTICAL APPLICATION OF THESE RESEARCH FINDINGS.

In this postgenomic era, gene manipulation techniques offer new ways to influence pheromone production in bark beetles. To enhance protection methods and prepare for future outbreaks, foresters are increasingly adopting innovative approaches that minimize the impact on non-target insects. One promising development is RNA *interference* (RNA*i*), which selectively silences specific genes, disrupting metabolic pathways to eliminate pests or inhibit pheromone production. RNA*i* allows for targeted pest management while minimizing ecological disruption (Gordon et al., 2007; Zotti et al., 2015).

While RNA*i* offers species-specific advantages, the complexity of gene silencing in Coleoptera insects poses significant challenges. Currently, there is limited evidence of RNAi research being applied to bark beetles (Joga et al., 2016). The objective is to target species-specific, non-lethal genes related to the bark beetle's aggregation behavior, thereby minimizing ecological harm. A similar strategy was demonstrated in the moth *Helicoverpa armigera*, where gene silencing altered reproduction by targeting genes responsible for sex pheromone production (Dong et al., 2017).

In wood-feeding insects, *ds*RNA can be delivered by spraying it onto the tree trunk (Li et al., 2015) or injecting it into the sap stream (Hunter et al., 2012), could effectively silencing pheromone biosynthetic genes during bark beetle feeding. Research into aggregation pheromones may provide insights into the ecology of aggressive species and inform strategies to control bark beetle populations, keeping them at endemic levels while preserving their ecological benefits.

8. CONCLUSION.

In conclusion, these findings establish a foundation for understanding the genetic mechanisms behind pheromone biosynthesis in *Ips typographus*. Juvenile hormone III (JH III) regulation on *I. typographus* was conducted for the first time and this approach facilitated the expression of relevant gene families from gut tissue, which are critical for pheromone production.

- We demonstrated the involvement of mevalonate pathway gene families in the gut of *I. typographus*, contributing to the *de novo* biosynthesis of the aggregation pheromones 2-methyl-3-buten-2-ol and ipsdienol during key life stages of the beetle.
- Furthermore, *cis*-verbenol and its relative precursors, verbenyl fatty acid esters, were identified in greater abundance from the immature stages of both sexes of *I. typographus*. This represents a novel finding that has not been previously documented in *Ips* species.
- A novel *isoprenoid diphosphate synthase* (IPDS) was identified as a key gene in the mevalonate pathway from *I. typographus* key life stages, making it a promising target for inhibiting the biosynthesis of 2-methyl-3-buten-2-ol.
- We identified cytochrome P450 (CYP450) gene families involved in the biosynthesis of *cis*-verbenol, as well as an esterase gene family related to *cis*-verbenol storage and release functions in *I. typographus*.
- CYP450 gene candidates implicated in ipsdienol biosynthesis were identified in *I. typographus* based on sequence similarity to functionally known genes from other bark beetle species.
- The JH III application on *I. typographus* evidently induced the *de novo* synthesis of 2-methyl-3-buten-2-ol and ipsdienol.
- In addition to these pheromonal components, *cis*-verbenol, verbenone other male-specific compounds with unknown functions, such as myrtenol and 2-phenylethanol, were identified and quantified from JHIII-treated *I. typographus* gut.

- JH III also induced the mevalonate pathway genes HMG-S and IPDS in the gut proteome analysis of male *I. typographus*.
- JH III induced CYP450 gene candidates involved in ipsdienol synthesis and detoxification over *cis*-verbenol synthesizing candidate genes.
- Additionally, JH III treatment induced esterase gene candidates implicated in the formation of verbenyl fatty acid esters in *I. typographus* gut tissue.
- By inducing verbenyl diglycosides in both sexes of *I. typographus*, JH III has influenced detoxification reactions related to pheromone components.

Taken together, this thesis synthesizes and contextualizes findings from four scientific articles, presenting novel results that were previously unknown in this field of *I. typographus* pheromone biosynthesis. Additionally, we suggest future research directions on aggregation pheromones of bark beetles, and potential applications of the findings for developing pest management strategies in forestry.

9. REFERENCES.

1. Amman GD. 1989. Proceedings-Symposium on the Management of Lodgepole Pine to Minimize Losses to the Mountain Pine Beetle. Intermountain Research Station, Forest Service, US Department of Agriculture, 262.
2. Andrle, M. 2017. Conifers are more at home here than previously thought. Charles University Archive, 1–4.
3. Annila, E. 1969. Influence of temperature upon the development and voltinism of *Ips typographus* L. (Coleoptera, Scolytidae). Annales Zoologici Fennici, Societas Biologica Fennica Vanamo, 161-208.
4. Aw, T., Schlauch, K., Keeling, C.I., Young, S., Bearfield, J.C., Blomquist, G.J., Tittiger, C. 2010. Functional genomics of mountain pine beetle *(Dendroctonus ponderosae*) midguts and fat bodies. BMC Genomics, 11, 1-12.
5. Bakke, A. 1976. Spruce Bark Beetle, *Ips typographus* " Pheromone Production and Field Response. Naturwissenschaften, 63.
6. Bakke, A., Froyen, P. & Skatteböl, L. 1977. Field response to a new pheromonal compound isolated from *Ips typographus*. Naturwissenschaften, 64(2), 98-99.
7. Basile S, Stříbrská B, Kalyniukova A, Hradecký J, Synek J, Gershenzon J and Jirošová A. 2024. Physiological and biochemical changes of *Picea abies* (L.) during acute drought stress and their correlation with susceptibility to *Ips typographus* (L.) and *I. duplicatus* (Sahlberg). Frontiers in Forest Global Change, 7:1436110.
8. Bearfield, J.C., Henry, A.G., Tittiger, C., Blomquist, G.J., Ginzel, M.D., 2009. Two Regulatory Mechanisms of Monoterpenoid Pheromone Production in *Ips* sp. Of Bark Beetles. Journal of chemical ecology, 689–697.
9. Benton, H.P., Want, E.J., Ebbels, T.M.D., 2010. Correction of mass calibration gaps in liquid chromatography-mass spectrometry metabolomics data. Bioinformatics, 26 2488–2489.
10. Bentz, B.J., Rgnire, J., Fettig, C.J., Hansen, E.M., Hayes, J.L., Hicke, J.A., Kelsey, R.G., Negron, J.F., Seybold, S.J., 2010. Climate change and bark beetles of the western United States and Canada: Direct and indirect effects. Bioscience, 60, 602–613
11. Biedermann, P.H.W., Müller, J., et al. 2019. Bark Beetle Population Dynamics in the Anthropocene: Challenges and Solutions. Trends in ecology & evolution, 34, 914–924.
12. Birgersson G. and Bergström G., 1989. Volatiles released from individual spruce bark beetle entrance holes Quantitative variations during the first week of attack. Journal of chemical ecology, 15(10):2465-83.
13. Birgersson, G., Schlyter F., Löfqvist J. & Bergström G. 1984. Quantitative variation of Pheromone components in the spruce bark beetle *Ips typographus* from different attack phases. Journal of chemical ecology, 10.
14. Blomquist, G. J., Tittiger, C., MacLean, M. & Keeling, C. I., 2021. Cytochromes P450: terpene detoxification and pheromone production in bark beetles. Current Opinion in Insect Science, 43, 97-102.

15. Blomquist, G.J., Figueroa-Teran, R., Aw, M., Song, M.M., Gorzalski, A., Abbott, N.L., Chang, E., Tittiger, C., 2010. Pheromone production in bark beetles. Insect Biochemistry and Molecular Biology, 40, 699–712.
16. Bohlmann, J., Gershenzon, J., 2009. Old substrates for new enzymes of terpenoid biosynthesis. Proceedings of the National Academy of Sciences, 106, 10402–10403.
17. Brand, J.M., Bracke, J.W., Britton, L.N., Markovetz, A.J., Barras, S.J., 1976. Bark beetle pheromones: production of verbenone by a mycangial fungus of *Dendroctonus frontalis*. Journal of Chemical Ecology 2, 195-199.
18. Brand, J.M., Bracke, J.W., Markovetz, A.J., Wood, D.L. and Browne, L.E. 1975. Production of verbenol pheromone by a bacterium isolated from bark beetles. Nature, 254(5496), 136-137.
19. Byers, J. A., & Birgersson, G. 2012. Host-tree monoterpenes and biosynthesis of aggregation pheromones in the bark beetle *Ips paraconfusus*. Psyche: A Journal of Entomology, 539624.
20. Byers, J.A. and Wood, D.L. 1981 Antibiotic-induced inhibition of pheromone synthesis in a bark beetle. Science, 213(4509), pp.763-764.
21. Byers, J.A., 1989. Chemical ecology of bark beetles. Experientia, 45(3), 271-283.
22. Byers, J.A., Birgersson, G., 1990. Pheromone production in a bark beetle independent of myrcene precursor in host pine species. Naturwissenschaften, 77, 385-387
23. Chakraborty, A., Modlinger, R., Ashraf, M. Z., Synek, J., Schlyter, F., and Roy, A. 2020. Core mycobiome and their ecological relevance in the gut of five *Ips* bark beetles (Coleoptera: Curculionidae: Scolytinae). Frontiers in Microbiology, 11:568853.
24. Chiu C.C., Keeling C.I., Henderson H.M., Bohlmann J. 2019a. Functions of mountain pine beetle cytochromes P450 CYP6DJ1, CYP6BW1 and CYP6BW3 in the oxidation of pine monoterpenes and diterpene resin acids. PLoS ONE, 14(5): e0216753.
25. Chiu, C. C., Keeling, C. I., and Bohlmann, J. 2019b. The cytochrome P450 CYP6DE1 catalyzes the conversion of *α*-pinene into the mountain pine beetle aggregation pheromone *trans*-verbenol. Scientific Reports, 9:1477.
26. Chiu, C.C., Keeling, C. I., Bohlmann J., 2017. Toxicity of pine monoterpenes to mountain pine beetle. Scientific Reports, 7:8858.
27. Chiu, C.C., Keeling, C.I., Bohlmann, J., 2018. Monoterpenyl esters in juvenile mountain pine beetle and sex-specific release of the aggregation pheromone *trans*-verbenol. Proceedings of the National Academy of Sciences of the United States of America, 2–7.
28. Chong, J., Soufan, O., Li, C., Caraus, I., Li, S.Z., Bourque, G., Wishart, D.S., Xia, J.G., 2018. MetaboAnalyst 4.0: towards more transparent and integrative metabolomics analysis. Nucleic acids research, 46, W486–W494.
29. Cloonan, N. et al. 2008 Stem cell transcriptome profiling via massive-scale mRNA sequencing. Nature Methods, 5, 613–619.
30. Cox, J. & Mann, M., 2008. MaxQuant enables high peptide identification rates, individualized p.p.b.-range mass accuracies and proteome-wide protein quantification. Nature Biotechnology, 26(12), 1367-1372.

31. Cox, J., Hein, M. Y., Luber, C. A., Paron, I., Nagaraj, N. & Mann, M., 2014. Accurate Proteome-wide Label-free Quantification by Delayed Normalization and Maximal Peptide Ratio Extraction, Termed MaxLFQ. Molecular & Cellular Proteomics, 13(9), 2513-2526.
32. Cristino, A. S., Nunes, F. M., Lobo, C. H., Bitondi, M. M., Simões, Z. L., da Fontoura Costa, L., Lattorff, H. M., Moritz, R. F., Evans, J. D., & Hartfelder, K., 2006. Caste development and reproduction: a genome-wide analysis of hallmarks of insect eusociality. Insect molecular biology, 15(5), 703–714.
33. Dickens, J. C. 1981. Behavioural and electrophysiological responses of the bark beetle, *Ips typographus*, to potential pheromone components. Physiological Entomology, 6(3), 251-261.
34. Dong K., Sun L., Liu J. T., Gu S. H., et al., 2017. RNA*i*-Induced Electrophysiological and Behavioral Changes Reveal Two Pheromone Binding Proteins of *Helicoverpa armigera* Involved in the Perception of the Main Sex Pheromone Component Z11-16, Ald. Journal of Chemical Ecology, 43(2):207-214.
35. EEA 2014. European forest ecosystems—state and trends. EEA Report 5, European Environment Agency, pp. 128.
36. Eigenheer, A.L., Keeling, C.I., Young, S. and Tittiger, C. 2003. Comparison of gene representation in midguts from two phytophagous insects, Bombyx mori and *Ips pini*, using expressed sequence tags. Gene, 316, pp.127-136.
37. Emlen, D., Szafran, Q., Corley, L. & Dworkin, I., 2006. Insulin signaling and limb-patterning: candidate pathways for the origin and evolutionary diversification of beetle 'horns. Heredity, 97, 179–191.
38. Erbilgin, N., Krokene, P., Kvamme, T., & Christiansen, E. 2007. A host monoterpene influences *Ips typographus* (Coleoptera: Curculionidae, Scolytinae) responses to its aggregation pheromone. Agricultural and Forest Entomology, 9(2), 135-140.
39. Ernst, U.R., Votavová, A., Hanus, R., Valterová, I., Jedlicka, P., 2016. Gene Expression Dynamics in Major Endocrine Regulatory Pathways along the Transition from Solitary to Social Life in a Bumblebee, *Bombus terrestris*. Frontiers in Physiology, 7, 1–20.
40. Fang, J. X., Du, H. C., Shi, X., Zhang, S. F., Liu, F., Zhang, Z., Zu, P. J. & Kong, X. B., 2021. Monoterpenoid signals and their transcriptional responses to feeding and juvenile hormone regulation in bark beetle *Ips hauseri*. Journal of Experimental Biology, 224(9), 9.
41. Felicijan, Mateja & Novak, Metka & Krasevec, Nada & Krajnc, Andreja. 2015. Antioxidant defences of Norway spruce bark against bark beetles and its associated blue-stain fungus. Agricultura. 12.
42. Figueroa-Teran, R., Pak, H., Blomquist, G. J., & Tittiger, C. 2016. High substrate specificity of ipsdienol dehydrogenase (IDOLDH), a short-chain dehydrogenase from *Ips pini* bark beetles. The journal of biochemistry, 160(3), 141-151.
43. Figueroa-Teran, R., Welch, W.H., Blomquist, G.J., Tittiger, C., 2012. Ipsdienol dehydrogenase (IDOLDH): a novel oxidoreductase important for *Ips pini* pheromone production. Insect biochemistry and molecular biology, 42, 81–90.

44. Fish, RH., Browne, LE., & Bergot, BJ. 1984. Pheromone biosynthetic pathways: Conversion of ipsdienone to (−)-ipsdienol, a mechanism for enantioselective reduction in the male bark beetle, *Ips paraconfusus*. Journal of chemical ecology, 10, 1057-1064.
45. Fish, RH., Browne, LE., Wood, DL., & Hendry, LB. 1979. Pheromone biosynthetic pathways: Conversions of deuterium labeled ipsdienol with sexual and enantioselectivity in *Ips paraconfusus* Lanier. Tetrahedron Letters, 20 (17), 1465-1468.
46. Fisher A. J., Baker B. M., Greenberg J.P. and Fall R. 2000. Enzymatic Synthesis of Methylbutenol from Dimethylallyl Diphosphate in Needles of *Pinus sabiniana*. Archives of Biochemistry and Biophysics, 128-134,
47. Fisher, K.E., Tillett, R.L., Fotoohi, M., Caldwell, C., Petereit, J., Schlauch, K., Tittiger, C., Blomquist, G.J. and MacLean, M. 2021. RNA-Seq used to identify ipsdienone reductase (IDONER): a novel monoterpene carbon-carbon double bond reductase central to *Ips confusus* pheromone production. Insect Biochemistry and Molecular Biology, 129, p.103513.
48. Frick, S., Nagel, R., Schmidt, A., Bodemann, R.R., Rahfeld, P., Pauls, G., Brandt, W., Gershenzon, J., Boland, W., Burse, A., 2013. Metal ions control product specificity of isoprenyl diphosphate synthases in the insect terpenoid pathway. Proceedings of the National Academy of Sciences of the United States of America, 110, 4194–4199
49. Frühbrodt, T., Schebeck, M., Andersson, M.N. et al. 2024. Verbenone—the universal bark beetle repellent? Its origin, effects, and ecological roles. Journal of Pest Sciences, 97, 35–71.
50. Galko, J., Nikolov, C., Kunca, A., Vakula, J., Gubka, A., Zúbrik, M., Rell, S., Konôpka, B., 2016. Effectiveness of pheromone traps for the European spruce bark beetle: A comparative study of four commercial products and two new models. Central European Forestry Journal, 62, 207–215.
51. Gilg, A. B., Bearfield, J. C., Tittiger, C., Welch, W. H. & Blomquist, G. J., 2005. Isolation and functional expression of an animal geranyl diphosphate synthase and its role in bark beetle pheromone biosynthesis. Proceedings of the National Academy of Sciences of the United States of America, 102(28), 9760-9765.
52. Gilg, A. B., Tittiger, C., Blomquist, G. J., 2009. Unique animal *prenyltransferase* with monoterpene synthase activity. Naturwissenschaften, 96, 731–735.
53. Goodman, W.G. & Cusson, M., 2012. The Juvenile Hormones. Insect Endocrinology, 8, 310-365.
54. Gordon K.H.J., Waterhouse P.M. 2006. Small RNA viruses of insects: expression in plants and RNA silencing B.C. Bonning (Ed.), Insect Viruses: Biotechnological Applications, Elsevier, San Diego, 459-502.
55. Gordon, K. H., and Waterhouse, P. M., 2007. RNAi for insect-proof plants. Nature Biotechnology, 25, 1231–1232.
56. Gray, D. W. 2002. Field response of *Ips paraconfusus, Dendroctonus brevicomis*, and their predators to 2-methyl-3-buten-2-ol, a novel alcohol emitted by ponderosa pine. Journal of Chemical Ecology, 28, 1583-1597.

57. Gries, 1990. Conversion of phenylalanine to toluene and 2-phenylethanol by the pine engraver, *Ips pini* (Say) (Coleoptera, Scolytidae). Experientia, 46, 329–331.
58. Hall, G.M., Tittiger, C., Andrews, G.L., Mastick, G.S., Kuenzli, M., Luo, X., Seybold, S.J., Blomquist, G.J., 2002. Midgut tissue of male pine engraver, *Ips pini*, synthesizes monoterpenoid pheromone component ipsdienol de novo. Naturwissenschaften, 89, 79–83.
59. Hebert, A. S., Richards, A. L., Bailey, D. J., Ulbrich, A., Coughlin, E. E., Westphall, M. S. & Coon, J. J., 2014. The One Hour Yeast Proteome. Molecular & Cellular Proteomics, 13(1), 339-347.
60. Hlásny T, Krokene P, Liebhold A, Montagné-Huck C, Müller J, Qin H, Raffa K, Schelhaas MJ, Seidl R, Svoboda M, Viiri H. 2019. Living with bark beetles: impacts, outlook and management options. European Forest Institute, 8. 1-52.
61. Hlásny, T., Konig, L., Krokene, P., Lindner, M., Montagné-Huck, C., Muller, J., Qin, H., Raffa, K. F., Schelhaas, M. J., Svoboda, M., Viiri, H. & Seidl, R., 2021. Bark Beetle Outbreaks in Europe: State of Knowledge and Ways Forward for Management. Current Forestry Reports, 7(3), 138-165.
62. Hlásny, T.; Barka, I.; Merganičová, K.; Křístek, Š.; Modlinger, R.; Turčáni, M.; Marušák, R. 2022. A New Framework for Prognosing Forest Resources under Intensified Disturbance Impacts: Case of the Czech Republic. Forest Ecology and Management, 523, 120483.
63. Huber, D.P.W., Erickson, M.L., Leutenegger, C.M., Bohlmann, J. and Seybold, S.J. 2007. Isolation and extreme sex-specific expression of cytochrome P450 genes in the bark beetle, *Ips paraconfusus*, following feeding on the phloem of host ponderosa pine, Pinus ponderosa. Insect molecular biology, 16(3), pp.335-349.
64. Hughes, P. R. (1974) Myrcene - Precursor of pheromones in *Ips* beetles. Journal of Insect Physiology, 20(7), 1271-1275.
65. Hunt, D. W., & Borden, J. H. 1990. Conversion of verbenols to verbenone by yeasts isolated from *Dendroctonus ponderosae* (Coleoptera: Scolytidae). Journal of Chemical Ecology, 16 (4), 1385-1397.
66. Hunter W.B., Glick E., Paldi N., Bextine B. R. 2012. Advances in RNA *interference*: *ds*RNA Treatment in Trees and Grapevines for Insect Pest Suppression. Southwestern Entomologist, 37(1):85-87.
67. Ivarsson P., Blomquist G. J. & Seybold S. J. 1997. In Vitro Production of the Pheromone Intermediates Ipsdienone and Ipsenone by the Bark Beetles *Ips pini* (Say) and *I. paraconfusus* Lanier (Coleoptera: Scolytidae). Naturwissenschaften, 84, 454–457.
68. Ivarsson, P. & Birgersson, G. 1995. Regulation and biosynthesis of pheromone components in the double-spined bark beetle *Ips duplicatus* (Coleoptera, Scolytidae). Journal of Insect Physiology, 41(10), 843-849.
69. Ivarsson, P., Schlyter, F., Birgersson, G., 1993. Demonstration of de novo pheromone biosynthesis in *Ips duplicatus* (Coleoptera: Scolytidae): inhibition of ipsdienol and *E*-

myrcenol production by compactin. Insect Biochemistry and Molecular Biology, 23, 655-662
70. Jansen, S., Konrad, H. & Geburek, T. The extent of historic translocation of Norway spruce forest reproductive material in Europe. Annals of Forest Science 74, 56 (2017).
71. Jindra, M. & Bittova, L. 2020. The juvenile hormone receptor as a target of juvenoid "insect growth regulators". Archives of Insect Biochemistry and Physiology, 103(3), 7.
72. Jindra, M., Palli, S. R. & Riddiford, L. M. 2013. The Juvenile Hormone Signaling Pathway in Insect Development. In: Berenbaum, M. R. (ed.) Annual Review of Entomology, Vol 58. 181-204.
73. Jindra, M., Palli, S. R. & Riddiford, L. M. 2013. The Juvenile Hormone Signaling Pathway in Insect Development. In: Berenbaum, M. R. (ed.). Annual Review of Entomology, Vol 58. 181-204.
74. Jirošová A, Modlinger R, Hradecký J, Ramakrishnan R, Beránková K and Kandasamy D. 2022. Ophiostomatoid fungi synergize attraction of the Eurasian spruce bark beetle, *Ips typographus* to its aggregation pheromone in field traps. Frontiers in Microbiology, 13:980251.
75. Joga MR, Zotti MJ, Smagghe G and Christiaens O. 2016. RNA*i* Efficiency, Systemic Properties, and Novel Delivery Methods for Pest Insect Control: What We Know So Far. Frontiers in physiology, 7:553.
76. Joga, M. R., Moglicherla K., Smagghe G and Roy A. 2021 RNA *interference*-based forest protection products (FPPs) against wood-boring coleopterans: Hope or hype? Frontiers in Plant Science, 12: 733608.
77. Kandasamy, D., Gershenzon, J., Andersson, M.N. et al. 2019. Volatile organic compounds influence the interaction of the Eurasian spruce bark beetle (*Ips typographus*) with its fungal symbionts. The ISME journal, 13, 1788–1800.
78. Kandasamy, D., Zaman R, Nakamura Y, Zhao T, Hartmann H, Andersson MN, et al. 2023. Conifer-killing bark beetles locate fungal symbionts by detecting volatile fungal metabolites of host tree resin monoterpenes. PLoS Biology, 21(2): e3001887.
79. Kautz, M.; Schopf, R.; Ohser, J. The “Sun-Effect”: Microclimatic Alterations Predispose Forest Edges to Bark Beetle Infestations. European Journal of Forest Research, 2013, 132, 453–465.
80. Keeling, C. I., & Bohlmann, J. 2006. Genes, enzymes and chemicals of terpenoid diversity in the constitutive and induced defence of conifers against insects and pathogens. New Phytologist, 170(4), 657-675.
81. Keeling, C. I., Bearfield, J. C., Young, S., Blomquist, G. J., & Tittiger, C. 2006. Effects of juvenile hormone on gene expression in the pheromone-producing midgut of the pine engraver beetle, *Ips pini*. Insect Molecular Biology, 15(2), 207-216.
82. Keeling, C.I., Blomquist, G.J., Tittiger, C., 2004. Coordinated gene expression for pheromone biosynthesis in the pine engraver beetle, *Ips pini* (Coleoptera: Scolytidae). Naturwissenschaften, 91, 324–328.
83. Keeling, C.I., Li, M., Sandhu, H.K., Henderson, H., Man, M., Yuen, S. 2016. Quantitative metabolome, proteome and transcriptome analysis of midgut and fat body tissues in

the mountain pine beetle, *Dendroctonus ponderosae* Hopkins, and insights into pheromone biosynthesis. Insect biochemistry and molecular biology, 70, 170–183.
84. Klimetzek, D., & Francke, W. 1980. Relationship between the enantiomeric composition of *α*-pinene in host trees and the production of verbenols in *Ips* species. Experientia, 36(12), 1343-1345.
85. Kogan, M., 1998. Integrated pest management: Historical perspectives and contemporary developments. Annual review of entomology, 43, 243–270.
86. Kohnle, U., Vité, J.P., Erbacher, C., Bartels, J. and Francke, W. 1988. Aggregation response of European engraver beetles of the genus *Ips* mediated by terpenoid pheromones. Entomologia experimentalis et applicata, 49(1-2), pp.43-53.
87. Kuhn A, Hautier L, San Martin G. 2022. Do pheromone traps help to reduce new attacks of *Ips typographus* at the local scale after a sanitary cut?. PeerJ, 10:e14093
88. Lancaster, et al., 2018. *De novo* formation of an aggregation pheromone precursor by an isoprenyl diphosphate synthase-related terpene synthase in the harlequin bug. Proceedings of the National Academy of Sciences of the United States of America, 115, E8634–E8641.
89. Lanne, B.S., Ivarsson, P., Johnson, P., Bergström, G., Wassgren, A.B., 1989. Biosynthesis of 2-methyl-3-buten-2-ol, a pheromone component of *Ips typographus* (Coleoptera: Scolytidae). Insect Biochemistry. 19, 163-168.
90. Lehmanski, L. M., Kandasamy, D., Andersson, M. N., Netherer, S., Alves, E. G., Huang, J., et al. 2023. Addressing a century old hypothesis–do pioneer beetles of *Ips typographus* use volatile cues to find suitable host trees?. New Phytologist, 238, 1762–1770.
91. Leinwand, S. G., & Scott, K., 2021. Juvenile hormone drives the maturation of spontaneous mushroom body neural activity and learned behavior. Neuron, 109(11), 1836–1847.
92. Leufvén, A., Bergström, G. & Falsen, E. Interconversion of verbenols and verbenone by identified yeasts isolated from the spruce bark beetle, *Ips typographus*. Journal of Chemical Ecology, 10, 1349–1361 (1984).
93. Li H., Guan R., Guo H., Miao X. 2015. New insights into an RNA*i* approach for plant defence against piercing-sucking and stem-borer insect pests. Plant Cell and Environment, 38(11), 2277-2285.
94. Lindström, M., Norin, T., Birgersson, G. et al. 1989. Variation of enantiomeric composition of α-pinene in norway spruce,Picea abies, and its influence on production of verbenol isomers by *Ips typographus* in the field. Journal of Chemical Ecology, 15, 541–548.
95. Lorio P. L., Mason G. N., Autry G. L., 1982. Stand Risk Rating for the Southern Pine Beetle: Integrating Pest Management with Forest Management, Journal of Forestry, Volume 80, 4, 212–214.
96. Lu, F. 1999. Origin and endocrine regulation of pheromone biosynthesis in the pine bark beetles, *Ips pini* (Say) and *Ips paraconfusus* Lanier (Coleoptera: Scolytidae). University of Nevada, Reno
97. Lubojácký, J., Lorenc, F., Véle, A., Knížek, M., & Liška, J. 2022. Výskyt lesních škodlivých faktorů v Česku v roce 2022. Zprav. Škodliví činitelé v lesích Česka

2021/2022–Škody zvěří. Sborník referátů z celostátního semináře s mezinárodní účastí. Průhonice, 6, 17–26.
98. MacLean M., Nadeau J., Gurnea T., Tittiger C., Blomquist G. J., 2018. Mountain pine beetle (*Dendroctonus ponderosae*) CYP4Gs convert long and short chain alcohols and aldehydes to hydrocarbons. Insect biochemistry and molecular biology, 102, 11-20.
99. Marini L., Okland B., Jönsson AM., Bentz B., Carroll A., Forster B., Grégoire J-C., Hurling R., Nageleisen LM., Netherer S., Ravn HP., Weed A., Schroeder M., 2017. Climate drivers of bark beetle outbreak dynamics in Norway spruce forests. Ecography 40: 1426-1435.
100. Martin D, Bohlmann J, Gershenzon J, Francke W, Seybold SJ. 2003. A novel sex-specific and inducible monoterpene synthase activity associated with a pine bark beetle, the pine engraver, *Ips pini*. Naturwissenschaften, 90, 173-179
101. Miyakawa H., Watanabe M., Araki M., Ogino Y., Miyagawa S., Iguchi T. 2018. Juvenile hormone-independent function of Krüppel homolog 1 in early development of water flea Daphnia pulex. Insect biochemistry and molecular biology, Volume 93, 12-18.
102. Moliterno A.A.C., Jakuš R., Modlinger R., Unelius C.R., Schlyter F. and Jirošová A. 2023. Field effects of oxygenated monoterpenes and estragole combined with pheromone on attraction of *Ips typographus* and its natural enemies. Frontiers in forests and global change, 6:1292581.
103. Nadeau, J.A., Petereit, J., Tillett, R.L., Jung, K., Fotoohi, M., MacLean, M., Young, S., Schlauch, K., Blomquist, G.J., Tittiger, C., 2017. Comparative transcriptomics of mountain pine beetle pheromone-biosynthetic tissues and functional analysis of CYP6DE3. BMC Genomics, 18, 311.
104. Nakamura, C.E., Abeles, R.H., 1985. Mode of interaction of b-hydroxy-b-methyl-glutaryl coenzyme A reductase with strong binding inhibitors: compactin and related compounds. Biochemistry, 24, 1364-1376
105. Nardi, J. B., Young, A. G., Ujhelyi, E., Tittiger, C., Lehane, M. J. & Blomquist, G. J., 2002 Specialization of midgut cells for synthesis of male isoprenoid pheromone components in two scolytid beetles, *Dendroctonus jeffreyi* and *Ips pini*. Tissue & Cell, 34(4), 221-231.
106. Naseer, A., Mogilicherla, K., Sellamuthu, G. & Roy, A., 2023. Age matters Life-stage, tissue, and sex-specific gene expression dynamics in *Ips typographus* (Coleoptera: Curculionidae: Scolytinae). Frontiers in forests and global change, 6.
107. Netherer, S., et al., 2024. Drought increases Norway spruce susceptibility to the Eurasian spruce bark beetle and its associated fungi. New Phytologist 242, 1000-1017.
108. Netherer, S., Kandasamy, D., Jirosová, A. et al. 2021. Interactions among Norway spruce, the bark beetle *Ips typographus* and its fungal symbionts in times of drought. Journal of Pest Science, 94, 591–614.
109. Paynter, Q.E., Anderbrant, O. & Schlyter, F. 1990. Behavior of male and female spruce bark beetles,*Ips typographus*, on the bark of host trees during mass attack. Journal of Insect Behavior, 3, 529–543.

110. Peltonen M., 1999. Windthrow and dead-standing trees as bark beetle breeding material at forest-clearcut edge. Scandinavian Journal of Forest Research, 14, pp. 505-511
111. Powell, D., Grosse-Wilde, E., Krokene, P., Roy, A., Chakraborty, A., Löfstedt, C., Vogel, H., Andersson, M. N. & Schlyter, F., 2021. A highly contiguous genome assembly of the Eurasian spruce bark beetle, *Ips typographus*, provides insight into a major forest pest. Communications Biology, 4(1), 9;4(1):1059.
112. Qiu, Y., Tittiger, C, et al. 2012. An insect–specific P450 oxidative decarbonylase for cuticular hydrocarbon biosynthesis. Proceedings of the National Academy of Sciences of the United States of America, 109, 14858–14863.
113. Raffa, K. F., Andersson, M.N., Schlyter, F., 2016. Host Selection by Bark Beetles: Playing the Odds in a High-Stakes Game, 1st ed. In Advances in insect physiology, 1-74.
114. Raffa, K., 1983. The Role of Host Plant Resistance in the Colonization Behavior and Ecology of Bark Beetles (Coleoptera: Scolytidae). Ecological monographs, 53, 27–49.
115. Ramakrishnan R., Roy A., Hradecký J., Kai M., Harant K., Svatoš A., Jirošová A*. 2024. Juvenile Hormone III Induction Reveals Key Genes in General Metabolism, Pheromone Biosynthesis, and Detoxification in Eurasian Spruce Bark Beetle. Frontiers in forests and global change, 6:1215813.
116. Ramakrishnan R., Shewale M. K., Strádal J., Hani U., Gershenzon J, Jirošová A*. Aggregation Pheromones in the Bark Beetle genus *Ips*: Advances in Biosynthesis, Sensory Perception, and Forest Management Applications (Manuscript).
117. Ramakrishnan, R., Hradecký, J., Roy, A., Kalinová, B., Mendezes C. R., Synek, J., Bláha, J., Svatoš, A., Jirošová, A., 2022a Metabolomics and transcriptomics of pheromone biosynthesis in an aggressive forest pest *Ips typographus*. Insect biochemistry and molecular biology, 0965-1748.
118. Ramakrishnan, R., Roy, A., Kai, M. R., Svatos, A. & Jirošová, A., 2022b. Metabolome and transcriptome related dataset for pheromone biosynthesis in an aggressive forest pest *Ips typographus*. Data in Brief, 41, 26.
119. Rappsilber, J., Mann, M. & Ishihama, Y., 2007. Protocol for micro-purification, enrichment, pre-fractionation and storage of peptides for proteomics using StageTips. Nature Protocols, 2(8), 1896-1906.
120. Reid, M.L., Purcell, J.R.C. 2011. Condition-dependent tolerance of monoterpenes in an insect herbivore. Arthropod-Plant Interactions 5, 331–337.
121. Renwick, J. A. A., Hughes, P. R. & Krull, I. S., 1976. Selective production of *cis*-verbenol and *trans*-verbenol from (-)- and (+)-*α*-pinene by a bark beetle. Science, 191(4223), 199-201.
122. Renwick, J.A.A. and Dickens, J.C. 1979. Control of pheromone production in the bark beetle, *Ips cembrae*. Physiological Entomology, 4(4), pp.377-381.
123. Riddiford LM. 2012. How does juvenile hormone control insect metamorphosis and reproduction?. General and comparative endocrinology, 179, pp. 477-484.

124. Riddiford, L. M., Cherbas, P. & Truman, J. W., 2001. Ecdysone receptors and their biological actions. Vitamins and Hormones - Advances in Research and Applications, Vol 60, 60, 1-73
125. Roy, A., George, S., Palli, S.R., 2017. Multiple functions of CREB-binding protein during postembryonic development: identification of target genes. BMC Genomics 1–14.
126. Sandstrom P, Welch WH, Blomquist GJ, Tittiger C. 2006. Functional expression of a bark beetle cytochrome P450 that hydroxylates myrcene to ipsdienol. Insect biochemistry and molecular biology, Nov; 36(11):835-45.
127. Sandstrom, P., Ginzel, M. D., Bearfield, J. C., Welch, W. H., Blomquist, G. J., & Tittiger, C. 2008. Myrcene hydroxylases do not determine enantiomeric composition of pheromonal ipsdienol in *Ips* spp. Journal of Chemical Ecology, 34, 1584-1592.
128. Schiebe, C., Unelius C. R., Ganji S., Binyameen M., Birgersson G., and SchlyterF. 2019. Styrene, (+)-*Trans*-(1*R*,4*S*,5*S*)-4-Thujanol and Oxygenated Monoterpenes Related to Host Stress Elicit Strong Electrophysiological Responses in the Bark Beetle *Ips typographus*. Journal of Chemical Ecology, 45 (5–6): 474–89.
129. Schlyter F., and Cederholm I. 1981. Separation of the sexes of living spruce bark beetles, *Ips typographus* (L.) (Coleoptera: Scolytidae). Zeitschrift für angewandte Entomologie, 92:42-47.
130. Schlyter F., and Löfqvist J. 1986. Response of walking spruce bark beetles *Ips typographus* to pheromone produced in different attack phases. Entomologia experimentalis et applicate, 41.3, 219-230.
131. Schlyter, F., Birgersson, G., Byers, J.A., Löfqvist, J., Bergström, G., 1987. Field response of spruce bark beetle, *Ips typographus* to aggregation pheromone candidates. Journal of Chemical Ecology, 13,701-716.
132. Schmidt-Vogt H, 1977. Die Fichte (1), 1st edn. Paul Parey, Hamburg, Berlin.
133. Schmitz RF., 1972. Behaviour of *Ips pini* during mating, oviposition and larval development. (Coleoptera: Scolytidae). The Canadian Entomologist, 104:1723–1728
134. Seidl R., Müller J., Hothorn T., Bässler C., Heurich M., Kautz M., Kaplan I. Small beetle, large-scale drivers: 2016. How regional and landscape factors affect outbreaks of the European spruce bark beetle. Journal of Applied Ecology, 53 (2), pp. 530-540,
135. Sellamuthu, G., Bily, J., Joga, M. R., Synek, J. & Roy, A., 2022. Identifying optimal reference genes for gene expression studies in Eurasian spruce bark beetle, *Ips typographus* (Coleoptera: Curculionidae: Scolytinae). Scientific Reports, 12(1), 17.
136. Seybold S. J. and Tittiger C. (2003) Biochemistry and molecular biology of de novo isoprenoid pheromone production in the Scolytidae. Annual review of entomology, vol. 48, pp. 425– 453.
137. Seybold, S.J., Ohtsuka, T., Wood, D.L., Kubo, I. (1995a). The enantiomeric composition of ipsdienol: a chemotaxonomic character for North American populations of *Ips* spp. in the pini subgeneric group (Coleoptera: Scolytidae). Journal of Chemical Ecology, 21, 995–1016
138. Seybold, S.J., Quilici, D.R., Tillman, J.A., Vanderwel, D., Wood, D.L. and Blomquist, G.J. (1995b) *De novo* biosynthesis of the aggregation pheromone components ipsenol

and ipsdienol by the pine bark beetles *Ips paraconfusus* Lanier and *Ips pini* (Say)(Coleoptera: Scolytidae). Proceedings of the National Academy of Sciences of the United States of America, 92(18), 8393-8397.
139. Silverstein, R.M., Rodin, J.O., Wood, D.L., 1966. Sex attractants in frass produced by male *Ips confusus* in ponderosa pine. Science, 154, 509-510
140. Smith, C.A., Want, E.J., O'Maille, G., Abagyan, R., Siuzdak, G., 2006. XCMS: processing mass spectrometry data for metabolite profiling using Nonlinear peak alignment, matching, and identification. Analytical chemistry, 78, 779–787.
141. Smykal, V., Daimon, T., Kayukawa, T., Takaki, K., Shinoda, T. and Jindra, M., 2014. Importance of juvenile hormone signaling arises with competence of insect larvae to metamorphose. Developmental Biology, 390(2), 221-230.
142. Song, M. M., Kim, A. C., Gorzalski, A. J., MacLean, M., Young, S., Ginzel, M. D., Blomquist, G. J. & Tittiger, C. 2013. Functional characterization of myrcene hydroxylases from two geographically distinct *Ips pini* populations. Insect Biochemistry and Molecular Biology, 43(4), 336-343.
143. Sparks, M.E.; Rhoades, J.H.; Nelson, D.R.; Kuhar, D.; Lancaster, J.; Lehner, B.; Tholl, D.; Weber, D.C.; Gundersen-Rindal, D.E. 2017. A Transcriptome Survey Spanning Life Stages and Sexes of the Harlequin Bug, *Murgantia histrionica*. Insects, 8, 55.
144. Šramel N., Kavčič A., Kolšek M., Groot M. 2021. Estimating the most effective and economical pheromone for monitoring the European spruce bark beetle. Journal of Applied Entomology, 145, 312-325.
145. Stark, R., Grzelak, M., Hadfield, J., 2019. RNA sequencing: the teenage years Nature Reviews Genetics, 20, 631–656
146. Szabó, P., Kuneš, P., Svobodová-Svitavská, H., Švarcová, M.G., Křížová, L., Suchánková, S., Müllerová, J., Hédl, R., 2017. Using historical ecology to reassess the conservation status of coniferous forests in Central Europe. Conservation Biology, 31, 150–160.
147. Tautenhahn, R., Böttcher, C., Neumann, S., 2008. Highly sensitive feature detection for high resolution LC/MS. BMC Bioinformatics, 9, 504.
148. Tillman, J. A., Holbrook, G. L., Dallara, P. L., Schal, C., Wood, D. L., Blomquist, G. J. & Seybold, S. J., 1998. Endocrine regulation of *de novo* aggregation pheromone biosynthesis in the pine engraver, *Ips pini* (Say) (Coleoptera: Scolytidae). Insect Biochemistry and Molecular Biology, 28(9), 705-715.
149. Tillman, J. A., Lu, F., Goddard, L. M., Donaldson, Z. R., Dwinell, S. C., Tittiger, C., Hall, G. M., Storer, A. J., Blomquist, G. J. & Seybold, S. J., 2004. Juvenile hormone regulates *de novo* isoprenoid aggregation pheromone biosynthesis in pine bark beetles, *Ips* spp., through transcriptional control of HMG-CoA reductase. Journal of chemical ecology, 30(12), 2459-2494.
150. Tittiger, C. and Blomquist, G.J. (2017). Pheromone biosynthesis in bark beetles. Current Opinion in Insect Science, 24, pp.68-74.
151. Tittiger, C., Blomquist, G.J., Ivarsson, P., Borgeson, C.E. and Seybold, S.J. (1999) Juvenile hormone regulation of HMG-R gene expression in the bark beetle *Ips*

paraconfusus (Coleoptera: Scolytidae): implications for male aggregation pheromone biosynthesis. Cellular and Molecular Life Sciences, 55, pp.121-127.

152. Treiblmayr, K., Pascual, N., Piulachs, M-D., Keller, T., Belles, X., 2006. Juvenile hormone titer versus juvenile hormone synthesis in female nymphs and adults of the German cockroach, Blattella germanica. Journal of Insect Science, 6:1–7.
153. Trumbo, S. T., 2018. Juvenile hormone and parental care in subsocial insects: implications for the role of juvenile hormone in the evolution of sociality. Current Opinion in Insect Science, 28, 13-18.
154. Tyanova, S., Temu, T., Sinitcyn, P., Carlson, A., Hein, M. Y., Geiger, T., Mann, M. & Cox, J., 2016. The Perseus computational platform for comprehensive analysis of (prote)omics data. Nature Methods, 13(9), 731-740.
155. Vanderwel D and Oehlschlager A.C. 1984. Biosynthesis of Pheromones and Endocrine Regulation of Pheromone Production in Coleoptera. Pheromone Biochemistry, Academic press, 175-215.
156. Venter, J.C., et al. 2004. Environmental genome shotgun sequencing of the Sargasso Sea. Science, 304, 66–74.
157. Wang, M., Carver, J., Phelan, V., et al. 2016. Sharing and community curation of mass spectrometry data with Global Natural Products Social Molecular Networking. Nature Biotechnology 34, 828-837.
158. Wang, Z., Gerstein, M., Snyder, M., 2009. RNA-Seq: a revolutionary tool for transcriptomics in Western Equatoria State. Nature reviews genetics, 10, 57.
159. Wermelinger B. 2004. Ecology and management of the spruce bark beetle *Ips typographus* - A review of recent research. Forest ecology and management, 202, 67–82.
160. Wermelinger, B. 2019. Pheromone production in bark beetles. Insect Biochemistry and Molecular Biology, 40, 0–2.
161. Zhao, T., Axelsson, K., Krokene, P., & Borg-Karlson, A. K. 2015. Fungal symbionts of the spruce bark beetle synthesize the beetle aggregation pheromone 2-methyl-3-buten-2-ol. Journal of chemical ecology, 41, 848-852.
162. Zhao, T., Ganji, S., Schiebe, C., Bohman, B., Weinstein, P., Krokene, P., ... & Unelius, C. R. 2019. Convergent evolution of semiochemicals across Kingdoms: bark beetles and their fungal symbionts. The ISME journal, 13(6), 1535-1545.
163. Zhu, H., Gegear, R. J., Casselman, A., Kanginakudru, S., & Reppert, S. M., 2009. Defining behavioral and molecular differences between summer and migratory monarch butterflies. BMC biology, 7, 14.
164. Zotti, M.J., Smagghe, G. 2015. RNAi Technology for Insect Management and Protection of Beneficial Insects from Diseases: Lessons, Challenges and Risk Assessments. Neotropical Entomology, 44, 197–213.